# SCREENING OF APTAMERS AND SELECTIVE INHIBITORS FOR MYOTONIC DYSTROPHY KINASE-RELATED CDC42-BINDING KINASE (MRCK) BY CE-SELEX AND CHEMICAL INHIBITION

LAI JESYIN

NATIONAL UNIVERSITY OF SINGAPORE

2009

# SCREENING OF APTAMERS AND SELECTIVE INHIBITORS FOR MYOTONIC DYSTROPHY KINASE-RELATED CDC42-BINDING KINASE (MRCK) BY CE-SELEX AND CHEMICAL INHIBITION

**LAI JESYIN**

*(B. Sc. (Hons),NUS)*

A THESIS SUBMITTED

FOR THE DEGREE OF MASTER OF SCIENCE

DEPARTMENT OF ANATOMY

NATIONAL UNIVERSITY OF SINGAPORE

2009

# Acknowledgements

First of all, I would like to express my deepest gratitude to Assoc Prof Thomas Leung (IMCB) and Prof Sam Li (Department of Chemistry, NUS) for giving me this precious opportunity to work with sGSK-IMCB group for my postgraduate degree. I am so much grateful to Prof Sam Li for hiring me as a research assistant so that my research experiences could be academically and intellectually enriched during the period of my study. Thousand thanks will be given to Assoc Prof Thomas Leung as well for being my chief supervisor who has been so patient to guide and to support me throughout the whole process of my master study. Besides, I would also like to offer my thanks to the Department of Anatomy.

All the friendship and help coming from the laboratory members of sGSK group would never ever be forgotten. My appreciation especially will be offered to the following people who had really cared for me, supported me, advised me and had experienced all the up and down of working life along with me in the laboratory. First, many thanks to Dr Ivan Tan for his critical reading of this thesis and for all his following thoughtful suggestions, advices and enlightenments cast on me. Subsequent thanks to Mr Jeffery Yong, Miss Irene Lee and Miss Chia Shu Mei who had accompanied me to go through every tough situation to finish this course of endeavour. Thanks to Miss Junie Tok, from NUS, too, who is a good collaborator of the aptamer project. Thanks to the ETC group and ICES group as well who had helped me in the MRCK inhibitor screening process. Furthermore, I must also express my gratitude to Dr Edward Manser, Dr Jackson Zhou, Dr Dong Jing Ming, Dr Perry Chan, Dr Wing Chan and Dr Yeohendran for their continuous encouragement and insightful discussions to help me finish this work.

Last but not least, my sincere thanks will be given to my dearest family members, all my sisters and brothers in Christ, and dearest Lamp particularly. Their love to me will always be in my heart. My appreciation to them is far beyond words.

# Table of contents

# Summary

MRCK is a downstream effector of Cdc42, a member of Rho GTPase and its main function is in regulating cytoskeletal reorganization. Upon binding to Cdc42-GTP, it is activated and its subsequent signalling mechanisms are turned on through multiple phosphorylation events. The regulation of MRCK activity and its binding partner(s) have recently been studied and unravelled. One of the most important roles of MRCK is in the regulation of lamellar actomyosin retrograde flow which is intimately linked to membrane protrusion at the leading edge in migrating cells and involved in directional cell motility. Owing to the significant functions of MRCK, studies regarding detection of MRCK by aptamers and inhibition of MRCK by chemical compounds were highlighted in this project.

Aptmers are short sequences of RNA/DNA which can form secondary structure and have binding capacity to various molecules including proteins. As such, they have been used as molecular probes for detection purposes and they may also have therapeutic potential. Here a screening process called systematic evolution of ligands by exponential enrichment (SELEX) that coupled with subsequent separation of aptamers by capillary electrophoresis (CE) was carried to identify specific MRCK aptamers. By performing CE-SELEX, MRCK aptamers were selected from a single stranded DNA (ssDNA) library consists of 40-mer random sequences. Non-SELEX, one of the protocols for performing CE-SELEX, omits DNA amplification and was used for selection. Owing to the novelty of this protocol, method development has been studied in detail for future work. A number of optimizations and adjustments were tested in order to improve the selection efficiency and quality. The original non-SELEX method and a modified non-SELEX method were used for selection in a comparative study. MRCK aptamers with dissociation constant ($K_d$) of about 100 nM were obtained from both methods. One of the aptamers, M6, was able to detect the active form of MRCK kinase domain but not the inactive form. Subsequently, MRCK binding affinity of

these two aptamers was further confirmed by demonstrating *in vitro* binding analysis with CE and an *in vitro* MRCK pull down assay.

Our initial interest was to identify aptamers that can inhibit MRCK. Nonetheless, no successful result was obtained from the selected aptamers. Therefore, a screen for chemical inhibitor of MRCK was concurrently implemented as the second part of this project. To search for a selective MRCK chemical inhibitor, screening for MRCK inhibitors from a group of chemicals was carried out. A total of about 170 chemicals were screened with an in vitro kinase assay. Chelerythrine chloride (che/chelerythrine) was identified from these compounds to have MRCK inhibitory effect. Its half maximal inhibitory concentration ($IC_{50}$) was later confirmed to be 0.86 μM by radioactive kinase assay. A much weaker inhibitory effects were observed on the related Rho Kinase and Citron Kinase with an $IC_{50}$ of 8.6 μM and 6.4 μM respectively. At a concentration of 5 μM, chelerythrine was able to perturb MRCK localization in HeLa cells. Reduced cell migration was also observed in chelerythrine treatment in an U2OS wound healing assay.

# List of Tables

# List of Figures

# Abbreviations

| | |
|---|---|
| 6His | hexahistidine |
| APS | ammonium persulphate |
| ATP | adenosine 5'-triphosphate |
| BSA | bovine serum albumin |
| CAT | catalytic |
| CC | coil-coil domain |
| CE | capillary electrophoresis |
| che/chelerythrine | chelerythrine chloride |
| Ci | curie |
| CL | cluster |
| CNH | citron homology chain |
| CRD | cystein-rich domain |
| CRIB | Cdc42/Rac interactive binding |
| DMPK | myotonic dystrophy protein kinase |
| DMSO | dimethyl sulfoxide |
| dsDNA | double-stranded DNA |
| ECEEM | equilibrium capillary electrophoresis of equilibrium mixtures |
| ECL | enhanced chemiluminescence |
| ECM | extracellular matrix |
| EDTA | ethylenediamine tetraacetic acid |
| FBS | fetal bovine serum |
| Fig. | Figure |
| FRET | fluorescence resonance energy transfer |
| GAP | GTPase activating protiens |
| GDI | guanine dissociation inhibitors |
| GDP | guonosine 5'-diphosphate |
| GEF | guanine exchange factor |
| GST | glutathione-*S*-transferase |
| GTP | guanosine 5'-triphosphate |
| HIV-1 RT | HIV-1 reverse transcriptase |
| HPLC | high performance liquid chromatography |
| IB | immunoblot |
| IF | intermediate filaments |
| Im | imidazole |
| IPTG | isopropyl β-D-thiogalactoside |
| Kd | dissociation constant |
| KIM | kinase inhibitory motif |
| Km | Michaelis constant |
| LB | Luria-Bertani |
| LIF | light-induced fluorescence |
| LMP | low-melting point |

| | |
|---|---|
| LRAP35a | Leucine repeat adaptor protein |
| M | molar |
| MAB | molecular aptamer beacon |
| MgCl2 | magnesium chloride |
| MAPK | mitogen-activated protein kinase |
| MLC2 | myosin light chain 2 |
| MLCK | myosin light chain kinase |
| μM | micromolar |
| mM | millomolar |
| MRCK | myotonic dystrophy kinase-related Cdc42 binding kinase |
| MYPT | myosin phosphatase |
| NaCl | sodium chloride |
| NECEEM | nonequilibrium capillary electrophoresis of equilibrium mixtures |
| NPY | neuropeptide Y |
| N-terminal | amino terminal |
| OD | optical density |
| PAK | p21-activated kinase |
| PBS | phosphate-buffered sa;ome |
| PCR | polymerase chain reaction |
| PH | pleckstrin homology domain |
| PKA | protein kinase A |
| PKC | protein kinase C |
| PVDF | polyvinylidene difluoride |
| RMLC | regulatory myosin light chain |
| ROK/ROCK/Rho kinase | Rho-associated kinase |
| SDS-PAGE | sodium dodecyl sulphate polyacrylamide gel electrophoresis |
| SELEX | systemic evolition of ligands by exponential enrichment |
| ssDNA | single-stranded DNA |
| TE | Tris-EDTA |
| TEMED | N,N,N',N'-tetramethylethylenediamine |
| Tris | tris-hydroxymethyl aminimethane |
| VEGF | vascular endothelial growth factor |
| WB | western blot |
| WT | wild-type |

# Chapter 1 Introduction

## Section 1 Screening of aptamers for myotonic dystrophy kinase-related Cdc42 binding kinase (MRCK) by CE-SELEX

### 1.1.1 Overview

Specific and effective protein detection is of vital importance in disease diagnoses and treatments. In addition, specific recognition of proteins is useful for the studies of protein function. It is therefore a need to generate protein detection methods with high specificity and efficiency. Commercially available antibodies specific for a wide variety of target protein are useful for both medical and scientific research. They are widely used in protein detection probes such as Western blot analysis and diagnoses. Some antibodies have even been tested in clinical trials and have received approval for disease treatments. For example muromonab-CD3, a monoclonal antibody, was the first antibody to be approved in 1986 as transplant rejection drug (62); Eculizumab, a humanized monoclonal antibody, was approved two years ago for the treatment of paroxysmal nocturnal hemoclobunuria (35).

Although antibodies have been very useful on monitoring of protein localization intracellularly, the problem of high background noise due to cross reactivity has been associated with its usage. In addition, the fluorescent signal of antibodies is constitutive that it does not change upon binding to the target. Furthermore, the whole process of antibody production is time consuming and costly. Its production also requires sacrifice of the immunized animals, a step when implicates ethic issues that should be avoided is possible. Consequently, a rapid and not hazardous method to generate a low cost tool for protein detection is of high demand and interest.

A relatively new protein detection tool, aptamer, is introduced here. Aptamers are short sequences of either DNA or RNA and with binding capacity to various types of targets, such as ions, proteins and small molecules (ATP, antibiotics, *etc.*). They have the potential to be used as effective molecular probes for the purpose of detecting and recognizing important biological targets. In order to select aptamers for a particular target, performing a screening

experiment is required. Systematic evolution of ligands by exponential enrichment (SELEX) is a screening technique that allows rapid selection and enrichment of specific ligands via repeated rounds of partition and amplification from a large combinatorial nucleic acid library (4). New SELEX approach using capillary electrophoresis (CE) has been exploited in this project as a quick and easy way to obtain specific aptamers for a particular target.

### 1.1.2 Aptamers

As aforementioned, aptamers are generated by an *in vitro* selection process, SELEX, from random sequences of DNA or RNA libraries. They are similar to antibodies in terms of their protein binding capacity. They can be isolated rapidly *in vitro* and have been shown not to elicit an immune response in the human body (13). Aptamers could be regenerated easily after denaturation. They are stable in long-term storage and can be transported at ambient temperature. Therefore, aptamers have distinct advantages over other reagents of being utilized as diagnostic, analytical and potential therapeutic agents (14). Moreover, aptamer can even be engineered into oligonucleotide probe called molecular aptamer beacon (MAB) that aids in protein detection.

Aptamers, as single-stranded oligonucleotides, have diverse biological functions and applications due to their ability to fold into three-dimensional shapes of flexible structure and form "pocket" structure which can bind to various target molecules, including proteins, small-molecule compounds, and even living cells (26, 102). Furthermore, DNA or RNA aptamers with the length of 40 random bases, for example, can give up to $10^{24}$ of different sequences. This enables them to have potentially diverse conformational structures and thus provides a higher probability to have at least one species that possesses high affinity to a target of interest (30).

#### 1.1.2.1 The applications of aptamers

As a consequence of the specific affinity and binding capacity of aptamers, numerous applications of aptamers are attributed. The major applications include pharmacological

probes as biosensors for *in vivo* and *in vitro* target validation (9, 90), intracellular probes for protein function analysis and drug discovery (25, 57), development of biosensors, small-molecule lead compounds for enzyme and receptor inhibition (17, 68), ligands for affinity chromatography and capillary electrophoresis (72), molecular probes for *in vivo* imaging (95), and candidate therapeutics for disease healing (15).

Pegaptanib (vascular endothelial growth factor aptamer, Macugen) is a modified RNA aptamer, consists of 28 nucleotides, which can specifically bind to extracellular vascular endothelial growth factor (VEGF) and inhibits VEGF (76). It prevents VEGF from interacting with its receptor on the surface of vascular endothelial cells and results in pathological angiogenesis suppression. Recently, this RNA aptamer has already received approval for the treatment of age-related macular degeneration (97). The inhibition of Pegaptanib in the interaction of VEGF with its receptors attributes to its potential for the treatment of diabetic retinopathy and it is now undergoing clinical trials to assess its treatment on this disease (19). Meanwhile, there are also several other aptamers undergoing clinical trials and development into drug candidates. These potential aptamer-based drugs are aptamers against amyloidogenic proteins such as the Aβ-peptide associated with Alzheimer disease (106), and aptamers against abnormal proteins found in prion disease (79).

Furthermore, the selectivity of aptamers makes them ideal to be developed into diagnostic reagents with conformational changes upon binding to ligand. In fact, aptamers have been modified and engineered into nucleic acid MAB that possesses a stem-loop structure. The loop sequence of MAB serves as a probe that is complementary to the target sequence, and the annealing of two complementary arm sequences forms the stem. The detection of the MAB is performed by either differential fluorescence quenching or fluorescence resonance energy transfer (FRET). The hairpin shaped MB, when encounters a target molecule, will form a probe-target hybrid that is more stable than the stem in the hairpin. This results in conformational changes and the stem-loop structure is open up to permit the release of fluorescent or FRET signal (Fig. 1.1). This feature makes MAB an extremely useful probe in monitoring protein in real time and in homogenous solution. It has

even been demonstrated in the detection of mRNA (81) and DNA-binding protein (53) in the living cells.

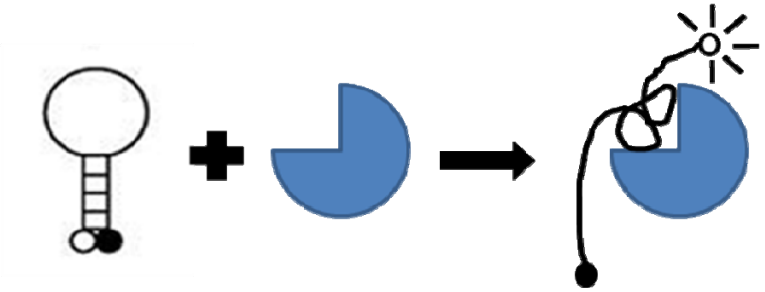


**Fig. 1.1 The working model of a MAB binding to its protein target.** The flourophore of a hairpin-structured MAB is quenched and gives no signal when it is not bound to the target. Interaction of MAB to its target opens up the MAB and releases the fluorescent signal.

### 1.1.2.2 The advantages and disadvantages of aptamers

Although aptamers have equivalent function as antibodies in recognizing target proteins, aptamers have a few advantages over antibodies. Aptamers can recognize the functional domains of proteins, such as catalytic domain of a protein, and thereby might be used in regulating the target's biological functions. In fact, a good aptamer can even distinguish between wild type and mutant protein or between active and inactive proteins or between different conformational states of a single molecule(14). Moreover, aptamers can be modified to be more useful in executing their functions, for example aptamers are immobilized onto to a solid support to form affinity column, bioengineered with fluorophore or quencher tag at either end for live cells imaging, and attached with appropriate functional groups for deliverance into living cells or animals. Despite the modifications, their target-recognition properties are still well preserved. As mentioned previously, aptamers are indeed rather safe in developing into therapeutic agents due to their lack of immunogenicity. In contrast, antibodies are often immunogenic and might not be as ideal as aptamers in exhibiting therapeutic functions. One of the most important benefits of aptamers, as compared to antibodies, is their remarkable stable properties in term of shelf life. They are more resistant towards temperature

changes and are thus easier to handle. Consequently, they have great potential in being exploited for the application in pharmacological areas.

However, as aptamers are more prone to be degraded by endogenous endonucleases and exonucleuses, research to overcome such a problem needs to be addressed. In fact, the aptamer structure is chemically modified to render it more stable for resistance towards generic nucleases to increase half-life of the aptamer (69). For example, Pegatapnib was indeed modified at the 2'position in several residues with F in pyrimidine bases or methoxy in purine bases to replace the natural OH groups in the RNA sequences.

### 1.1.3 The selection of aptamer

SELEX is the most versatile and common method to select nucleic acid aptamers for a target. It was first reported in 1990 by Gold's group (93) to study the interaction between a T4 DNA polymerase and mRNA, and Szostak (23) to isolate RNA molecules that bind specifically to a variety of organic dyes. Later on, it was subsequently developed into a technology for *in vitro* selection of specific aptamers for a chosen target from a random pool of DNA or RNA library (58). This method starts from an automated chemical generated random library of DNA or RNA molecules. The three main procedures are shown in Fig. 1.2 and the details of SELEX are as below:

1. Selection

A library of nucleotide sequences is incubated with the target for a given period of time. The molecules in the library without affinity to the target will remain free in the solution while those with affinity to the target will be bound to the target. Target-bound and unbound molecules can be separated by using various techniques, such as affinity chromatography, membrane filter, capillary electrophoresis, and etc. Finally, aptamers with higher affinity to the target will be eluted or collected from the target and they will form into an enriched pool of DNA for the subsequent steps.

2. Amplification

The collected and purified sequences are amplified by polymerase chain reaction (PCR) to

yield a pool of aptamers that binds to target with higher affinity. This enriched pool generated from the PCR-amplified sequences is used for the next round of selection, partition and amplification.

3. Aptamer isolation

In some cases, the selection conditions are changed to more stringent conditions to allow purification of tight and specific binders only. Selection and amplification procedures will be repeated for several rounds till the enriched library achieves a certain level of bulk affinity. After that, individual aptamer sequences from the enriched library are selected and identified by molecular cloning and DNA sequencing. Lastly, the individual aptamers are chemically synthesized for the testing of their binding affinities to the target (5).

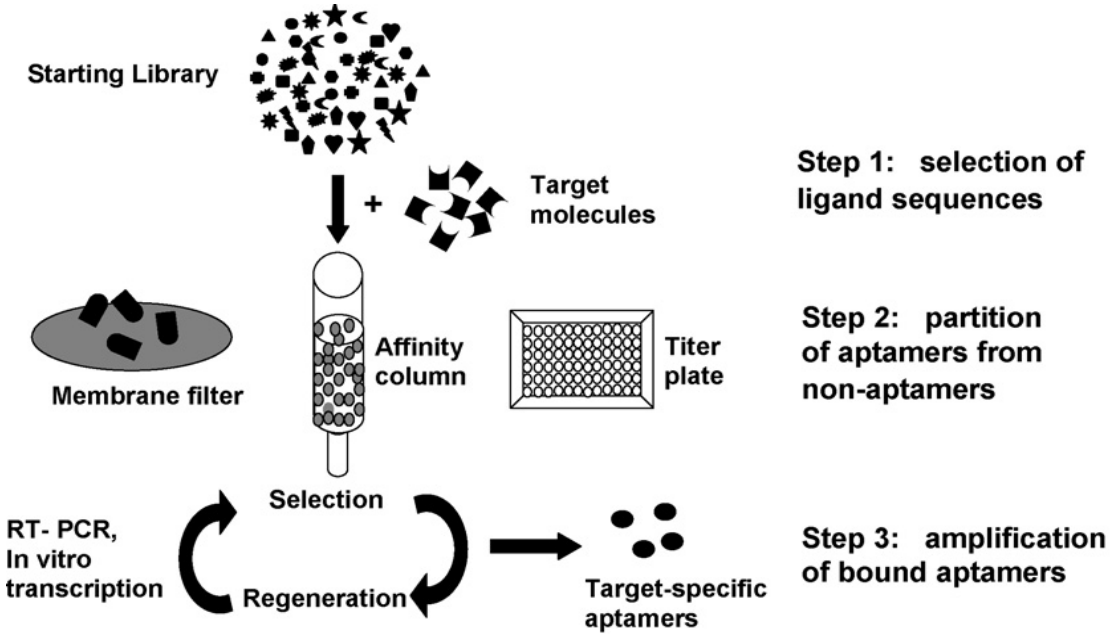


**Fig. 1.2 The three main processes which are involved in SELEX.** Random sequences of DNA/RNA library is incubated with the target; various partitioning techniques, such as membrane filter, affinity column or titer plate, are used for partitioning of target-bound aptamers from non aptamers; the selected aptamers are regenerated by PCR amplification for the next round of selection. (Adapted from Yang Y *et al*. (104))

### 1.1.3.1 Capillary electrophoresis (CE) as a technique for SELEX

The conventional approach of SELEX was done by passing the aptamers through a column with target molecules immobilized on a stationary support by a linker molecule. The linker might also form steric hindrance on some parts of the target and might prevent the

aptamers to have complete access towards the target. Moreover, this method requires a blocking step and it is generally difficult to recover strong target binders from the column (44). In contrast, membrane filtration method, normally used for large SELEX targets like proteins, allows aptamers to interact freely with target in solution and eliminates linker bias (34). Unfortunately, both column purification and membrane filtration processes require 10-15 cycles of selections to obtain high-affinity aptamers. To overcome this problem, a modified technique, CE, has been utilized as an alternative enrichment method for improving the efficiency of selection in the SELEX procedure. CE was designed to separate samples based on their size to charge ratio in the interior of a small capillary filled with an electrolyte using electrical field (Fig. 1.3). One major advantage of CE is that only a small volume of sample in nanoliter range is required. In brief, CE-SELEX applies electrophoresis principle to separate aptamer-target binding complexes from free aptamers. A library of aptamers is incubated with the target first before they are injected into a capillary. Separation is done in the capillary, which is filled with running buffer, with electrical polarity applied at the two ends. Specific binders are separated from nonbinding molecules based on a mobility shift induced by the formation of aptamer-target complexes (33)(Fig. 1.4). In principle, the modern CE technology is applicable in SELEX for selection of target-specific aptamers.

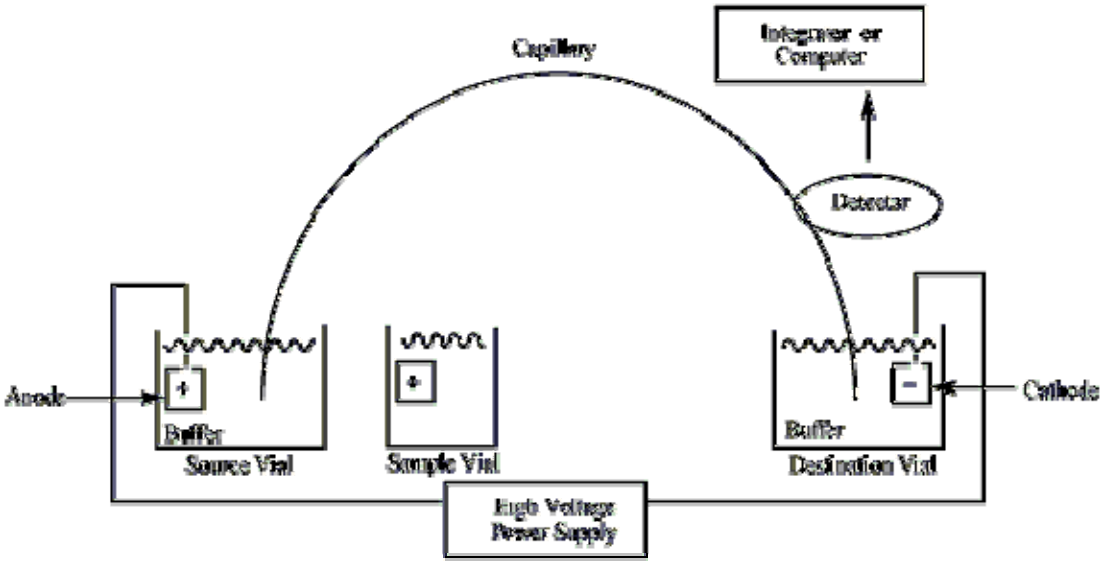


**Fig. 1.3 A diagram of capillary electrophoresis system.** The main components of the system contain source and destination vials, a sample vial, a capillary, electrodes, a high-voltage power supply, a detector, and a data output. The source vial, destination vial and capillary are filled with an electrolyte such as an aqueous buffer solution. Normally, anode is at the source vial while cathode is linked to the destination vial. (Adapted from http://en.wikipedia.org/wiki/Capillary_electrophoresis)

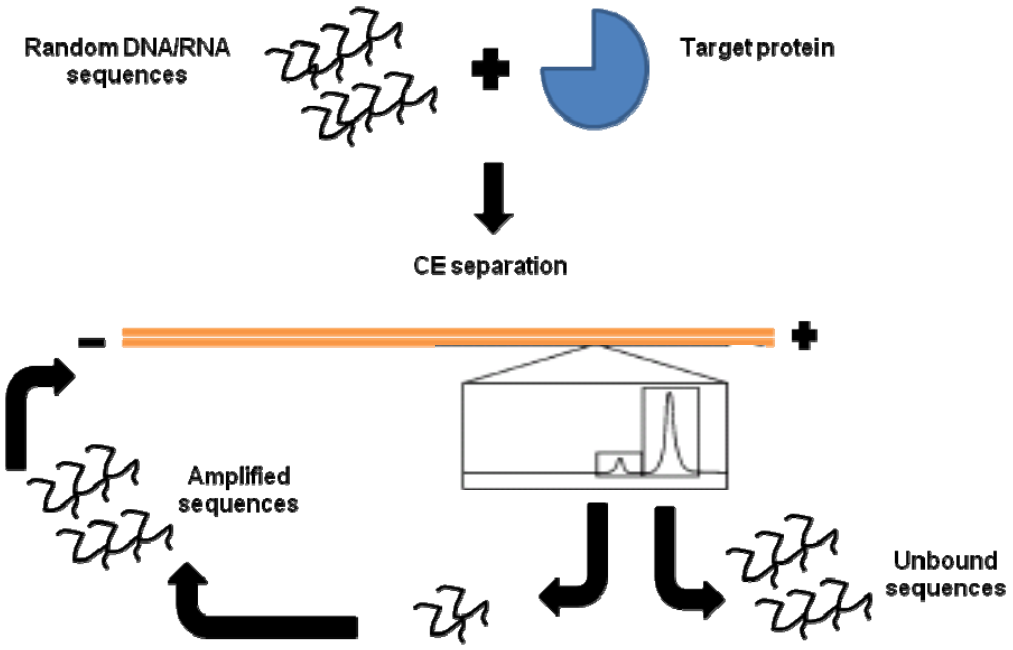


**Fig. 1.4 The complete procedures of aptmers selection using CE-SELEX.** The nucleic acid library is incubated and mixed with the target protein. The mixtures are injected into the CE and separated in a free solution. Same as conventional SELEX, binding sequences are partitioned from nonbinding sequences based on a mobility shift induced by the formation of aptmer-target complexes. Collected sequences are PCR amplified to generate a new pool for further rounds of selections.

### 1.1.4 CE partitioning methods: NECEEM and ECEEM

Two types of partitioning process have been recently introduced for CE-SELEX: nonequilibrium capillary electrophoresis of equilibrium mixtures (NECEEM) and equilibrium capillary electrophoresis of equilibrium mixtures (ECEEM).

NECEEM is an approach in which the equilibrium fraction of target-bound DNA is partitioned from the equilibrium mixture of free DNA without having components of the DNA library or the target in the running buffer (Fig. 1.5). As a result, complexes with weak interaction tend to dissociate during their migration along the capillary while binders with high affinity to the target are eventually selected. NECEEM was claimed to be more advanced than conventional SELEX methods in three aspects: (i) high efficiency of aptamer selection, (ii) accurate determination of binding parameters (e.g. dissociation constant, $K_d$), and (iii) capable to quantitate targets with their aptamers. Berezovski M *et al*. (5) even demonstrated that a single round of NECEEM-based SELEX was sufficient for obtaining a pool of aptamers for PFTase with $K_d$ in the range of 1 nM (5), in contrast to conventional methods which require 8-12 rounds. Bowser's group also successfully selected a pool of high-affinity DNA aptamers for human IgE and HIV-1 reverse transcriptase (HIV-1 RT) using NECEEM. The average $K_d$ of the sequences in the enriched pool for IgE was in nanomolar range (60) and picomolar affinity for HIV-1 RT (64) after 4 rounds of selection. Moreover, they proved that NECEEM is applicable in isolating aptamers for targets smaller than the DNA sequences by performing 80-mer aptamers (~25kDa) selection against neuropeptide Y (NPY)(~4kDa). It is much simpler to select aptamers for high molecular weight targets because they retard the mobility of DNA upon binding. Though the mobility of a DNA sequence only changed slightly upon binding to NPY, enriched pool in low nanomolar $K_d$ was obtained when they performed three CE collections for every round of selection to increase the number of DNA sequences for partition (59). High-affinity DNA aptamers for Protein kinase C δ (PKCδ) have also been selected using NECEEM. Nine rounds of selection, which the others only did 3-4 rounds, were carried out and the lowest $K_d$ of the aptamer-protein binding is 122 nM (55). Last but not least, DNA aptamers that specifically recognize ricin toxin were selected with

NECEEM and the enrichment achieved 87.2% purity (based on percentage of bound aptamers) after 4 rounds of selection. The aptamers derived were found to possess high affinity and specificity for ricin with 80±38nM as the lowest $K_d$ value (89).

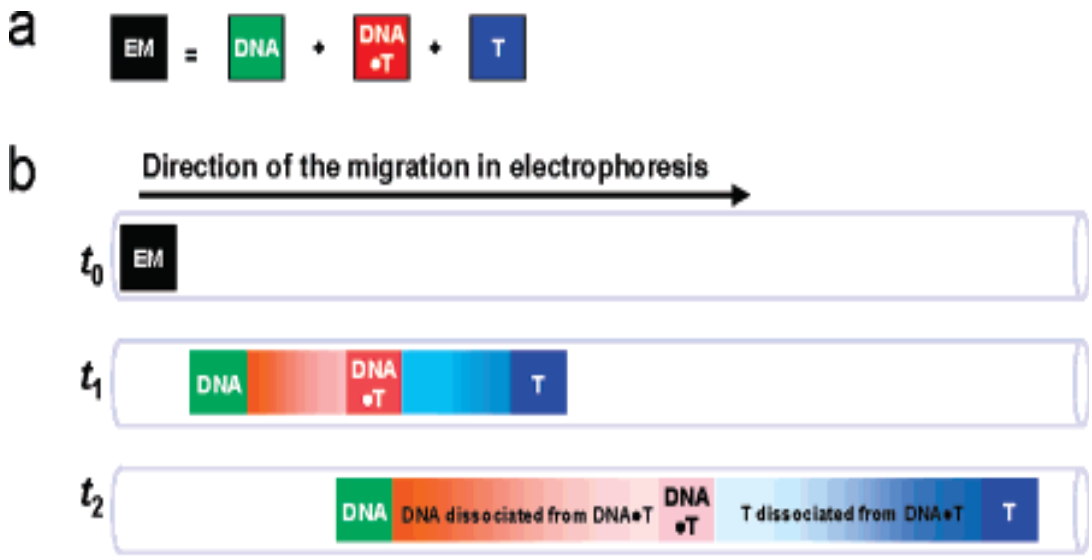


**Fig. 1.5 Schematic representation of NECEE-based selection of DNA aptamers.** (a)The equilibrium mixture (EM) consists of free DNA, DNA-target complex (DNA.T), and free target (T). (b)NECEEM-based separation of the EM. Target-bound DNA (red) is separated from the free DNA (green). Here shows the spatial distribution of the separated components in the capillary at different times ($t_0$=0, $t_2$>$t_1$>$t_0$) from the beginning of separation. (Adapted from Berezovski M *et al*. (5))

As for ECEEM, in which aptamer-target equilibrium is maintained during partitioning, it is able to select aptamers with predefined values of $K_d$ (21) . This method, however, required target presence in the running buffer at the concentration equal to that of the target concentration in the equilibrium mixture and this will increase target consumption in comparison with NECEEM. Moreover, the completion of ECEEM requires NECEEM to determine the migration times of complexes and free aptamers, and $K_d$ values as well. ECEEM combined with NECEEM was reported in aptamer selection for MutS and the best candidate selected had an affinity of 3.6nM±0.5nM (22). Three rounds of ECEEM-based selection were performed to develop aptamers with predefined $K_d$ and NECEEM to find out the real $K_d$ of each aptamer for further selection.

### 1.1.5 Non-SELEX

Non-SELEX is a modified CE-SELEX technique which employs NECEEM-based partitioning, with enhanced efficiency by excluding the steps of PCR amplification in between rounds of selection. Fig. 1.6 depicts the difference between conventional SELEX and non-SELEX while Fig. 1.7 describes the procedures of non-SELEX. Non-SELEX has at least two advantages over SELEX: (i) more rounds of aptamer selection can be done in one day, and (ii) aptamer selection can be performed in an automated fashion using a commercially available CE instrument (6). For better understanding to these distinct methodologies, the similarities and differences of conventional SELEX, CE-SELEX and non-SELEX were summarized in Table 8 (Appendix). In a proof-of-principle work, aptamers for h-Ras were partitioned via non-SELEX. Three rounds of non-SELEX were able to generate an enriched pool of DNA with average 300nM $K_d$ value.

### 1.1.6 Aim of research

CE-SELEX is a novel technique which can be applied to aptamer selection for any target of interest. As CE-SELEX is still in its infancy, careful optimization and development of this technique is required for proper selection of aptamers. The main objective of this study is to optimize the CE selection method and conditions for the selectiong of aptamers specific to our protein of interest, MRCK. Subsequently, the binding ability of the selected aptamers is analyzed and designed into molecular probe for target protein recognition in the cell.

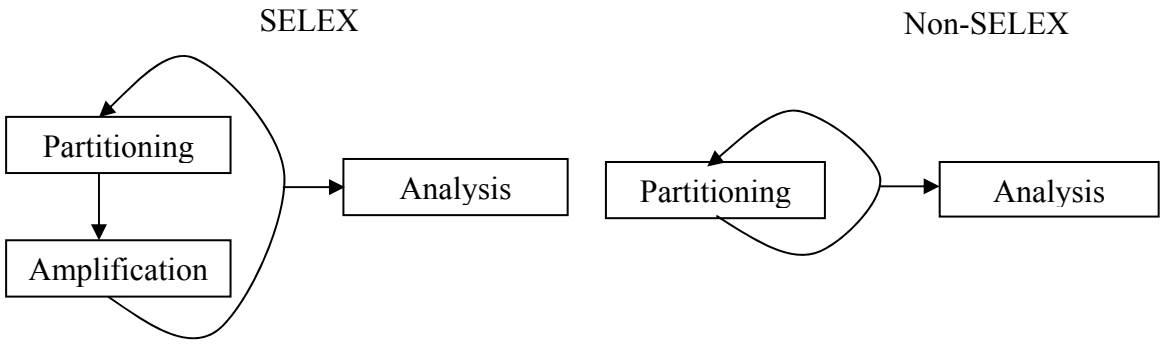


**Fig. 1.6 Schematic of the differences between SELEX and non-SELEX procedures.** The only difference between SELEX and non-SELEX is that the step of amplification is omitted in non-SELEX.

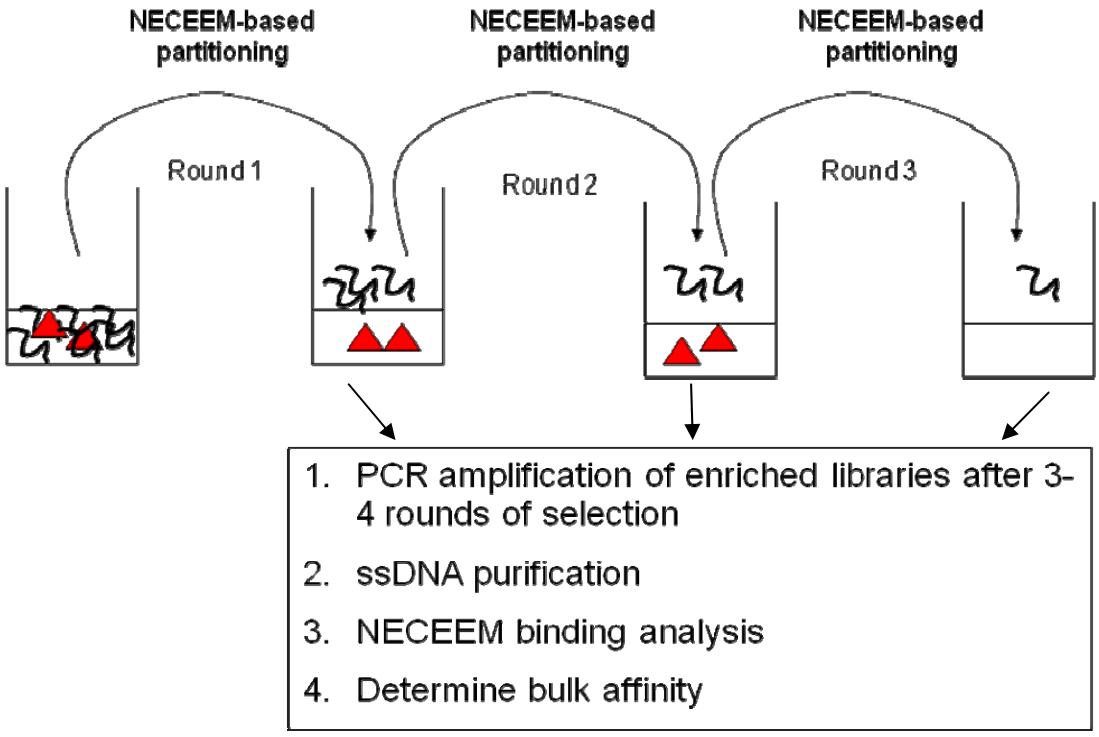


**Fig. 1.7 Diagram shows all the procedures of a complete set of aptamer selection using non-SELEX method.** Three steps of NECEEM-based partitioning are involved in non-SELEX selection of aptamers.

## Section 2 Screening of selective inhibitors for myotonic dystrophy kinase-related Cdc42 binding kinase (MRCK) by chemical inhibition

### 1.2.1 Overview

Cell migration is an essential event that takes place throughout the entire lifespan of all multicellular organisms. Rho family of GTPases was found to play a central role in this process through their regulation on cytoskeletal reorganization. The functions of Rho, Rac and Cdc42 have especially been well established over the past decades. In brief, Cdc42 regulates the direction of migration, Rac induces membrane protrusion at the front edge of the cell via actin polymerization and integrin adhesion complexes, and Rho promotes actomyosin contraction in the cell body and at the rear. These GTPases act as molecular switches via their respective sets of downstream effector proteins in the regulation of cell motility and cytoskeletal changes.

MRCK, a Rac/Cdc42-binding kinase, was reported to function downstream of Cdc42 in regulating cytoskeletal reorganization and lamellar actomyosin retrograde flow, which is crucial to membrane protrusion and cell migration. MRCK inhibition therefore could result in cell motility inhibition. However, no known selective MRCK inhibitor is available. Thus, it is of our interest to screen and identify such inhibitors. In an initial screen performed in this project, around 170 chemicals were screened for this ability to inhibit MRCK. The highest hit was obtained from a compound named chelerythrine chloride. It was shown to inhibit MRCK activity an with $IC_{50}$ of 0.86 μM while it only inhibits Rho-associated kinase (ROK) and Citron Rho-interacting kinase (CRIK) at higher concentrations. The $IC_{50}$ for ROK and CRIK are 8.6 μM and 6.5 μM respectively. Chelerythrine chloride, at a concentration of 5 μM, was able to perturb MRCK localization in the cells and results in a reduced cell migration rate in U2OS cells using wound healing assay.

### 1.2.2 Cell migration and Rho GTPase

Cell migration is an event that can be observed in wound healing, immune

surveillance, and also during the growth and development of multicellular organisms. In fact, cell migration is mainly controlled by internal and external signals, such as attractants or repellents from distant environment, neighboring cells or extracellular matrix (ECM) (71). These signals in turn activate complex signal transduction cascades that result in highly dynamic changes in actomyosin cytoskeleton, microtubules, vesicular transport pathways, genes transcription and protein-protein interaction. Actomyosin cytoskeleton, microtubule system with motors, and also intermediate filament system, coordinate with each other like an orchestra to modulate the whole process of cell movement (20).

A huge variety of intracellular signaling molecules has been implicated in cell migration, including MAPK cascades, lipid kinases, phospholipases, serine/threonine and tyrosine kinases and scaffold proteins. Rho GTPase as one particular family of proteins seems to play a pivotal role in regulating the biochemical pathways most relevant to cell migration. Therefore, Rho GTPase is believed to be one of the key contributions that regulate the process of cell migration.

The Ras-related Rho family of GTPases is constituted with small signaling G proteins which are usually 21 kDa. The primary roles of Rho GTPases include regulating the actin cytoskeleton, cell polarity, microtubule dynamics, membrane transportation and transcription factor activity. These low molecular weight GTPases act as molecular switch to control complex cellular processes by shuttling between two conformational states, the inactive GDP-bound form and the active GTP-bound form. The GTP-bound Rho GTPases interact with their respective downstream effectors to generate a response till they hydrolyse GTP to GDP; the GDP-bound Rho GTPases are inactive and can be extracted from the membranes by guanine dissociation inhibitors (GDI). This cycle process, as shown in Fig. 1.8, is tightly regulated by guanine exchange factors (GEFs), GTPase activating proteins (GAPs), and GDIs. Sixty effectors of Rho GTPases have been identified so far in which Rho, Rac and Cdc42 are the three best-characterized target proteins.

The widely accepted model of cell migration is shown in Fig. 1.9. It is a cyclic process which initiates from a migration-induced signal. This signal activates Rac in

promoting actin polymerization to form peripheral lamellipodial protrusions (73) while Cdc42 stimulates cell polarization in the front of the cells (24) and also caused the formation of actin-rich membrane extension structures called filopodia (47, 67). Actin polymerization provides driving force for the extension of protrusions in the direction of migration while contraction, promoted by Rho, happens at the cell body and the back of the cell (73). These protrusions are stabilized by ECM or adjacent cells via formation of new focal adhesion or transmembrane receptors linked to the actin cytoskeleton. As the cell moves forward, the adhesions at the rear are disassembled and allow cell membrane to detach from the ECM (20, 49, 74).

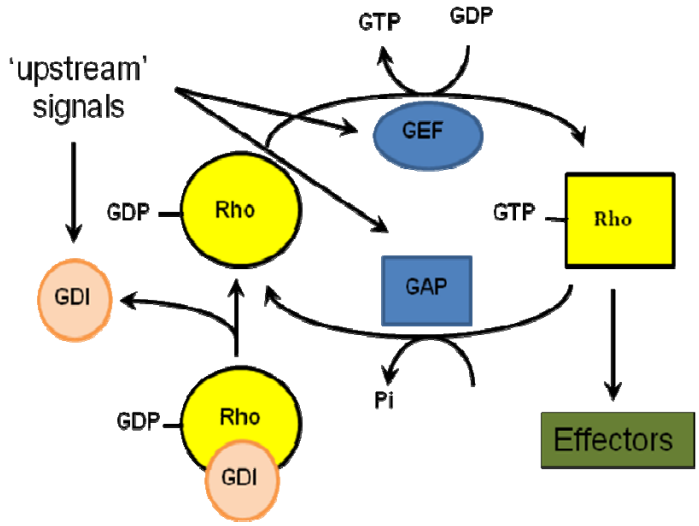


**Fig. 1.8 The Rho GTPase cycle.** Rho GTPases cycle between an inactive GDP-bound and an active GTP-bound conformation. Guanine nucleotide exchange factors (GEFs), when activated by upstream signals, can cause exchange of GDP to GTP and lead to activation of Rho GTPases. Active Rho-GTPs then interacts with their downstream effectors. GTPase activating proteins (GAPs) enhance GTP hydrolysis and inactivate Rho GTPases. Meanwhile, guanine dissociation inhibitors (GDIs) can block the cycle and solubilize the GDP-Rho.

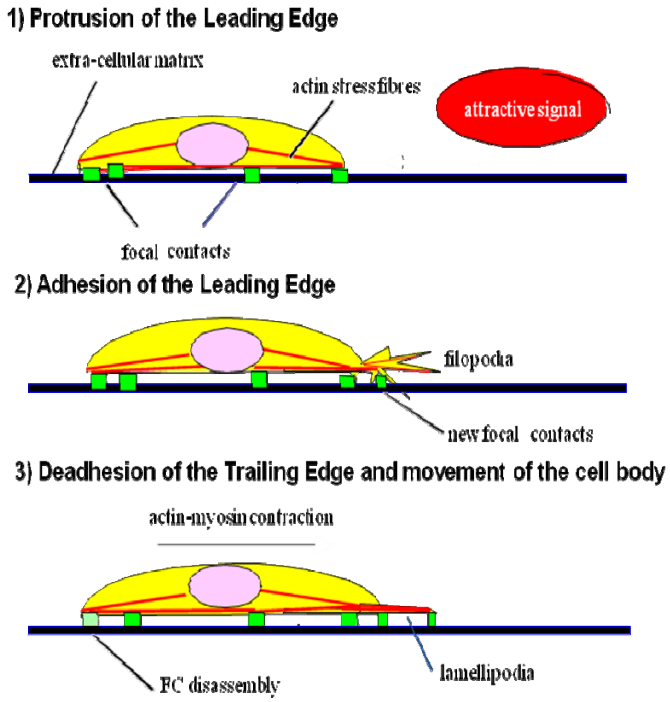


**Fig. 1.9 A schematic of the three stages of cell movement.** An external migration-induced signal, sensed by the cell, determines the direction of cell motion. The cell then extends a protrusion in this direction by actin polymerization at the leading edge. It adheres its leading edge to the surface on which it is moving and detaches at the cell body and the rear. Finally, it pulls the whole cell body forward by contractile forces generated at the cell body and the rear.

### 1.2.3 Myotonic dystrophy kinase-related Cdc42-binding kinase (MRCK)

Myotonic dystrophy kinase-related Cdc42-binding kinase (MRCK), is one of the downstream effectors of Cdc42. MRCK together with p21-activated kinases (PAKs) was identified in our laboratory from a binding assay searching for potential targets of the p21 Rho family (51). Two isoforms of MRCKs, MRCKα and MRCKβ, were identified while the other isoform, MRCKγ, was depicted by Jobert G. *et al.* (41) and Pirone D.M. *et al*. (70). The significant functions, properties and protein signaling mechanisms of MRCKα, but not MRCKβ, have been studied more intensively by our research group for the past ten years. MRCKα is a relatively large protein with molecular weight of about 180-200 kDa. According to the work of isolation and characterization of MRCKs, MRCKs belong to a family of serine/threonine kinases highly related to the myotonic dystrophy protein kinase (DMPK) (11, 29) and Rho-associated kinases (ROKs/ROCKs/Rho-kinases) in terms of protein sequences similarity and their downstream phorsphorylation targets (39, 52, 56).

Multiple functional domains were discovered and characterized from MRCKs. All the isoforms of MRCKs, including MRCKα, MRCKβ and MRCKγ, contain a highly conserved N-terminal serine/threonine kinase domain. An extended coiled-coil domain (CC), a kinase inhibitory motif (KIM), a cysteine-rich domain (CRD) that binds phorbol ester, a pleckstrin homology domain (PH), a citron homology domain (CNH) and the Cdc42/Rac interactive binding (CRIB) domain, are the following functional domains located in order after the kinase domain (Fig. 1.10).

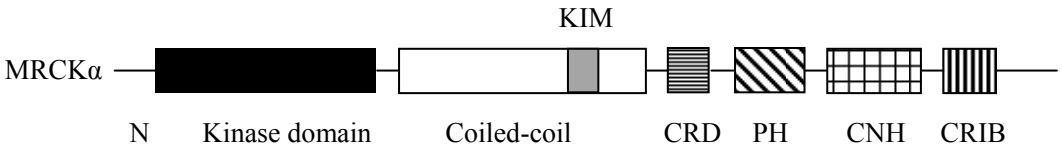


**Fig. 1.10 Functional domains of MRCKα.** Kinase domain of MRCKα is flanked by an N-terminal sequence and a coiled-coil domain. Cysteine-rich domain (CRD) with kinase inhibitory motif (KIM), pleckstrin homology domain (PH), citron homology domain (CNH), and Cdc-42/Rac-interactive binding (CRIB) domain are the various functional domains presenting between the kinase domain and the C termini.

In fact, much work was focused on the functional and characteristic studies of MRCKα. MRCKα, as suggested by its name, was discovered to be the effector of Cdc42 and Rac acting downstream of these Rho GTPase. According to an *in vitro* binding assay, however, MRCKα was found to be capable of binding strongly to Cdc42-GTP than to Rac1-GTP. Moreover, MRCKα, acting as the effector of Cdc42, has the function in promoting cystoskeletal reorganization (51). There are evidences showing that MRCKα has implication in Cdc42-mediated peripheral actin formation and neurite outgrowth in HeLa and PC12 cells respectively (16). The mechanism where MRCKα regulates actin cytoskeletal reorganization is via phosphorylation of a myosin-binding subunit (MBS) of myosin phosphatase 1 (MYPT1) (86) and myosin light chain 2(MLC2) (101). Recently, our laboratory discovered that MRCKα, by forming a tripartite complex with LRAP3a (Leucine repeat adaptor protein) and myosin 18a, is also involved in modulating lamellar actomyosin retrograde flow which is crucial to cell protrusion and migration (88).

#### 1.2.3.1 MRCK-related kinases

MRCKs belong to a large subclass of protein kinases termed the AGC kinases, which denote protein kinase A, G and C and other kinases, like protein kinase B/Akt, p70 and 90 ribosomal S6 kinases, phosphoinositide-dependent kinase-1, ROK, DMPK, and Citron Rho-interacting kinase (CRIK) (Fig. 1.11). Phosphorylation is vital in the activation of all the AGC kinases, though additional regulatory mechanisms are involved for each kinase.

According to sequence homology and the AGC kinases tree, MRCKs are most closely related to DMPK, ROK and CRIK. Their N-terminal kinase domains are very homologous in terms of amino acid sequences, for example, the kinase domain of MRCK is about 78.3% similar to DMPK. They all have a CC domain following the highly conserved kinase domains (87). Furthermore, they also have similar domain arrangement, even sharing similar downstream phosphorylation substrate. Fig. 1.12 shows the alignment of the MRCK kinase domain with DMPK, ROK, CRIK, and other related kinases (MLCK, PAK, PKA and PKC). MRCK, ROK and DMPK can phosphorylate the MYPT1 of the myosin light chain phosphatase (65, 86), while MRCK, ROK and CRIK can phosphorylate the myosin light chain (MLC) of myosin II. Myosin II plays a critical role in regulating actomyosin cytoskeleton in cell spreading and migration. The activities of myosin II are highly mediated by phosphorylation of its regulatory light chain (RLC). Monophosphorylation of RLC at Ser19 increases the actin-activated $Mg^{2+}$-ATPase activity while diphosphorylation at both Thr18 and Ser19 further increases the actin-activated $Mg^{2+}$-ATPase activity (36). In terms of MLC2 phosphorylation, Ser19 is the common phosphorylation site for MRCK (88) but CRIK and ROK can phosphorylate both Thr18 and Ser19 of MLC2 (103).

Although the kinase domains of MRCK, DMPK, ROK and CRIK are highly homologous, each of them plays different roles in the cells with quite distinct *in vivo* functions. As mentioned earlier, the main function of MRCK is related to the regulation of actin cytoskeleton organization. ROK, unlike MRCK, interacts with Rho-GTP but not Cdc42-GTP and Rac1-GTP. As the effector of Rho, ROK promotes formation of stress fibers and

focal adhesion complexes (52) via MLC2 phosphorylation to enhance actomyosin contraction (48) and intermediate filaments (IFs) organization (80). DMPK was reported to have functional implication in the generation and maintenance of the skeletal muscle, cardiac muscle atrioventricular conduction, cellular ion homeostasis regulation and glucose metabolism (42) while CRIK is primarily involved in the regulation of cell-cycle progression (83).

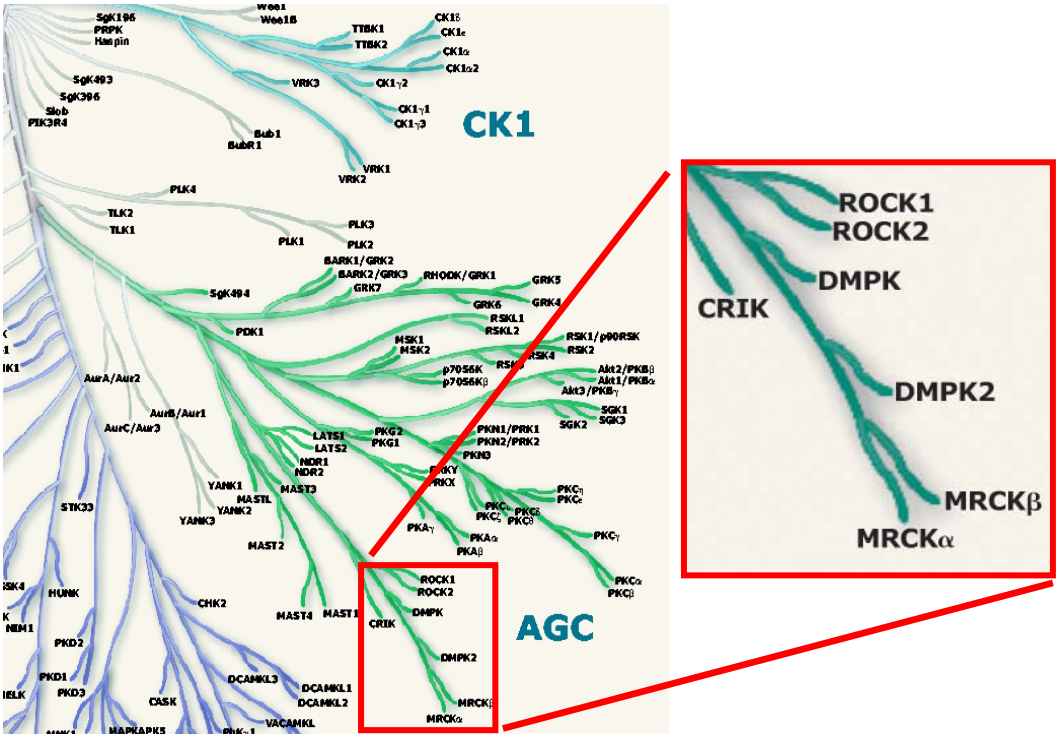


**Fig. 1.11 AGC kinases tree.** Red square marks out the most closely related kinases of MRCK, which are Rho-associated kinase (ROK/ROCK/Rho-kinase), myotonic dystrophy protein kinases (DMPK), and Citron Rho-interacting kinase (CRIK).

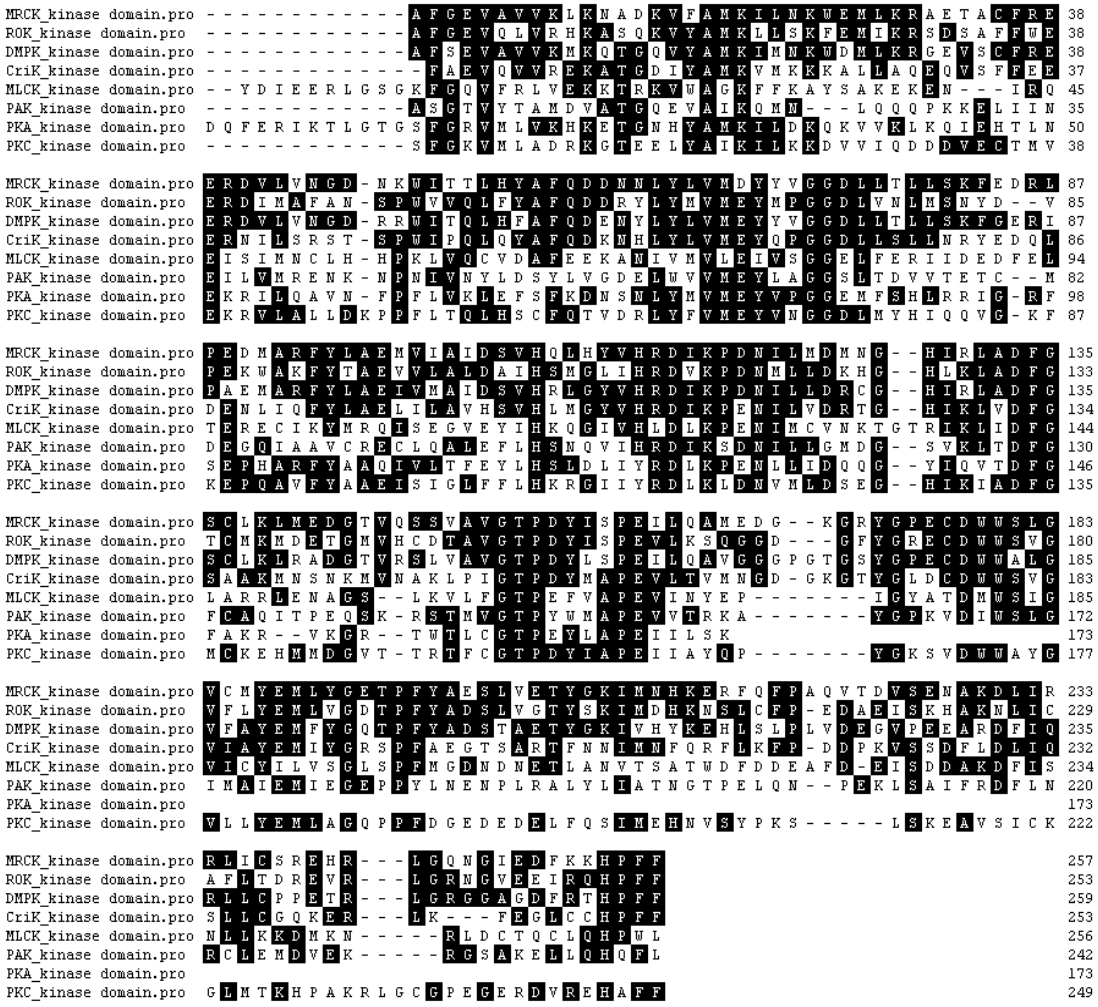


**Fig. 1.12 The amino acid sequences alignment of the kinase domain of MRCK and other kinases.** Kinase domain sequences alignment of MRCK with ROK, DMPK, CRIK, MLCK (myosin light chain kinse), PAK and PKA (protein kinse A). Areas of amino acid identity are labelled, and numbers indicate the positions of residues.

### 1.2.4 Effects and methods of MRCK inhibition

According to the previous effort carried out by our laboratory, the kinase domain of MRCK is negatively regulated by the KIM domain located within the distal CC domain (87). This means that the interaction between the KIM domain and the kinase domain results in the inactivation of MRCK catalytic activity. A loss of the actomyosin networks in the lamellar and subnuclear region was reported in active MRCK-depleted cells (88). Consequently, cell migration was impaired due to the disruption of actomyosin retrograde flow (31). Biological molecules or chemical compounds which can inhibit MRCK activity will thus potentially be

useful in controlling cell motility. For example, MRCK inhibitor might be applied to stop metastasis of cancerous cells.

There are basically two commonly available methods being used to reduce or downregulate MRCK *in vivo* catalytic activity in. The first method is the use of siRNA, which is specific for MRCK, to knockdown the expression of endogenous MRCK and thus lead to depletion of the active MRCK. Secondly, introduction of the kinase-dead mutant of MRCK, either through transfection or microinjection, into the cells can also bring the same effect as decreasing MRCK activity. However, transfection technique is required for the introduction of siRNA or kinase-dead MRCK into the cells while highly microinjection has the problem of being laborious and low efficiency. Therefore, there is still a lack of a more convenient and immediate way to achieve the immediate effect of MRCK inhibition. One of the most ideal ways to perturb or to knockout the functions of MRCK would thus rely on the use of a chemical drug that can specifically inhibit MRCK enzymatic activity.

#### 1.2.4.1 ROK inhibitors

Unlike MRCK, six ROK inhibitors are available in the market and many more ROK inhibitors have been published in the literature. The most popular and generally used inhibitor of ROK is Y-27632. It was discovered and described by Narumiya's research group in 1997. They identified that Y-27632, a pyridine derivative, can target to ROK and can consistently suppress ROK-mediated formation and contraction of stress fibers in cultured cells. They also found that the compound is able to reduce dramatically high blood pressure in several hypertension rat models (94). The working principle of Y-27632 is predicted by targeting and blocking ROK from phosphorylating smooth muscle MYPT and MLC2 (43). A decrease of myosin phosphorylation subsequently leads to arterial smooth muscle relaxation and vasodilation of blood vessels. Other than this, it was also reported to inhibit RhoA-mediated cell transformation (77), tumour-cell invasion (40) and neutrophil chemotaxis (66). Therefore, from the effects of ROK inhibition, ROK inhibitors are indeed highly potential for anti-cancer or anti-inflammatory treatment.

HA1077, also known as fasudil hydrochloride, is another compound reported to have inhibition effect on ROK (3). This compound has been shown to act as a drug for cerebral vasospasm treatment by increasing cerebral blood flow and inhibiting inflammatory response (84). Rockout, 3-(4-Pyridyl)-1H-indole, is a selective and ATP-competitor inhibitor of ROK activity. It was discovered through an image-based, high-throughput screen of cell monolayer wound healing (105). N-(4-Pyridyl)-N′-(2,4,6-trichlorophenyl)urea is also another ATP-competitive inhibitor of ROK. It was designed via docking simulation of a number or compounds on the target protein (85). H-1152 was designed as a more specific, stronger and membrane-permeable inhibitor of ROK with a dissociation constant of 1.6nM (38). Lastly, N-(4-(1H-pyrazol-4-yl)phenyl)-2,3-dihydrobenzo[b][1,4]dioxine-2-carboxamide is a ROKII inhibitor reported to have high potency in both biochemical and cell-based assays with $IC_{50}$ in nM range. It was also revealed to be highly selective to ROK against other related kinses (27). In conclusion, a few chemical compounds that can effectively inhibit ROK activity have been identified but inhibitors for MRCK remain yet to be discovered.

### 1.2.5 Aims of research

As mentioned above, a few chemical compounds available in the market can act as ROK inhibitors. These drugs are useful in assisting the studies of cell migration involving ROK pathways. In fact, they can be further tested on clinical trials for therapeutic purposes, such as anti-cancer or anti-inflammatory treatment. In contrast, the inhibitor for MRCK, also as one of the main components mediating cell migration, is not available. It is therefore of our interest to screen and find out the chemical compound(s) that can inhibit MRCK specifically *in vitro* and *in vivo*. The main objective of this study is first to look for MRCK inhibitor and then to characterize the compound biochemically and physiologically.

## Chapter 2 Materials and methods

### Section 1

### 2.1 Protein methodology

#### 2.1.1 Transformation and protein expression in competent cells

DNA plasmid, pQE60 MRCKα CAT, pGEX PAK 404 or pQE30 Cdc42wt which had been prepared in the laboratory from previous work, was used for transformation. The DNA plasmid, with the amount of 5-50 ng, was mixed with 50 µl of *E. coli* competent cells and was incubated on ice for 20 min. The cells were treated with heat-shock for 45 s at 42$^{o}$C and were then chilled on ice for 1-2 min. The heat-shock treated cells were recovered in 100-200 µl Luria-Bertani (LB) broth without ampicillin and were shaken for at least 30 min at 37$^{o}$C. Subsequently, the recombinant competent cells were cultivated overnight in 100-200 ml LB culture containing 50 µg/ml ampicillin at optimized temperature. The strain of *E. coli* competent cells used for protein expression and the different conditions for growing the transformed cells are listed in the table below.

| Fusion protein | *E. coli* strain | Growing temperature | LB culture |
|---|---|---|---|
| 6His-MRCKα CAT | XL-1 blue | 37$^{o}$C | LB with ampicillin |
| GST-PAK 404 | BL 21 codon plus | 30$^{o}$C | LB supplement with 20 mM glucose and ampicillin |
| 6His-Cdc42wt | XL-1 blue | 37$^{o}$C | LB with ampicillin |

**Table 1. *E. coli* strain and conditions for protein expression**

On the next day, the bacterial culture was diluted about 20 folds in LB with ampicillin and grown to achieve $OD_{600}$ of 0.7-0.8. Induction with 0.5 mM IPTG (Invitrogen) for protein expression was done by shaking the cells at room temperature for 3-4 hr. Lastly, the cells were harvested by centrifugation at 5000-7000 rpm for 10-15 min and ready for fusion protein purification. The pelleted cells could be frozen and stored up to a few months before further process.

### 2.1.2 Protein purification and ion-exchange

Hexahistadine(6His)-tagged MRCKα CAT or Cdc42wt was purified in 6His-tag lysis buffer (50 mM Hepes pH 8, 300 mM NaCl, 25 mM Im, and 0.1% Triton X-100) while GST-PAK 404 was purified in GST lysis buffer (50 mM Hepes pH8, 150 mM NaCl, 0.5 mM $MgCl_2$ and 0.1% Triton X-100). The pelleted cells were first resuspended in respective lysis buffer. With the addition of 1 mg/ml Lysozyme, 5 mM DTT (not for 6His-tagged protein), 2 μg/ml peptide inhibitor Leupeptin and 0.5mM protease inhibitors PMSF in lysis buffer, the cells were incubated on ice for 20 min and subjected sonication at 4°C using the Microson ultrasonic cell disruptor. Sonication programme was set as 3 × 20 s sonication with 10 s interval in between. The crude lysate was then spun by ultracentrifugation using Beckman Ti50.2 rotor at 35,000 rpm for 35 min at 4°C. The supernatant was subsequently collected into a new falcon tube and 400 μl of either Nikel beads (Qiagen) or glutathione sepharose beads (Genscript) was added to fish out 6His- or GST-tagged protein. After 2-3 hr rolling at 4°C, the bound protein was collected in a column. The collected beads were washed with 5 × 10 ml of lysis buffer and eluted as shown in the following table.

| Protein | Elution buffer | Elution fraction(s) and volume |
|---|---|---|
| 6His-MRCKα CAT | 6His lysis buffer with 250 mM Im | 1 × 150 μl , 3 × 300 μl |
| GST-PAK 404 | GST lysis buffer with 5 mM glutathione | 4 × 500 μl |
| 6His-Cdc42wt | 6His lysis buffer with 100, 200, 300 and 400 mM Im (stepwise elution) | 4 × 300 μl |

**Table 2. The elution buffers, the elution fraction(s) and volume of purified protein respectively.**

In some cases, thrombin cleavage was performed to remove GST tag. Briefly, glutathione beads were resuspended in 500 μl of GST buffer containing 10U/ml thrombin and incubated at 37°C for 1 hr. Benzamidine beads (Amersham Biosciences) were then added to remove thrombin and rolled at 4°C for about 30 min. The cleaved proteins were eventually collected in the flow through fraction.

Protein concentration of all the eluents was determined by spectrometer measurement

using Bradford assay. Overnight dialysis was required for 6His-tagged protein to remove Imidazole (Im) from the buffer. Lastly, 5% glycerol was added before aliquoting to smaller volume and snap-frozen in liquid nigrogen for storage at -80$^{o}$C.

In order to achieve high protein purity for capillary electrophoresis experiment, protein was further purified in anion-exchange column using SMART$^{TM}$ system (Pharmacia Biotech) or HPLC. As such, pure protein fraction was then ready for aptamers screening.

### 2.1.3 Cdc42 GTP exchange reaction and PAK activation

GTP was used to generate active Ccd42-GTP in solution. GTP exchange reaction of Cdc42 was performed in 2 × exchange buffer (25 mM EDTA, 25 mM DTT, 1 M NaCl and 0.5 M MES-NaOH, pH6.5) with the addition of 2 mM GTP and incubated at 30$^{o}$C for 10 min. The exchange reaction was terminated via addition of 0.05 M $MgCl_2$. Cdc42-GTP was required for PAK activation reaction.

Glutathione bound GST-PAK 404 was resuspended in 300-500 μl lysis buffer after 5 extensive washes. The beads were spun down in cold at 1,000 rpm for 2 min. Extra buffer was removed and the beads were added into kinase buffer (25 mM Hepes, pH 7.3, 25 mM NaCl, 5 mM β-glycerolphosphate, 2.5 mM NaF, 0.025% Triton X -100, 5 mM $MgCl_2$) containing 2 mM ATP and Cdc42-GTP. The molar ratio of Cdc42-GTP: GST-PAK 404= 3:1 was used for PAK activation. The reaction was carried out at 37$^{o}$C for 45-35 min. Glutathione bound active GST-PAK 404 was collected in a column and washed to removed Cdc42-GTP and excess ATP, and was finally eluted with glutathione.

### 2.1.4 Testing kinase activity of MRCKα

Either radioactive method or non-radioactive method of kinase assay was carried out to test the kinase activity of MRCKα. For radioactive method, MRCKα was incubated with 5 μg GST-MLC2 (myosin light chain 2) as substrate and 10 μM ATP with 0.2 μl [γ-$^{32}$P]ATP (3,000 Ci/mmol; NEN) in kinase buffer at 30$^{o}$C for 15-20 min. For non-radioactive method, it was

done similarly without [γ-$^{32}$P]ATP and the phosphorylation of substrate was detected in Western blot using anti-pS19 MLC2 (Cell Signaling Technology) at 1:2000 dilution.

### 2.1.5 Sodium dodecyl sulphate polyacrylamide gel electrophoresis (SDS-PAGE)

Polyacrylamide gels were used for proteins analysis and separation. Bio-Rad Mini-PROTEAN gel casting system was used to cast gels with desired percentage of acrylamide concentration. The recipe of a typical 10% gel is shown as below:

| Ingredients | Resolving gel | Stacking gel |
|---|---|---|
| $H_2O$ | 2.395 ml | 1.05 ml |
| 1.5M Tris-HCl pH8.8 | 2.5 ml | - |
| 0.5M Tris-HCl pH6.8 | - | 0.625 ml |
| 10%SDS | 100 μl | 25 μl |
| 50% glycerol | 1.616 ml | 0.4 ml |
| 30% Acylamide/Bisacrylamide (29:1) | 3.25 ml | 0.4 ml |
| 10% ammonium persulphate (APS) | 62.5 μl | 12.5 μl |
| N,N,N,N,-Tetramethyl-Ethylenediamine (TEMED) | 6.25 μl | 5 μl |

**Table 3. The recipe of a typical 10% polyacylamide gel.**

Protein samples were mixed with 2 × sample buffer (50 mM Tris-HCl pH6.8, 6% SDS, 2% β-mercaptoethanol, 0.1% bromophemol blue and 50% glycerol) and were boiled for 5-7 min prior to loading. Gel electrophoresis was carried out in running buffer containing 25 mM Tris-HCl pH 8.0, 192 mM glycine and 0.1% SDS at a constant voltage of 150-180V for 1-1.5 hr.

### 2.1.6 Coomassie blue staining

For protein analysis with Coomassie Blue staining, gels were soaked in staining solution containing 1% (w/v) Coomassie brilliant blue, 40% (v/v) methanol and 10% (v/v) acetic acid for more than 1 hr or overnight. The gels were subsequently destained in destaining solution (40% methanol and 5% acetic acid in $H_2O$) until the background was fairly clean.

### 2.1.7 Western blot

For protein detection using Western blotting, proteins were first transferred to polyvinylidene difluoride (PVDF) membranes using Bio-Rad semi-dry transfer apparatus. After that, the PVDF membrane was blocked in PBS containing 5% skimmed milk and 0.1% Tween for at least 30 min. The membrane was then washed with PBS containing 0.1% Tween and was probed with specific primary antibody in PBS 0.1% Tween for 2 hr with rolling at room temperature (RT) or overnight at 4$^{o}$C. The membrane was washed extensively to remove unbound primary antibody before probing with horseradish peroxidase (HRP)-conjubated anti-mouse or anti-rabbit IgG (Dako) at RT for 1 hr. The membrane was again washed extensively prior to visualization of protein bands by enhanced chemiluminescence (ECL) reactions and exposed onto X-ray films, which were developed by a Kodak X-ray film processor.

## 2.2 Aptamer selection methodology

### 2.2.1 Single-stranded DNA (ssDNA) and MRCKα incubation

A FAM-tagged ssDNA library consisting of 40-base random sequences flanked by 20-base constant sequences at two sites: 5'-/6-FAM/ AGCAGCACAGAGGTCAGATG (40N) TTCAGCGTAGCACGCATAGG-3', was purchased from Integrated DNA Technology, Inc.
A 100 μM concentration of ssDNA library was dissolved in Tris-EDTA (TE) buffer (10mM Tris, pH7.5, 1mM EDTA) and was kept as stock in cold. Prior to CE selection, 50 μM of ssDNA library, diluted in MRCKα binding buffer (50 mM Tris, pH 8.3, 50 mM NaCl and 5mM $MgCl_2$), was first denatured at 95$^{o}$C for 10 min and then cooled down to 20$^{o}$C at a rate of 0.5$^{o}$C/s. Final concentration of 25 μM ssDNA library was incubated with 500 nM or 10 μM active MRCKα at RT for 15 min.

### 2.2.2 Capillary electrophoresis

Before selection of aptamers for MRCKα, the elution time of ssDNA library and MRCKα migration pattern was tested on a few different running buffers containing Tris-borate, Tris-HCl (Promega), sodium borate (Merck) or sodium phosphate, in which concentration ranged from 20 to 100 mM and pH ranged from 7 to 9. These buffers were used as their buffering capacity and their properties would not be too harsh to MRKC kinase domain (pI value is 5.08). The type of capillary used for CE run was also optimized and a 60 cm long (50 cm to detector) fused-silica capillary purchased from Polymicro Techonologies (Phoenix, USA) with an inner diameter of 50 μm and outer diameter of 360 μm was chosen. The elution time of ssDNA library or MRCKα was detected at wavelength 260 nm or 200/280 nm respectively. The real elution time of ssDNA or MRCKα to the end of capillary was obtained by multiplying the elution time, taken from the electropherogram, with 1.2 ($f$ = $L_{total}/L_{detector}$). The elution time of MRCKα was further confirmed by doing collecting fraction at 1 min interval over 5 min where the peak of MRCKα was detected for 10 times. The collected fractions were run on a 10% polyacrylamide gel and Western blot was done to visualize the intensity of the protein bands. With the optimized running buffer, the aptamers collection window was determined according to the elution time of ssDNA library and MRCKα.

### 2.2.3 Non-SELEX

Non-SELEX was used as the separation method for aptamer selection by using a P/ACE MDQ apparatus (Beckman Coulter, Mississauga, ON, Canada) equipped with Photodiode array detector. Both the inlet and the outlet reservoirs of the capillary were supplied with CE running buffer. The capillary was rinsed with 0.1 M HCl (Fisher Scientific), 0.1 M NaOH (Fluka), deionized $H_2O$ and followed by the CE running buffer for 2 min each between each run. After rinsing, ssDNA aptamers and MRCKα incubation sample were then injected into the capillary by a pressure pulse of 5 psi × 15 s or 5 psi × 10 s. The partition was performed under the following conditions: 20 kV, 333 V/cm, 20$^{o}$C and normal polarity (cathode at outlet

end). Approximately $10^{12}$ sequences were injected into the capillary for the first selection. The MRCKα bound ssDNA fractions were collected in an automated mode by replacing the regular outlet reservoir with a collection vial containing 5 µl of 500nM MRCKα in binding buffer. The collected fractions were subjected to the next round of separation. A few rounds of selection were carried out until an enriched pool of aptamers with reasonably high affinity to MRCKα was obtained. At the end of every run, the capillaries were rinsed as described previously excluding the CE running buffer.

### 2.2.4 Enriched aptamer pools, clusters and single clones binding analysis

The binding affinities of collected fractions amplified by polymerase chain reaction (PCR), of ssDNA aligned clusters and of ssDNA single clones were analyzed by CE-P2 machine equipped with light-induced fluorescence (LIF) detector at Department of Chemistry, NUS. In most cases unless otherwise stated, 100nM of the corresponding ssDNA samples were denatured by heat as done previously and incubated with 1 µM MRCKα for 15 min or overnight. The ssDNA and MRCKα mixture was injected into the capillary at a pressure of 1 psi × 10 s. The dissociation constant ($K_d$) of the corresponding ssDNA samples towards MRCKα was calculated using the formula as shown below. The free ssDNA peak area, ssDNA-MRCKα complex peak areas and the complex dissociating area were integrated from the electropherograms using the software Clarity 5.5.0.

$$K_d = \frac{\{[T]_0(1+A_{DNA}/(A_{DNA\cdot T}+A_{diss}))-[DNA]_0\}}{\{1+(A_{DNA\cdot T}+A_{diss})/A_{DNA}\}}$$

Here $[T]_0$ and $[DNA]_0$ are the total concentrations of the target and DNA respectively. $A_{DNA}$ is the area of the peak of free DNA divided by the migration time of free DNA, $A_{DNA\cdot T}$ is the area of the peak of DNA that dissociated from the complex during NECEEM divided by the migration time of free DNA and $A_{diss}$ is the area of the peak of the intact complex that reached the detector divided by the migration time of the complex.

### 2.3 DNA methodology

#### 2.3.1 Enriched aptamer pools amplification

The collected fractions of aptamers were amplified via PCR. Vent taq polymerase (New England Biolabs; 0.06 U/μl), collected aptamers as templates, a FAM-tagged forward primer (5'/-FAM6/AGC AGC ACA GAG GTC AGA TG; 1.5 μM), a biotinylated reverse primer (5'/biotin/-TTC ACG GTA GCA CGC ATA GC-3'; 1,5 μM), $MgCl_2$ (4 mM) and dNTPs (250 μM each, New England Biolabs, Inc.) were used for PCR amplification. The PCR mixed sample was first denatured at 94$^{o}$C for 5 min. Subsequently, a total of 23 cycles of denaturation (30 s, 94$^{o}$C), annealing (30 s, 53$^{o}$C), and extension (20 s, 72$^{o}$C) were performed and the reaction was terminated after a final extension for 5 min at 72$^{o}$C. The PCR product was analyzed on a 2 % agarose gel containing 0.5 mg/ml ethidium bromide. DNA samples were mixed with 5 × sample buffer (10 mM Tris-HCl (pH 7.6), 0.03 % (w/v) bromophenol blue, 0.03 % (w/v) xylene cyanol, 60 % (v/v) glycerol, and 60 mM EDTA) before loading onto the gels. TAE buffer (0.04 M Tris-acetate, 0.01 M EDTA) was used as the running buffer and a complete DNA agarose gel electrophoresis on a 2% agarose gel was done at a constant voltage of 120 V for 30 min. The DNA bands were visualized with ethidium bromide stained by using UV illumination.

#### 2.3.2 ssDNA aptamers pufication

The amplified double-stranded DNA (dsDNA) product was purified into ssDNA by passing through a streptavidin-agarose (Upstate, USA) column. The streptavidin agarose beads were first packed in a 1 ml blue tip and equilibrated with streptavidin binding buffer (10 mM Tris, pH 7.5, 50 mM NaCl, and 1 mM EDTA). The PCR product was diluted half with the streptavidin binding buffer and passed through the equilibrated streptavidin-agarose column. After the whole sample has passed through the column, it was washed with 1 ml of streptavidin buffer for 5 times. dsDNA with a biotinylated complementary strand would bind streptavidin to the column and remain in the column. Finally, the wanted desired ssDNA

aptamers were eluted with 400 μl of 0.15 M NaOH at 37$^{o}$C. 60 μl of 1 M HCl was added into the eluted fraction to bring the pH down to neutral. Ethanol precipitation was done to concentrate the eluted ssDNA and this formed the enriched pool of ssDNA aptamers.

### 2.3.3 Cloning and sequencing of enriched aptamer pools

After 4 rounds of selection, the enriched pools with improved binding affinity were cloned and sequenced. The enriched pools were re-amplified with primers that contained BamHI and SalI restriction sites added to the 5' end with no FAM or biotin tag. High fidelity PCR using taq DNA polymerase (NEB) was performed to amplify the enriched pool for cloning. The PCR conditions were similar to the PCR conditions described above, except only 12 cycles and a final extension of 10 min at 72$^{o}$C were carried out.

After PCR, the dsDNA product was cleaned up by a miniprep column to separate desired dsDNA product from primers and dNTPs. An aliquot of the dsDNA with restriction enzyme cut sites and 1 μg of pGEX 4T-1 plasmid vector were digested with BamHI and SalI restriction enzymes for 1-2 hr. The digested DNA and vector were then separated by electrophoresis on a 2 % low-melting point (LMP) agarose gel. The electrophoresis procedure was done as described above. The DNA and vector bands were excited out from LMP gel according to their base pair size. The cut DNA fragments were subsequently cloned into the plasmid vector by doing in-gel ligation. The excised DNA fragments and vector bands were washed with $H_2O$ and were melted in 150-200 μl of $H_2O$ respectively at 70$^{o}$C for 5 min. Ligation mixture containing 3 μl of plasmid vector, 12 μl of DNA fragment, T4 ligase in ligation buffer was prepared. In-gel ligation reactions were performed for more than 1 hr or overnight at RT or 16$^{o}$C respectively.

After ligation, the ligase was inactivated by heat at 70$^{o}$C for 5 min. The ligated constructs were transformed into XL-1 Blue *E. coli* bacteria. Colonies were picked as many as possible and were then sequenced by the GST forward primer.

### 2.3.4 Sequences alignment

DNA aptamer sequences that were collected from the sequencing results were aligned together by using clustalW program from the website (http://www.ebi.ac.uk/Tools/clustalw2/index.html). A phylogenetic tree was generated and clusters were determined. DNA sequences in the same clusters were re-aligned to identify consensus regions.

### 2.3.5 Clusters and single clone amplification

Aptamer sequences, which were previously cloned into pGEX 4T-1 plasmid vector, were cut out from the construct with BamHI and SalI restriction enzymes. The enzymatic digested DNA fracgment was purified on a 2% LMP agarose gel. The excised DNA fragment was melted in 200 µl of water and was then used as template in asymmetric PCR reaction. For one reaction of asymmetric PCR mixture, it contained 1 µM of FAM-tagged forward primer (5'/-FAM6/AGC AGC ACA GAG GTC AGA TG; 1.5 µM) with less reverse primer (5'-TTC ACG GTA GCA CGC ATA GC-3'), which was 1 nM, 250 µM of each dNTPs, 0.05 U of Hot Star Taq polymerase, and 10 µl of DNA template in a total volume of 100 µl. Initial denaturation was done at 95$^{o}$C for 15 min, followed by 40 cycles of denaturation at 94$^{o}$C for 30 sec, annealing at 58$^{o}$C for 1 min, and extension at 72$^{o}$C for 30 sec. The PCR reaction was completed with a final extension at 72$^{o}$C for 5 min.

### 2.3.6 Aptamer-MRCKα *in vitro* pull-down assay

Aptamers-MRCKα pull-down assay was done as an alternative method to confirm the binding of the aptamer to MRCKα. Biotinylated ssDNA aptamer (aitbiotech; 0.4 µM), MRCKα-CAT (2 µM), poly-dIdC (0.09-0.08 µg/µl), with total volume of 200 µl, were incubated in MRCKα binding buffer at 4$^{o}$C for 2 hr. Prior to incubation, all ssDNA aptamers were heat denatured first as described above. Streptavidin beads (30 µl /reaction) were pre-blocked in 1 % BSA and equilibrated with MRCKα binding buffer. 30 µl beads were then

packed into a yellow tip and used as a column for aptamer-MRCKα pull-down assay. The incubated mixtures were passed through the streptavidin column 2 times to pull down biotin-tagged aptamers. After that, 5-6 washes with 200 µl binding buffer were carried out to wash away unspecific binding. The aptamer-bound MRCKα was then eluted with 30 µl of 2 X sample buffer by boiling at 100$^{o}$C for 7 min. For analysis, SDS-PAGE using 10 % gel was run and western blot using anti-6Histidines antibody (1:1000; Sigma) was performed to detect the binding of MRCKα to the biotinylated aptamer.

**Section 2**

**2.4 MRCKα inhibitors screening**

The screening was done with the help from ETC (Experimental Therapeutics Center) group by using an automatic robot at Nanos, Biopolis. Chemical compounds were screen in duplicates in a 384-well plate to identify MRCKα kinase inhibitor. Firstly, 2 µl of 20% DMSO, as control, or compound was added into each well. The final concentration of compound used for screening is 1 µM. Purified recombinant 6His-MRCKα CAT (2.72 ng) was added into all wells subsequently. Substrates mixture including 3.15 µg of purified GST-PIM (phosphatase inhibitory motif) and 5 µM of ATP was subsequently added into the mixture of compound/solvent and MRCKα CAT. The total volume of the whole incubation mixture in a well was 20 µl. The *in vitro* kinase reaction was done at RT for 20 min or 1 hr. After 20 min or 1 hr incubation, equal volume (20 µl) of Kinase-Glo Reagent (Promega) was added into each well to stop the kinase reaction. The Kinase-Glo Reagent contains flyer fly luciferase which will convert ATP into light signal. Ten-minute incubation was required before proceeding to luminescent signal measurement with Safire II, Tecan.

**2.5 Protein methodology**

**2.5.1 Preparation and cloning for constructs of MRCKα-CAT and other kinases**

DNA constructs of ROKα-CAT$^{1-543}$, CRIK-CAT$^{1-520}$, DMPK-CAT$^{1-466}$, MLCK-CAT$^{1424-1740}$,

and PKCα-CAT$^{308-673}$ were prepared and cloned into either pQE30 bacterial vector or pxj-6His-biotin mammalian vector. Constructs of MRCKα-CAT$^{1-473}$, PAK full length and PKA full length were already prepared and available for used. Detailed information with respect to the types of cloned vector and cloning sites for each DNA constructs is presented in Table 4.

| Gene | Cloned vector | Cloning sites | |
|---|---|---|---|
| | | Start site | End site |
| ROKα-CAT$^{1-543}$ | pxj-6His-biotin | BamH I | Not I |
| CRIK-CAT$^{1-520}$ | pQE30 | Xho I | Pst I |
| DMPK-CAT$^{1-466}$ | pQE30 | BamH I | Sac I |
| MLCK-CAT$^{1424-1740}$ | pxj-6His-biotin | BamH I | Pst I |
| PKCα-CAT$^{308-673}$ | pxj-6His-biotin | BamH I | Sph I |
| | | | |

**Table 4. Types of cloned vector and cloning sites for constructs of catalytic domain of some kinases in this study.**

### 2.5.2 Protein expression and purification of MRCKα, PIM, MLC2 and other kinases

Hexahistidine-MRCKα CAT, GST-PIM (phosphatase inhibitory motif) MYPT (myosin light chain phosphatase) and GST-MLC2 were purified as mentioned in 2.1.2. Radioactive kinase assay was also done to confirm that GST-PIM and GST-MLC2 can be phosphorylated by 6His-MRCKα CAT.

Kinase catalytic domains of ROKα, CRIK, DMPK, MLCK and PKCα were expressed and purified while GST-PAK 404 was prepared as aforementioned and 6His-PKA was already available in our laboratory. CRIK and DMPK were tagged with 6 Histidines and were expressed and purified from *E. coli* XL-1 Blue. The purification method was same as 6His-MRCKα CAT as mentioned previously. Mammalian constructs of ROKα, MLCK and PKCα were transfected into 60-70% confluent COS7 cell line. The transfected cells were harvested on the next day in lysis buffer (25 mM Hepes, pH7.3, 1.5 mM $MgCl_2$, 0.2 mM EDTA, 5% glycerol, 1 mM sodium orthovanadate, 20 mM β-glycerol phosphate) with 0.5% Triton-X 100, 300 mM NaCl, 25 mM Im and proteases inhibitors cocktail. After homogenization of the harvested cells, the membrane fractions and cell debris were spun down at 4$^{o}$C at 13,000 r.p.m. The supernatant was transferred into a new tube and 30 µl of Nikel beads were added into the

supernatant. Hexahistidine-tagged kinases were pulled down by rolling the tubes in the cold for 2-3 hrs. After that, the beads were spun down in cold at 1,000 r.p.m. Subsequently, the beads were washed 4 times with 500 µl of washing buffer (same as lysis buffer but with 0.25% Triton-X 100) in a column. Low salt washing buffer (50mM NaCl) was used for the last wash. The kinases were eventually eluted in elution buffer (same as lysis buffer but with 50mM NaCl, 300mM Im and 0.25% Triton-X 100). Purified kinases were run on 12-10% of polyacrylamide gels for analysis. Eventually, the activity of the purified kinases was tested by doing radioactive kinase assay as describe in 2.1.5.

### 2.5.3 Studies of substrate specificity for MRCKα-related kinases

Kinase assay was carried out in a total of 30 µl of reaction mixture containing about 40 ng of kinases, 5 µg of substrate (GST-PIM or GST-MLC2) and 10 µM ATP in kinase buffer. ATP supplement with 0.1 µl [$\gamma$-$^{32}$P]ATP was used in kinase reaction containing GST-PIM as substrate. The kinase reaction was done at RT for 20 min. The phosphorylation state of the substrate was analyzed by 12% SDS-PAGE and Western blot using anti-pS19 MLC2 (1:2000) or anti-ppT18/S19 MLC2 (1:2000; Cell Signaling Technology) as primary antibodies in kinase reaction when GST-MLC2 was used as substrate.

## 2.6 MRCKα inhibitors characterization

### 2.6.1 Selectivity studies of inhibitors

The inhibition effects of 5 µM or 10 µM of Chelerythrine chloride (LC lab) was tested on 40 ng of MRCKα, DMPK, CRIK, MLCK, PAK, PKA and 10ng of ROKα . MRCKα and ROKα were also tested with 5 µM of Y-27632 (Calbiochem), 10nM or 50nM of Staurosporine (Sigma), 10 µM of ML-7 (Calbiochem), and 1 µM of H89 (LC lab) for inhibitors selectivity studies. Concurrently, MLCK, PKA and PKCα were incubated with their respective known inhibitors as controls. Kinase assay was carried out by incubating the kinases with the chemical inhibitors for 5 min prior to the addition of 5 µg substrate and 10 µM ATP

supplement with 0.1 µl [γ-$^{32}$P]ATP to initiate the kinase reaction. The effects of the chemical inhibitors were analyzed using 12 % SDS-PAGE.

### 2.6.2 $IC_{50}$ estimation for inhibitors

Chelerythrine chloride and Y-27632 (ROKα inhibitor) were diluted serially from the range of 0.2 µM to 5µM. A higher range, 2.5 µM to 10 µM, was used for chelerythrine chloride selectivity study on ROKα and CRIK. Serial concentrations of the inhibitor were pre-incubated with 40ng MRCKα, 10ng ROKα or 40ng CRIK for 5 min. Kinase assays were carried out at RT for 20 min by adding in 5 µg of GST-PIM or GST-MLC2 as the substrate, 100 µM or 10 µM ATP with 0.1 µl [γ-$^{32}$P]ATP in kinase buffer (as described above). The effect of the inhibitors on the kinase activity was confirmed by 12 % SDS-PAGE and the remaining kinase activities were quantified by the Molecular Dynamics PhosphorImager System (Fuji). In this process, the signal from $^{32}$P was exposed shortly (within 30 mins) to the PhosphoImager and scanned into computer. Short exposure time was performed due to the high level of phosphorylation in this assay. Next, a program, Multi Gauge, was used to quantify the signals by comparing them with the background and the control. Subsequently, a curve was plotted using the values from the program for $IC_{50}$ estimation.

In this study, the radioactive kinase assay was preferred over the conventional filter binding assays due to the high background coming from MRCK autophosphorylation. It is a reasonable assumption that the resolution of $^{32}$P labeled substrate on PAGE gel should allow more accurate quantification of substrate phosphorylation.

### 2.6.3 Drugs treatment in HeLa cells and immunofluorescent staining of cells

Around 60-70% confluent HeLa cells were cultured onto coverslips. On the next day, desired concentrations of the inhibitors (2.5 µM and 5 µM of Chlerythrine chloride, 5 µM Sanguinarine, 5 µM of Y-27632, 10 µM of ML-7, 1 µM H89) were treated onto HeLa cells for 30 mins or 1 hr. After the incubation period, cells were washed with PBS and fixed in 4% paraformaldehyde for 20 min at RT or fixed in cold methanol for 10 min at 4$^{o}$C, following by

washing in PBS and permeabilization with 0.2 % Triton-X100/PBS for 10 min. The physiological effects of the inhibitors were confirmed by doing immunofluorescent staining using self-raised anti-MRCKα mouse (1:50) and anti-pS19 MLC2 (1:75) or anti-ppT18/S19 MLC2 (1:75) antibodies as primary antibodies. The primary antibodies diluted in 0.5% Triton-X 100/PBS were incubated onto the cells overnight at 4$^{o}$C. On the next day, the cells were washed two times with 0.1% Triton-X 100/PBS and were then incubated with Cy3-conjugated anti-mouse (Jackson Immmuno Research Laboratory) and Alexa-488 conjugated anti-rabbit (Molecular Probes) as secondary antiboies and Alexa-647 phalloidin (1:300; Molecular Probes) for 1 hr at RT in the dark. Eventually, two washes were performed and the coverslips were mounted onto glass slides for image capture using a Coolshap HQ (Roper Scientific) adapted to a Zeiss Axioplan wide-field fluorescent microscope.

**2.6.4 Wound healing assay**

U2OS cells were plated onto coverslip at about 90% confluence in Dulbecco's modified Eagle's medium containing 1% FBS. The confluent cells were scratched with a pipette tip and replaced in medium containing either DMSO as control or 2.5 μM Chelerythrine chloride as treatment. The process of cell migration was recorded for 4 hrs after recovery. The distance of cell migration of either control or treatment was calculated using Metamorph program for statistical analysis.

**Chapter 3**

**Screening of Aptamers for Myotonic Dystrophy Kinase-Related Cdc42 Binding Kinase (MRCK) by CE-SELEX**

## 3.1 Introduction

SELEX (Systematic evolution of ligands by exponential enrichment) is a method commonly used in RNA and DNA aptamer selection for specific targets of interest. Hundreds of RNA aptamers specific to small molecule and protein targets have been successfully selected through the use of this method. They include from small molecules like ATP and GTP, to larger molecules, such as thrombin (33, 102). The widespread success in the selection of functional RNAs raised the issue of whether DNA could also give rise to functional sequences. In recent years, single-stranded DNA (ssDNA) aptamers against many different targets have been selected (102). The conventional SELEX methods, such as affinity column method and membrane filtration method, have been used for aptamer selection. This leads to the identification of a nucleic acid aptamer against thrombin using affinity column SELEX method (10).

Many improvements have been made on the conventional SELEX method in recent years. CE-SELEX, a non-conventional SELEX, is one of the methods reported to be able to improve the efficiency of selection by reducing the number of selection cycles and shortening the time to isolate high-affinity aptamers (58, 104). By applying CE-SELEX, aptamers against many targets, such as IgE (60) and neuropeptide Y (59), have been selected. Introduction of non-SELEX selection process further decreases the aptamer selection time as repeated partitioning steps are carried out without amplification (6). In this study, we have applied this method in a screening of aptamers specific for MRCK kinase domain (refer to MRCK in this study) due to the convenience and rapid processing time. Moreover, we also design to select aptamers with the ability in discerning conformational differences between active and inactive MRCK.

Though CE in combination with non-SELEX is a relatively new technique for

aptamer selection, it has some other inherent problems such as the small volume injection of aptamers for partition. Some initial modifications on the original non-SELEX protocol were thus implemented to solve this problem and to increase the efficiency of MRCK aptamer selection.

### 3.2 Non-SELEX conditions for MRCK aptamer selection

Method development of NECEEM-based non-SELEX was performed to determine the optimal conditions for aptamer selection. It is crucial to determine a proper aptamer-collection window for MRCK-aptamer selection as this will affect the selection of aptamers with high affinity to the targets. In order to obtain a wider collection window, parameters that need to be optimized are the choices of buffer, its concentration and pH of CE running buffer. In addition, salt composition of selection buffer, protein concentration and sample injection size are also taken into consideration (7).

The CE running buffer was chosen according to the separation distance of a target from DNA. Tris, phosphate and borate buffers are the three buffers which are normally employed for the purpose of separating biological analytes (12). Suitable pH within the buffering range of the buffer and the buffer concentration need to be considered. A few concentrations of Tris, phosphate and borate buffer with pH 7-9 were tested. Fig. 3.1 shows the migration pattern of MRCK under phosphate buffer pH 7 and borate buffer pH 9.

Prior to CE separation, aptamers and target protein are incubated in selection buffer which contains NaCl and $MgCl_2$. The components of the selection buffer also require optimization. Various concentrations of NaCl in the selection buffer were studied. When phosphate buffer was used as CE running buffer, the optimized selection buffer that gave rise to observable MRCK-aptamer complex peaks was found to be 50 mM Tris, 50 mM NaCl and 5 mM $MgCl_2$ (Fig. 3.2) The bulk affinity of naïve DNA library under these conditions was calculated to be 150 μM. As 500 nM MRCK concentration was used, the protein peak is too low to be detected but complex peaks were still detectable.

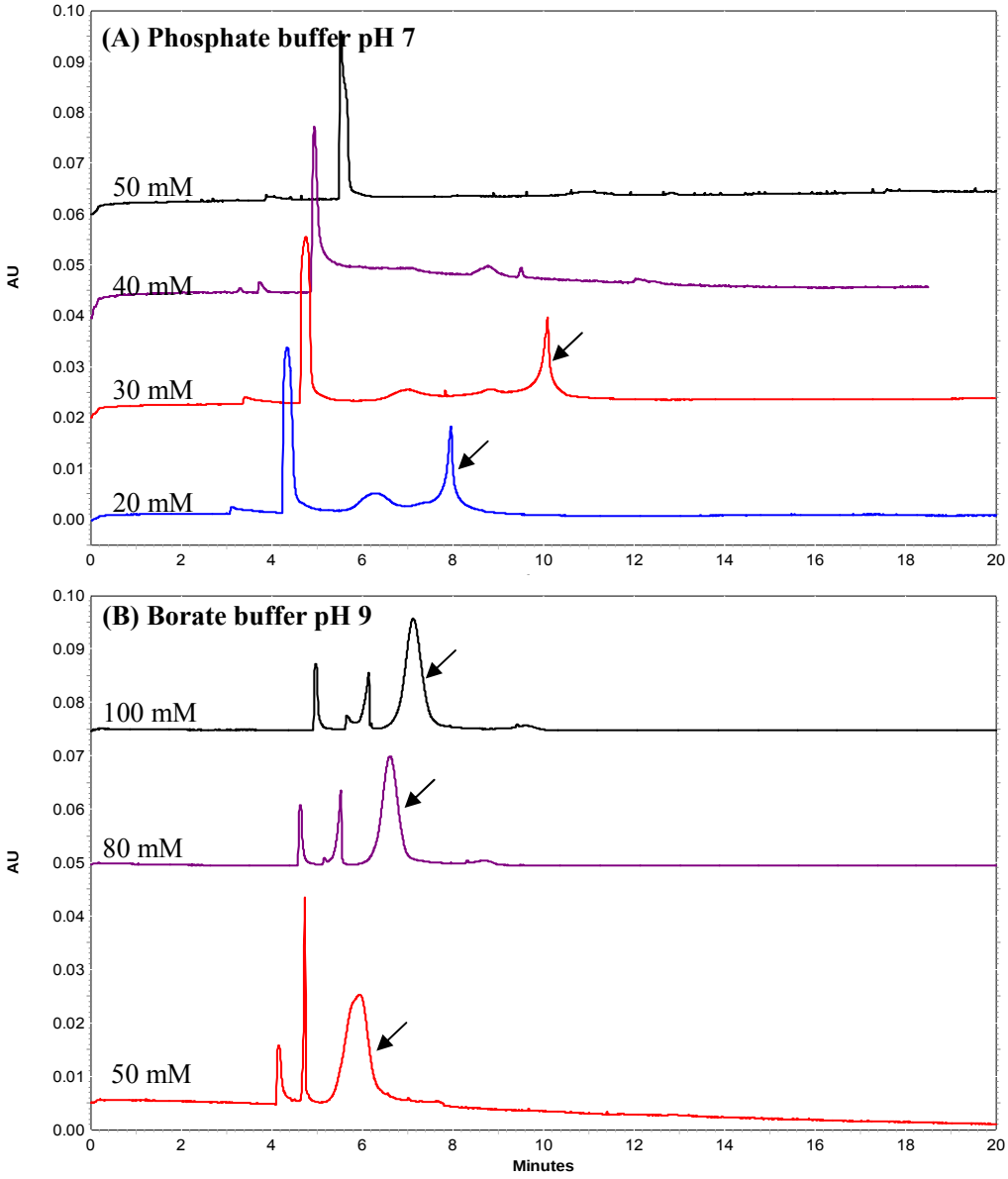


**Fig. 3.1 Optimization of CE running buffer for MRCK aptamer selection.** The migration pattern of MRCK protein peak in (A) Phosphate buffer pH 7 and (B) borate buffer pH 9 at different buffer concentrations. The migration pattern of MRCK protein peak was affected by the buffer types, concentration and pH of the CE running buffer. Black arrows indicate the protein peak of MRCK under each condition.

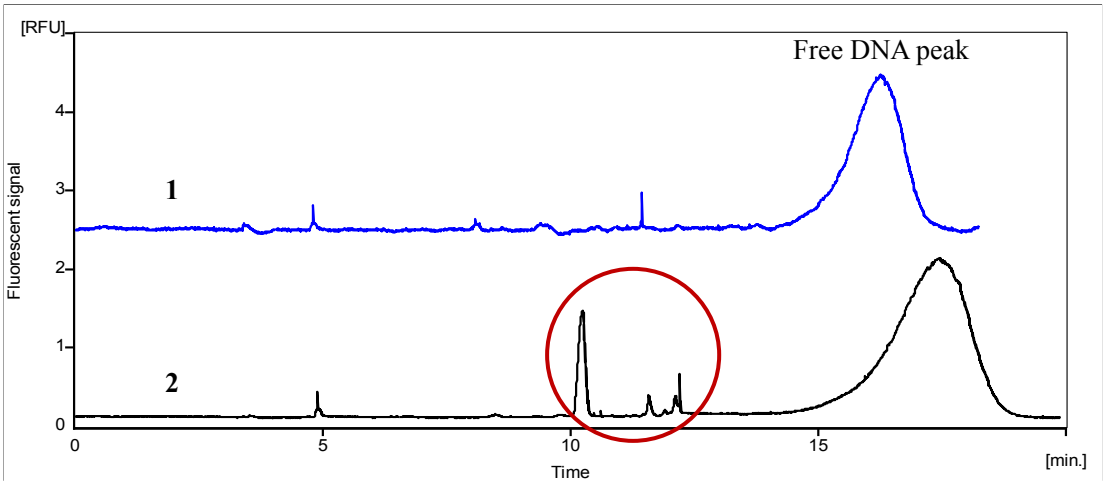


**Fig. 3.2 Electropherograms of DNA library and MRCK.** (1) 100 nM FAM-tagged naïve DNA library and (2) 17.5 µM MRCK incubated with 100 nM FAM-tagged naïve DNA library. 50 mM phosphate buffer pH 7 was used as CE running buffer. Red circle indicates the complex peaks.

One of the advantages of using CE is that it requires only a small amount of analytes and the sample injection size is in the scale of nanolitres. However, this small injection volume disallowed injection of a large number of DNA library sequences in one single round of selection. One solution is to use a highly concentrated library to increase the number of DNA molecules per injection. However, high DNA concentrations gave rise to broad peaks that worsens the separation between free and target-bound DNA, leading to poor partitioning efficiency. A library with a concentration of 25 µM of DNA with an injection pressure of 5 psi for 15 seconds was used as a compromise between injection size and resolution. This loading size contained a total of 2 x $10^{12}$ sequences that were screened for binding with MRCK upon the first round of non-SELEX.

### 3.3 Original non-SELEX approach as an initial screening of MRCK aptamers

In an initial screening of MRCK aptamers, an original non-SELEX approach as described by Berezovski M *et al.* (6) was applied. Phosphate buffer with pH 7 was used in this CE protocol. DNA library at 25 μM concentration was incubated with 500 nM of MRCK prior to injection. Fig. 3.3 shows the enriched aptamer pools obtained up to three rounds of positive selection against MRCK. As more than one complex peak was observed, it suggests that MRCK may interact with DNA with several stoichiometries. In order to calculate the dissociation constant ($K_d$) of enriched aptamer pool, peak areas of all complexes were integrated and the $K_d$ values were calculated using the formula in Section 2.2.4. Table 4 summarized the $K_d$ values of these three enriched aptamer pools. The bulk affinity of the best enriched aptamer pool obtained was approximately 450 nM after two rounds of positive selection. The second and third enriched aptamer pools have almost the same $K_d$. As a result, no significant improvement of $K_d$ was observed from the third round of selection.

| **Enriched aptamer pool** | **$K_d$ / nM** |
|---|---|
| First | 7557 |
| Second | 449 |
| Third | 485 |

**Table 4. Dissociation constant ($K_d$) of the first to third enriched aptamer pool from original non-SELEX method.**

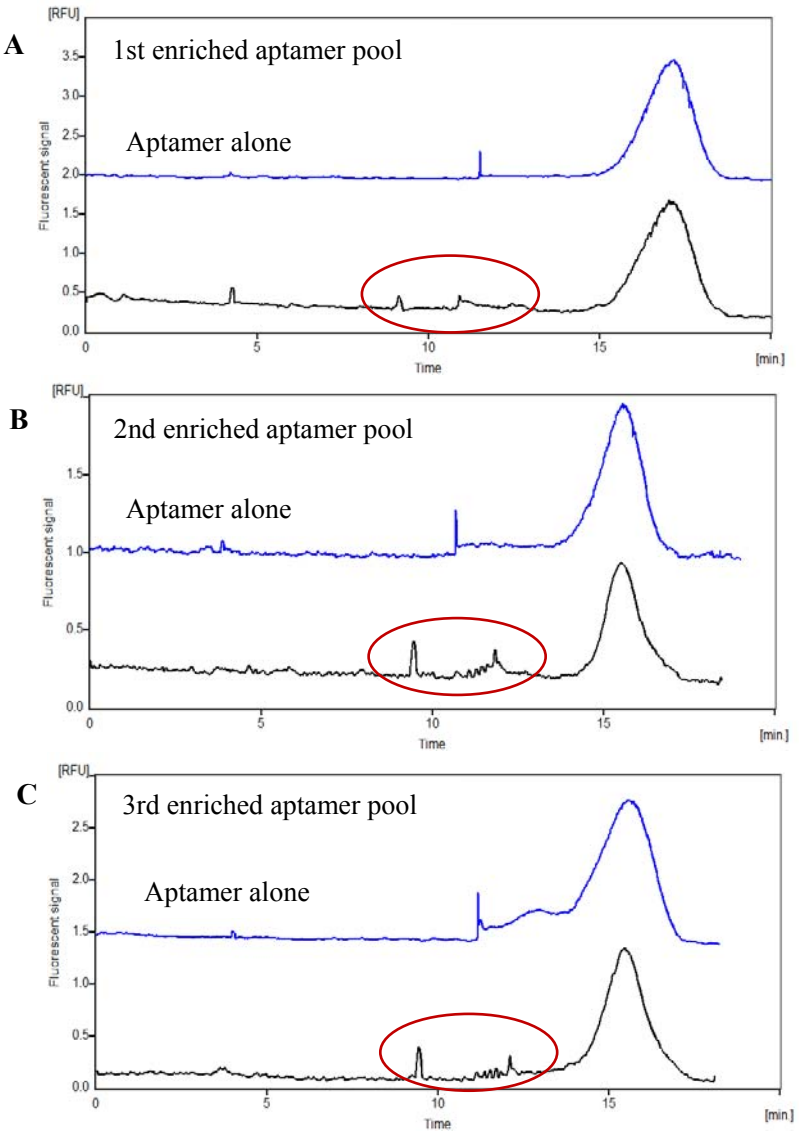


**Fig. 3.3 Electropherograms of enriched aptamer pools from the original non-SELEX method.** 1 μM of MRCK was incubated with 100 nM of first (A), second (B), and third (C) enriched aptamer pools. Aptamers alone without MRCK were run as controls. Other peaks, circled in red, which migrated before the free DNA peak were observed to be complex peaks.

### 3.4 Modified non-SELEX approach for improvement in MRCK aptamer selection

#### 3.4.1 Confirmation of MRCK and aptamers retention time

In order to improve the quality of aptamer selection for MRCK, some modifications were made on the original non-SELEX protocol. Before applying the new approach of non-SELEX method, the retention time of MRCK and DNA aptamers in the capillary was checked and confirmed respectively. According to Fig 3.4A, MRCK protein peak was confirmed by UV detection at wavelengths of 200 nm, 260 nm and 280 nm. When 100 mM borate buffer was used as CE running buffer, the migration time of MRCK was predicted to be around 8 minutes. By running different concentrations of MRCK, the detection limit of CE at wavelength of 200 nm was found to be 10 μM of MRCK as showed in Fig 3.4B. Apparently, 10 μM of MRCK was still able to be detected but not 1 μM MRCK. To further confirm the observed peak belongs to MRCK, a mixture of MRCK and aptamers were injected into CE and five fractions were collected at every 1 minute interval from 7 to 12 minutes. The five collected fractions were analyzed by western blotting (Fig 3.5). The retention time of MRCK was confirmed at the regions from 8-9 minutes. As mentioned previously, DNA aptamers are more negatively charged than MRCK and thus migrate later than the protein. The retention time of DNA aptamer was found to be at approximately 11-12 minutes as shown in the electropherogram in Fig 3.4C.

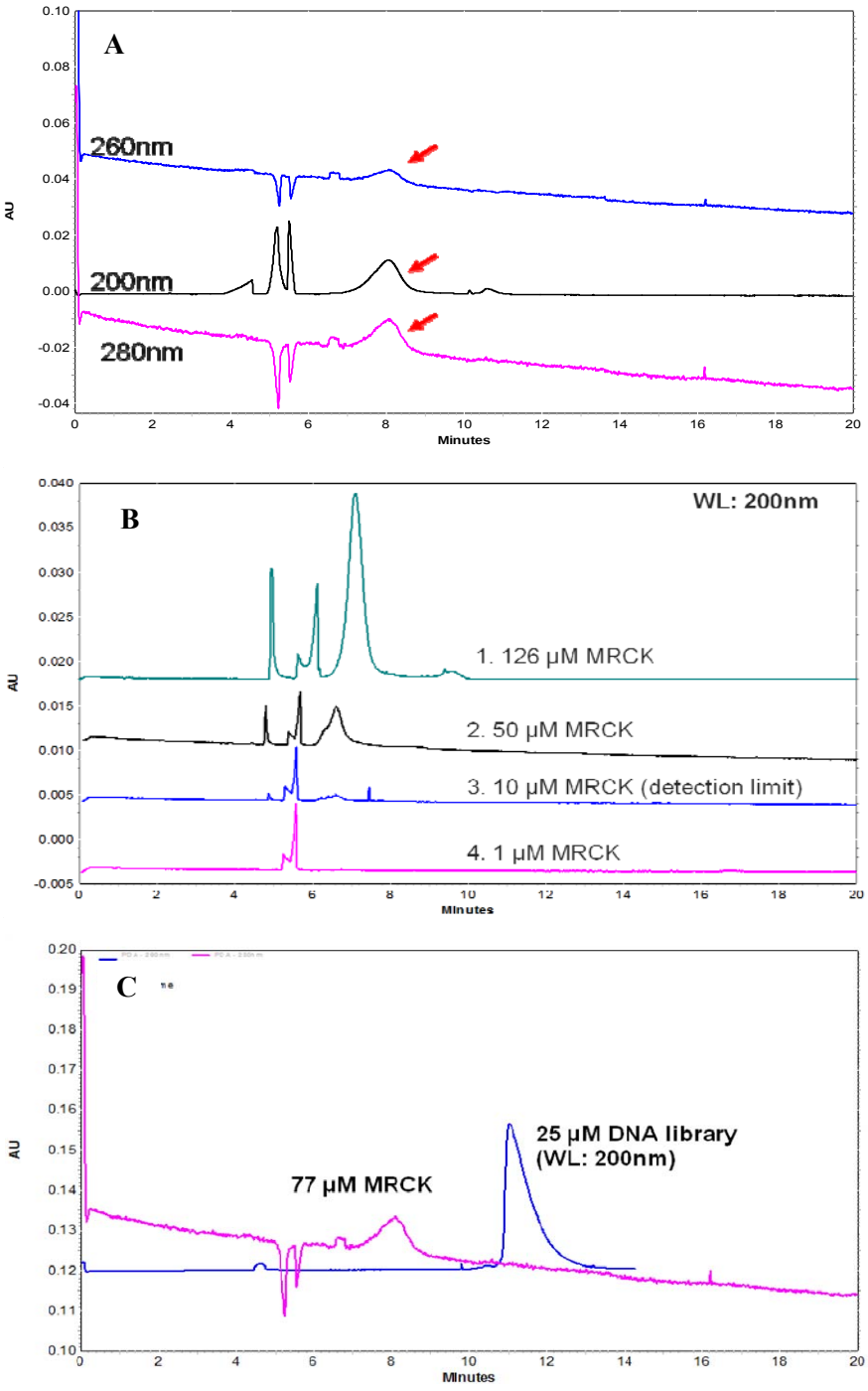


**Fig. 3.4 Electropherograms for MRCK protein peak and DNA aptamer peak detection.** (A) MRCK peak can be detected by UV at wavelengths of 200 nm, 260 nm and 280 nm. Red arrows point to the protein peak of MRCK. (B) Serials concentrations (126 µM, 50 µM, 10 µM and 1 µM) of MRCK were run on CE to check the detection limit of the UV detector. The detection limit was found to be 10 µM of MRCK. (C) The electrophoretic migration profiles of the target protein, MRCK, at a concentration of 77 µM MRCK and DNA library at a concentration of 25 µM were aligned side by side. All the runs were performed in CE running buffer using borate buffer at pH 9.

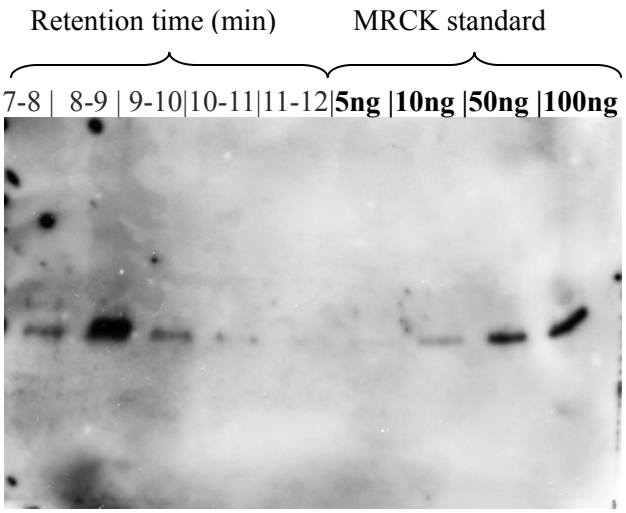


**Fig. 3.5 Confirmation of MRCK migration time using western blot.** Five fractions were collected at every 1minute interval from 7-12 minutes. The collected fractions were run on a protein gel and subjected to western blot (IB) using anti-6 histidines antibody. MRCK standard with the amount of 5 ng, 10 ng, 50 ng and 100 ng was as control and for the estimation of protein amount. Sensitive enhanced chemiluminescence (ECL) used in the blot here gave rise to the high background.

### 3.4.2 MRCK aptamer selection using modified non-SELEX approach

The main problem of the non-SELEX approach is that the number of DNA aptamer molecules which can be injected into the capillary for partition is rather restricted due to the small injection volume. In order to solve this problem, an incubation of 25 μM of DNA with 10 μM of MRCK and 0.09-0.08 μg/μl of poly-dIdC was injected 10 times into the capillary. Meanwhile, 10 collections on the aptamer-collection window were also carried out. The collection window in the first round of selection was determined to be around the MRCK protein peak, which was 7.5-10.5 min as shown in Fig. 3.6. In brief, these collected fractions were ethanol precipitated in the presence of poly-dIdC and resuspended in the desired volume for the next round of selection. In the subsequent rounds of selection, the selection processes were performed using 500 nM of MRCK as target concentration to reduce the unspecific and weakly bound aptamers. Simultaneously, the collection window was changed to 6.5-10.5 min to avoid missing out of specific binders for MRCK. Ten collections were performed in each round of selection and a total of three positive selections against MRCK were implemented. These ten collections from each round of selection eventually formed the first to third

enriched aptamer pools.

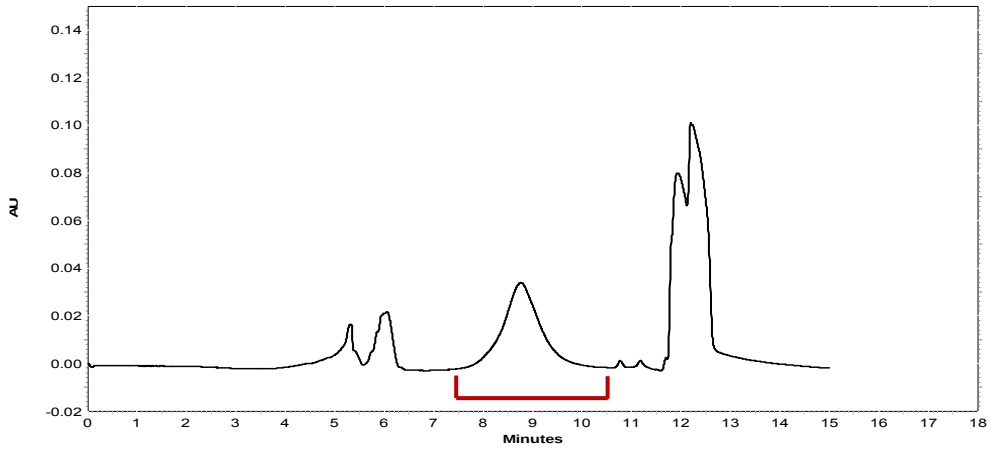


**Fig. 3.6 Electrophoretic migration profile of MRCK together with DNA library and poly-dIdC.** In the modified non-SELEX method, 10 µM of MRCK was incubated with 25 µM of DNA library and poly-dIdC. The mixture was injected into capillary for separation after 15 minutes of incubation. Aptamer collection window, as indicated, which is marked, was determined at the region from 7.5 to 10.5 minutes.

Similar to the original non-SELEX protocol, three rounds of selection were also performed in this modified non-SELEX method. Fig 3.7 shows the electropherograms of the binding analysis of these three enriched aptamer pools. The amplified enriched aptamer pools were either incubated with MRCK for 15 minutes or overnight. In the first enriched aptamer pool, 15 minutes incubation gave no obvious complex peak and only one complex peak was detected in the overnight incubation. One complex peak migrated just before the free DNA peak was observed in the second enriched pool and many more complex peaks were found in the third enriched pool. The $K_d$ values of each enriched aptamer pool for MRCK were calculated and summarized in Table 5.

| **Enriched aptamer pool** | **$K_d$ / µM** |
|---|---|
| First | 8 |
| Second | 1.6 |
| Third | 1.04 |

**Table 5. Dissociation constant ($K_d$) of the first to third enriched aptamer pools from modified non-SELEX method.**

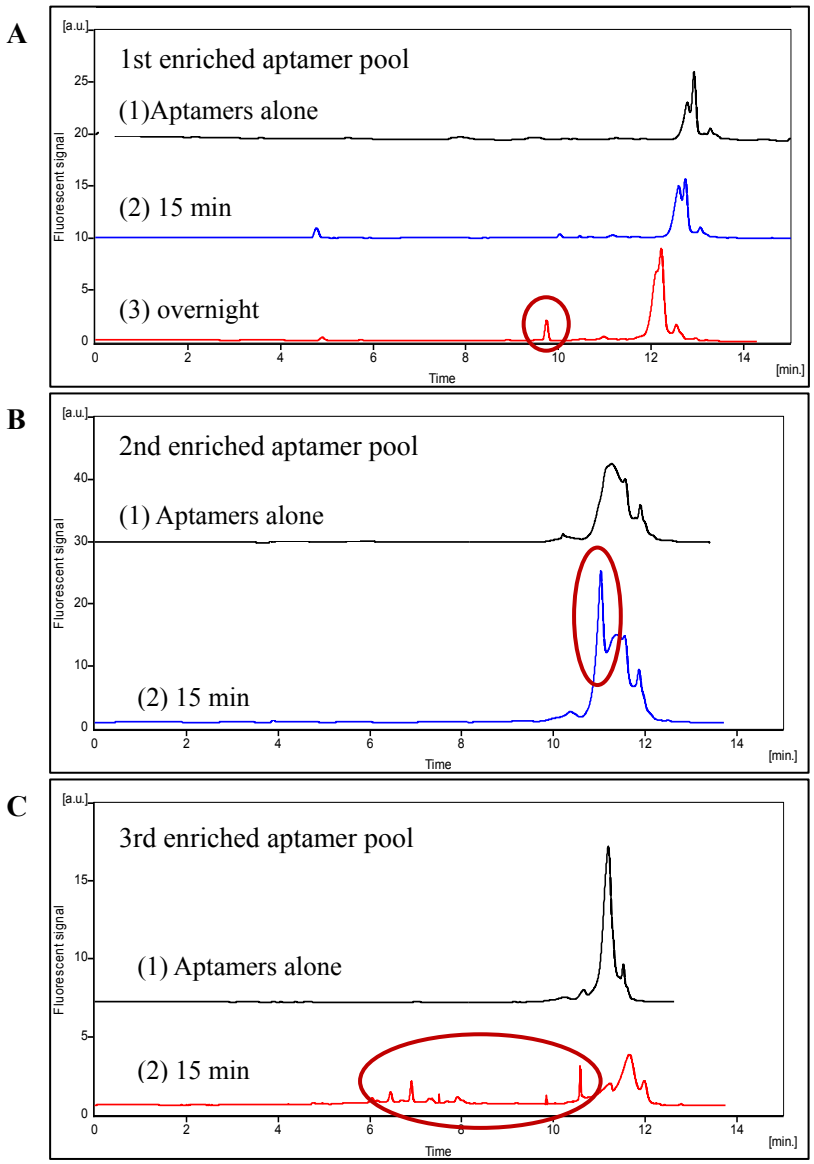


**Fig. 3.7 Electropherograms of enriched aptamer pools from the novel non-SELEX method.** 1 µM of MRCK was incubated with 100 nM of first (A), second (B), and third (C) enriched aptamer pools. Aptamers alone without MRCK were run as controls. Other peaks, circled in red, which migrated before the free DNA peak are observed to be complex peaks.

### 3.5 Comparison of the original and modified approach non-SELEX protocol

Two non-SELEX approaches were performed and the enriched aptamer pools from each approach were compared in terms of their binding affinities towards MRCK using CE and an *in vitro* MRCK pull-down assay.

#### 3.5.1 Original non-SELEX

In the original approach, the second enriched aptamer pool was cloned and sequenced for further analysis. A total of 46 clones from the aptamer pool were cloned and sequenced to obtain the individual DNA sequences. Sequence alignment was done using ClustalW2 software to generate a phylogenetic tree. The length of the branches in the phylogenetic tree implies the similarity in sequences between two aptamers. The shorter the branches length between two aptamers, the more similarity of sequences is in these aptamers. According to the phylogenetic tree, a few aptamers that branched closely were aligned together to obtain their consensus sequences. Among the aligned sequences, aptamers that are most similar to their consensus sequences were selected as representatives for binding analysis and $K_d$ calculation. Out of all the analyzed aptamers, five aptamers (named M6, M16, M31, M40 and M43) have $K_d$ values in the nanomolar range, indicating their high affinity towards MRCK. In contrast, they showed no cross-reactivity to inactive MRCK and thrombin, which was used as a negative control. This indicates that these aptamers are able to discern the conformational difference between active and inactive MRCK. The aptamer M6 was the best binder among these five aptamers. Fig. 3.8 shows the electropherograms of the binding profile of M6 to MRCK, inactive MRCK and thrombin. Thus, aptamer M6 was used in the further analysis.

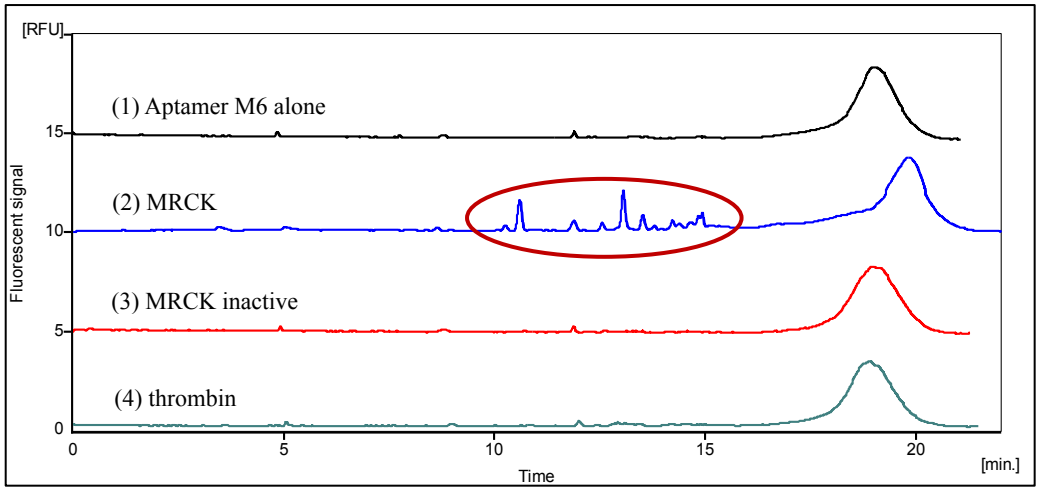


**Fig. 3.8 Binding analysis of M6.** 100 nM of M6 was incubated with either 1 µM MRCK or 1 µM of inactive MRCK or 1 µM of thrombin. Aptamer M6 alone was run as control. Complex peaks, circled in red, were only observed when M6 aptamer was incubated with MRCK, indicating the specific binding of M6 to MRCK.

### 3.5.2 Modified non-SELEX

Second and third enriched aptamer pools obtained from the modified non-SELEX method showed $K_d$ values of about 1 µM. These two enriched aptamer pools were therefore cloned and sequenced for subsequent analysis. A total of 86 sequences were cloned and sequenced from these two enriched aptamer pools. All the sequences obtained were again aligned using the ClustalW2 programme. The phylogenetic tree generated from the multiple sequences alignment was shown in Fig. 3.9. In order to make sure that all the cloned aptamers were included in our analysis, 19 clusters were drawn from the phylogenetic tree as what is shown in Fig. 3.9. Every cluster contains aptamers with close similarity in DNA sequences. These 19 clusters were amplified and purified to form smaller pools of aptamers. Binding analysis using CE was subsequently performed on these 19 clusters. Out of these 19 clusters, four clusters (CL 2, CL 3, CL 6 and CL 18) gave positive results. A total of 22 aptamers were included in these four clusters and their individual binding affinities towards MRCK were tested. Among the 22 sequences, 9 of them have a total shift in aptamer peak when they were incubated with MRCK. In comparison to the free DNA peak of the control (DNA aptamers

alone without MRCK), a complete shift was observed. One aptamer F3.11 has the lowest $K_d$ (109 nM) among the 9 aptamers The migration profile of F3.11 alone and F3.11 in the presence of MRCK is shown in Fig. 3.10. F3.11 together with M6 was eventually used in a comparison study between the conventional and the modified non-SELEX methods.

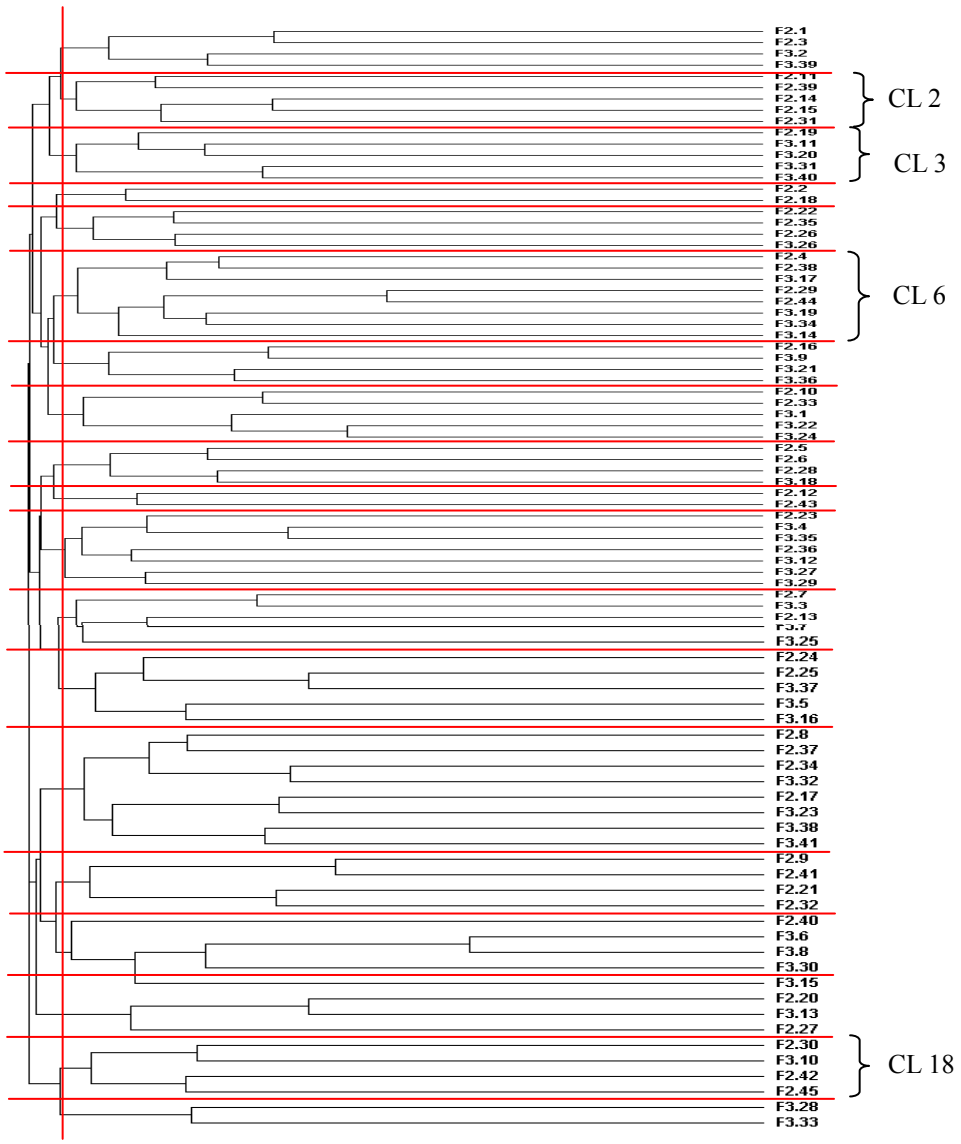


**Fig. 3.9 Phylogenetic tree of aptamers from second and third enriched aptamer pools from novel non-SELEX.** Clusters CL2, CL3, CL6 and CL18 are the clusters that gave positive results in binding analysis.

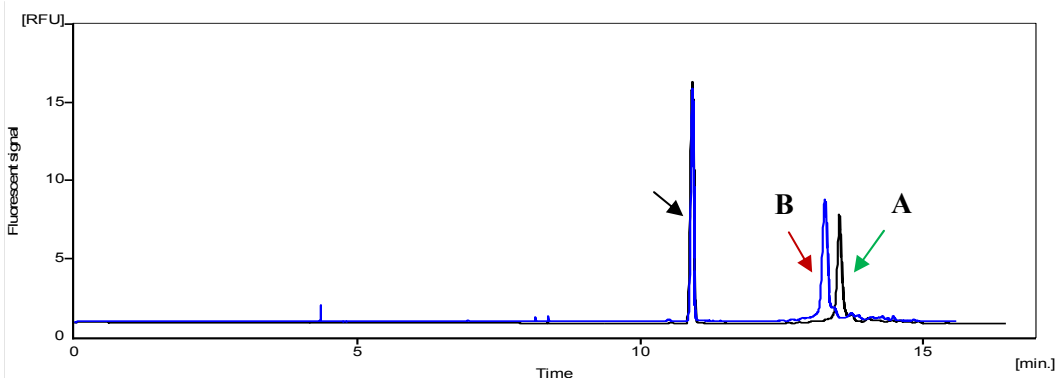


**Fig. 3.10 Electropherograms of aptamer F3.11 alone and F3.11 together with MRCK.** (A) Aptamer F3.11 alone was run on CE as a control. The free DNA aptamer peak of F3.11 is indicated by green arrow. (B) 100 nM of aptamer F3.11 was incubated with 1 µM MRCK for 15 minutes before subjected for separation using CE. The whole aptamer peak, as indicated by red arrow, was shifted when MRCK bound to F3.11. The black arrow points at the peak of FITC which was used as internal standard to check for shift in aptamer peak.

### 3.6 Affinity binding of aptamers M6 and F3.11 to MRCK was confirmed by an *in vitro* MRCK pull-down assay

Two aptamers, namely M6 and F3.11 were found to have binding affinities to MRCK from a ssDNA library by using an original and a modified non-SELEX method respectively. The DNA sequences and the $K_d$ for MRCK of M6 and F3.11 were summarized in Table 6. By using an alternative method to CE, binding affinities of these two aptamers were confirmed in an *in vitro* MRCK pull-down assay. In this *in vitro* MRCK pull-down assay, an incubation containing biotinylated aptamer, MRCK and poly-dIdC was prepared and biotinylated aptamer was pulled down in cold using a streptavidin column. The binding of the aptamer to MRCK, was scored by the presence of MRCK in the pull-down of biotinylated aptamer. Fig. 3.11 shows the results of this *in vitro* MRCK pull-down assay for M6 and F3.11. For M6 (Lane 2) and F3.11 (Lane 5), higher amounts of MRCK were detected in the eluents from streptavidin column. This is in contrast to the low amount of MRCK which was detected in the eluents from the streptavadin columns of negative control (Lane 1 and Lane 4), where no aptamer was present, or with scrambled DNA aptamer (Lane 3 and Lane 6). We therefore conclude that both M6 and F3.11 are able to pull-down MRCK in this *in vitro* system, indicating that they can serve as molecular probe for MRCK detection.

| Clone # | Aptamer sequence | $K_d$ / nM |
|---|---|---|
| **M6** | AATGATAAACCACTGGTGAATCGCTCAAGTCAGTAGTAGG | 125 |
| **F3.11** | CGAGCTGATGCGTGTCACCTCGTAGGACAGTCATCGAGGC | 109 |

**Table 6. DNA sequences and $K_d$ for MRCK aptamers M6 and F3.11.**

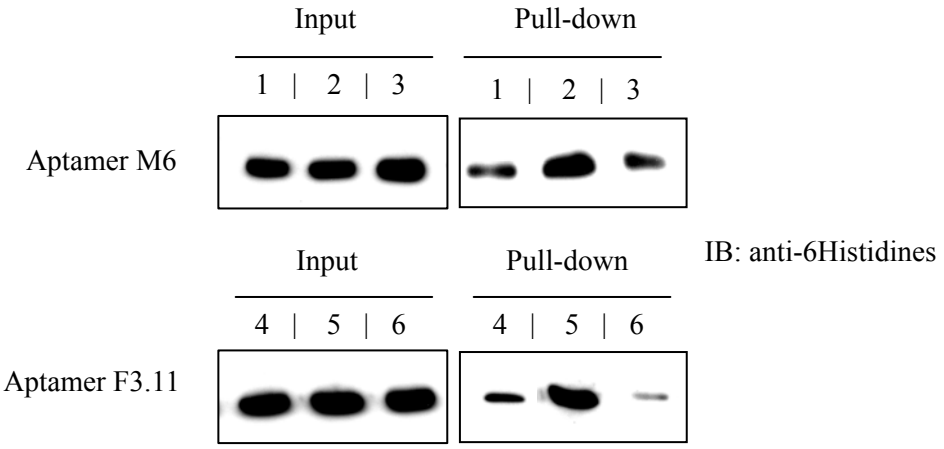


**Fig. 3.11 Confirmation of the binding abilities of aptamers M6 and F3.11 to MRCK using an *in vitro* MRCK pull-down assay.** Biotinylated ssDNA aptamer at a concentration of 0.4 μM was incubated with 2 μM MRCK and poly-dIdC (0.09-0.08 μg/μl) in the cold for 2 hours. A streptavidin column was used to pull-down the biotinylated aptamer. Aptamer which has affinity to MRCK will be able to pull-down MRCK as well. The presence of MRCK in the pull-down was analyzed by western blotting (IB) with anti-6Histidines antibody. Input indicates the initial amount of MRCK in the incubation. Pull-down implies the amount of MRCK in the eluent that was released from the streptavidin column. Low amount of MRCK (background signal) was present in the pull-downs of control (lane 1 and lane 4), without aptamer, and aptamer with scramble sequences (lane 3 and lane 6). Aptamer M6 (lane 2) and F3.11 (lane 5) were able to pull-down higher amount of MRCK.

### 3.7 Discussion

The utilization of CE technology in SELEX for aptamer selection is a new attempt. Although certain areas of this approach are still required to be improved, the rapid selection process by CE-SELEX does offer a great advantage over the conventional method, making it a suitable technology for high-throughput screening. In this project, a screen for MRCK-specific aptamers has been described as collaboration between our group and the Department of Chemistry in NUS.

The selection of MRCK aptamers was first investigated with the optimization of the choices of buffer, its concentration and optimal pH for CE running. The CE running buffer composition is one of the major conditions that affect the detection of protein and aptamer-protein complexes. It controls the ionization state of the protein and aptamer, and prevents adsorption of protein and DNA onto the capillary. The components of the buffer must be compatible with the formation and stabilization of the complexes (12) without affecting their specific association. Following this was the optimization of the selection buffer. Optimal NaCl concentration in the selection buffer is vital to prevent unspecific ionic interaction between the aptamers and targets, and to increase the stringency of the selection (7). Besides, magnesium is required to stabilize the aptamer secondary structure (2) and to promote the formation of complexes during migration. Buffer systems of extreme pH were avoided to prevent denaturation of aptamer and protein, or alteration of the functional groups crucial for interaction (12).

CE-SELEX includes two types of partitioning proceses: nonequilibrium capillary electrophoresis of equilibrium mixtures (NECEEM) and equilibrium capillary electrophoresis of equilibrium mixtures (ECEEM). NECEEM-based non-SELEX was applied in an initial screening for MRCK aptamers. Non-SELEX omits the step of amplification and renders it to be more efficient. Owing to its fast and rapid process, non-SELEX was performed here. Simultaneously, some modifications were introduced into the original non-SELEX for the purpose to improve the quality of the screening process.

Before performing non-SELEX, concentration of the target protein needed to be

considered. The concentration of target protein used in the original non-SELEX was actually adapted from the protocol published by Berezovski M.V. *et al.* (7). For the modified non-SELEX, serial concentrations of protein, from low to high (1 μM to 126 μM in Fig. 3.4B), were run on CE for target protein determination prior to MRCK aptamers screening.

In the screening of these two methods, the $K_d$ values of both the second and the third enriched aptamer pools were found to be quite similar (Table 4 and Table 5). This suggests that further selection did not actually improve the quality of selection. It is likely that having more rounds of selection in CE-SELEX may not actually mean one will collect aptamers with lower "bulk" $K_d$. In fact, a recent report has suggested that the $K_d$ measurements of the 2nd enriched pool and the 3rd enriched pool were higher than the 1st enriched pool (64). There are a few reasons which may give rise to this observation. After the 2nd round of selection, almost all the aptamers in the pool possessed affinity to the target. When 3rd round of selection was performed, no significant improvement of binding could be observed due to the same sequences of aptamers, which were already present in the 2nd enriched pool, were selected. Moreover, contamination of the target protein or experimental error could also be possible in contributing to the lack of improvement in further rounds of selection.

From the results of the original non-SELEX, aptamer (M6) with the lowest $K_d$ of 125 nM was selected. This aptamer was able to recognize conformation of active MRCK and not inactive MRCK. In an attempt to select aptamer with higher affinity to MRCK, the original non-SELEX protocol was revised and we realized that only part of the incubated DNA aptamers and targets was injected into CE for partition. The ssDNA library which was used here has 40 random bases and thus contains $10^{24}$ ($40^4$) different sequences. An injection of 150 nL of 25 μM DNA library in the first round of selection contained only $10^{12}$ molecules of the DNA aptamer and many other sequences were missed out. Therefore, some adjustments were made to increase the loading size of CE. By performing ten injections and ten collections, we hope to increase the number of DNA molecules that would be subjected for partition. In this modified non-SELEX approach, however, the lowest $K_d$ of aptamer (F3.11)

which was obtained is 109 nM. In fact, no significant improvement in MRCK binding affinity could be concluded from the modified approach. Although the $K_d$ value of M6 (from the original non-SELEX) is comparable to the $K_d$ value of F3.11 (from the modified non-SELEX), the MRCK binding profiles of these two aptamers were different. Many complex peaks were observed for M6-MRCK complex while a total shift in aptamer peak was observed for F3.11. These observations suggest that M6 might interact with MRCK at different sites and thus results in M6-MRCK complexes with different charge-to-mass ratio. Difference in charge-to-mass ratio consequently affects the retention time of the complexes. In contrast, aptamer F3.11 might bind to MRCK at a more consistent manner and caused a complete shift in aptamer peak.

As mentioned previously, the interaction of M6 and F3.11 to MRCK was also further confirmed by *in vitro* MRCK pull-down assay. Aptamer M6 and F3.11 could precipitate equal amount of MRCK in the pull-down suggesting M6 and F3.11 have similar affinity to MRCK which is consistent with their calculated $K_d$ values.

The main focus of the first part of this project, that is MRCK aptamers screening, was actually more for the purposes in developing CE-SELEX method and to validate the feasibility of using DNA aptamers as molecular probes for protein recognition. The two selected aptamers, M6 and F3.11, were subsequently sent to our collaborator at the Department of Chemistry, NUS, for the design of molecular aptamer beacon (MAB, described in Section 1.1.2). In addition to *in vitro* studies, we have also tried to microinject into HeLa cells for MRCK interference and cytoskeletal organization studies. The preliminary data showed that M6 did not exhibit strong binding to endogenous MRCK when introduced into HeLa cells as majority of the aptamer was detected in the cell nucleus (data not shown). From these preliminary studies, there are three main reasons which hindered us from carrying out further investigation. First, the aptamers fluoresce by themselves even without binding to the targets and this is thus unsure as whether they bind to the real targets. Second, ssDNA aptamer have high affinity to nuclear DNA and RNA (61, 82). They tend to migrate into cell nucleus which would attenuate the amount of aptamers available for targets detection in the

cytosol. Third, the binding affinity of aptamer M6, with $K_d$ value of 125 nM, may not be high enough and thus may affect the detection limit in cell staining. All these have thus precluded more functional studies on M6 aptamer, including the study on MRKC inhibitory effects.

In our initial proposal, we also planned to look for aptamers that can inhibit MRCK activity. Owing to the tendency of aptamer's association with the cellular RNA and DNA which may reduce its efficacy, inhibition of MRCK with the use of chemical compounds was also concurrently pursued. The findings are described in the next chapter.

## Chapter 4

## Screening of Selective Inhibitors for Myotonic Dystrophy Kinase-Related Cdc42 Binding Kinase (MRCK) by Chemical Inhibition

### 4.1 Introduction

MRCK was discovered to be the key regulator of myosin activity underlying cell protrusion and neurite outgrowth (16, 51) and together with ROK and MLCK (36) they regulate *in vivo* phosphorylation of myosin light chain (MLC) and the phosphatase inhibitory motif (PIM) of myosin phosphatase. Besides, MRCK is also engaged in the lamellar retrograde flow that may direct nuclear movement in migrating cells (31). It was found that MRCK exists as a tripartite complex containing LRAP35a, a Leucine repeat adaptor protein, and MYO18A. This MRCK-LRAP35a-MYO18A complex plays a major role in the assembly of the lamellar actomyosin flow bundles that are important for persistent membrane protrusion (88). Various means of inhibiting MRCK have been used, including introduction of siRNA and dominant negative constructs into the cells. However, the most effective and rapid way of inhibition would be the use of a chemical compound that can cause immediate inhibition on MRCK kinase activity.

High-throughput screening for specific inhibitors for various kinases have been widely carried out and found to be successful. For example, JX401 was identified as a mitogen-activated protein kinase p38alpha via a high-throughput screen using yeast cells(28). In this project, an *in vitro* screening method using Kinase-Glo Luminescent kinase assay was applied to facilitate the screening process of MRCK inhibitors. In brief, MRCK kinase reaction was performed in the presence of a compound and the remaining ATP in the solution after the kinase reaction was detected by the addition of a Kinase-Glo Luminescent Reagent which converts ATP to luminescent signal (Fig. 4.1A). Therefore, the release of luminescent signal is inversely related to kinase activity.

**4.2 MRCK enzymatic kinetic studies**

Before the actual screening process, some enzymatic kinetic studies on MRCK were done in order to obtain an optimal condition to carry out MRCK kinase reaction for inhibitors screening. Fig. 4.1B shows the sigmoidal kinetic curve of MRCK kinase activity. As reported previously, there is a relationship between MRCK N-terminus-dependent kinase domain dimerization and kinase activity (87). Dimerization of MRCK N-terminus and trans-autophosphorylation of key residues within the activation loop and the extended hydrophobic phosphorylation motif are required for MRCK activation. As shown in Fig. 4.1B, MRCK is not enzymatically active at low concentrations (<0.01 μM). A critical concentration of MRCK is required to achieve dimerization and activation of MRCK. Upon dimerization, MRCK activity resembles a normal progress curve for a first order enzymatic reaction, i.e. the production rate is approximately linear at the initial stage for a short period and the rate gradually slows down as the reaction proceeds when the substrate is consumed. Furthermore, according to the time course study of a serial concentration of MRCK as shown in Fig. 4.1C, the kinetic curve of 0.05 μM of MRCK is linear within the first 30 minutes. As a result, 0.05 μM MRCK and 20 minutes kinase reaction time are chosen for MRCK inhibitors screening as MRCK activity is within the linear range in terms of enzymatic rate and reaction time.

Other than MRCK concentration and kinase reaction time, ATP concentration and substrate concentration are the other two factors which need to be determined. The detection window of ATP level of the Kinase-Glo assay is from 0 to 10 μM. There is a linear relationship between the luminescent signal and the amount of ATP in the kinase reaction from 0–10 μM using this assay. 5 μM of ATP is the minimum ATP concentration (4) that is normally used for kinase assays and this concentration is at the linear portion of the detection window of Kinase-Glo assay. The $K_m$ for ATP for MRCK was estimated to be approximately 1.5 μM (Fig. 4.1D). As 5 μM of ATP is near to the $K_m$ for ATP for MRCK and the ATP detection ability of the Kinase-Glo reagent is also quite sensitive around this region, 5 μM ATP is thus ideal for kinase assay. For the substrate, phosphatase inhibitory motif (PIM) of myosin-binding subunit was used as the substrate and the $K_m$ for PIM for MRCK was

predicted to be about 1 µM in Fig. 4.1E. 5 µM of PIM, which is higher than the $K_m$ for PIM, was used so that the kinase reaction would not be restricted by the substrate.

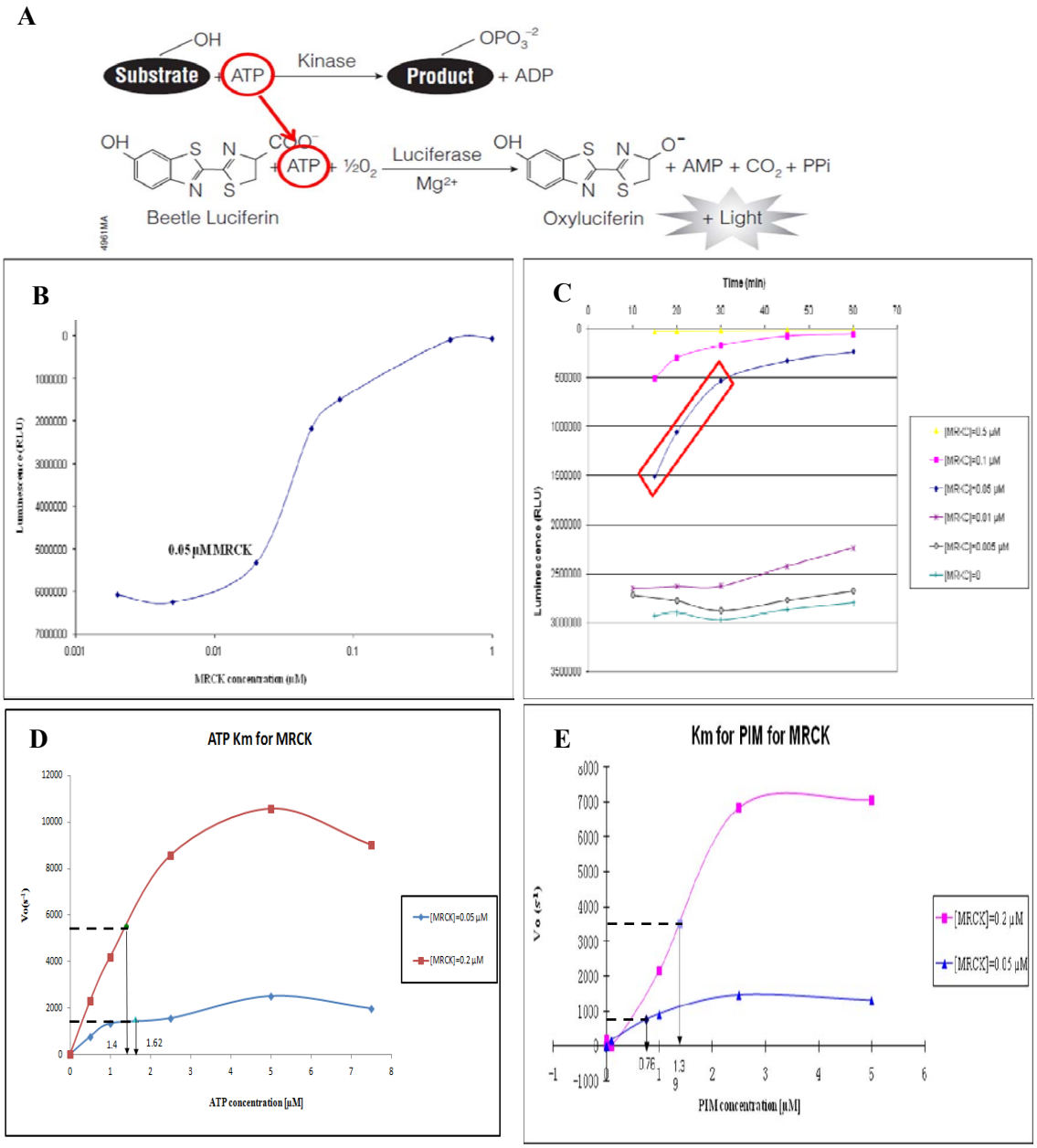


**Fig. 4.1 Enzymatic kinetic studies on MRCK.** (A) The Kinase-Glo assay reactions. Kinase reaction was conducted at room temperature for 20 minutes. The level of ATP remaining after the kinase reaction was detected by adding Kinase-Glo Luminescent Reagent. ATP acts as a substrate for Kinase-Glo Luciferase in the reagent to catalyze the mono-oxygenation of luciferin. The luciferase reaction produces one photon of light per turnover. (B) The sigmoidal kinetic curve of MRCK activity. (C) Time course study of MRCK activity at different MRCK concentrations. The red box marks out the linear range of MRCK activity at 0.05 µM in the first 30 min. (D) The initial reaction velocity, Vo, of 0.05 µM and 0.2 µM MRCK was plotted against ATP concentration for the estimation of ATP Km for MRCK. (E) The Vo of 0.05 µM and 0.2 µM MRCK, were plotted against PIM substrate concentration for the estimation of the substrate $K_m$ for MRCK. $K_m$ is the half of the concentration of substrate (or ATP) that leads to half-maximal velocity.

### 4.3 MRCK inhibitors screening and discovered chelerythrine chloride as a potential MRCK inhibitor

In the initial screen, approximately 155 chemical compounds, among which most of them are known kinase inhibitors, were screened initially in order to obtain a common chemical structure that can inhibit MRCK. From the screening results shown in Fig. 4.2A, luminescent signal released from a chemical compound called chelerythrine chloride (che/chelerythrine; 10 μM) was close to the negative controls, indicating that no active MRCK was present to consume ATP. Chelerythrine produced the highest inhibition among all the screened compounds. In the functional studies of selected chemicals, more investigation was focus on chelerythrine but not INCA-6 because its effect on MRCK is more direct and promising. Although INCA-6 seemed to be an effective inhibitor from the *in vitro* screening, it did not produced obvious *in vivo* inhibitory effect when HeLa cells were treated with 10 μM of INCA-6 for 1 hr (data not shown). One possible explanation on the inhibitory mechanism of INCA-6 is that it may block the substrate recognition site of MRCK but not the catalytic site. This deduction is according to its known inhibitory action on calcineurin where INCA-6 interrupts the interaction between calcineurin and its substrate, nuclear factor of activated T cells (NFTA) (75). However, this still does not fully explain why INCA-6 does not affect active MRCK *in vivo* localization because lamellar and cell central localization of active MRCK depends on both its catalytic activity and substrate recognition ability. MRCK localization should be perturbed when MRCK has no activity and cannot recognize its substrate. As the real working mechanism of INCA-6 is still unknown, we did not carry out further functional studies on INCA-6.

Chelerythrine (Fig. 4.2B, **1**) was reported in 1990 by Herbert's group to be a potent and specific inhibitor for PKCα with an $IC_{50}$ of 660 nM (32). It has a wide range of biological activities, including antiplatelet, anti-inflammatory, antibacterial and antitumor effects. It can also activate MAPK (mitogen-activated protein kinases) pathways which is independent of PKC inhibition. Moreover, chelerythrine can inhibit the binding of BclXL to Bak at $IC_{50}$=100 μM to stimulate apoptosis (8, 100). However, a more recent study was not able to confirm the

inhibitory effect of chelerythrine on PKC (50). It is of our interest to compare the inhibitory effects of this compound on the kinase activity of MRCK, PKC and other MRCK-related kinases.

A second screen was also carried out with another 19 compounds that are structurally similar to chelerythrine. Of these, Sanguinarine (Fig 4.2B, **2**) which has the most similar structure as chelerythrine can also inhibit MRCK. Fig. 4.2D shows that both chelerythrine and sanguinarine inhibited MRCK activity in a concentration-dependent manner. MRCK activity was completely inhibited at 2 μM of both chelerythrine and sanguinarine. The MRCK inhibitory property of chelerythrine and sanguinarine is probably due to their highly similar structure. In contrast, Y-27632, a ROK inhibitor, has no inhibitory effect on MRCK activity at this concentration. Moreover, a compound no. **15** (Fig. 4.2C) from the second screen can also perturb MRCK localization in HeLa cells (Fig 4.2E) but it has no inhibitory effect on MRCK activity in an *in vitro* kinase assay (data not shown). These results suggested that its target is not MRCK and it probably inhibits another target along the pathway of MRCK. Therefore, more investigation should be carried out to search for the actual target of compound **15** and the mechanism of how MRCK *in vivo* localization is affected.

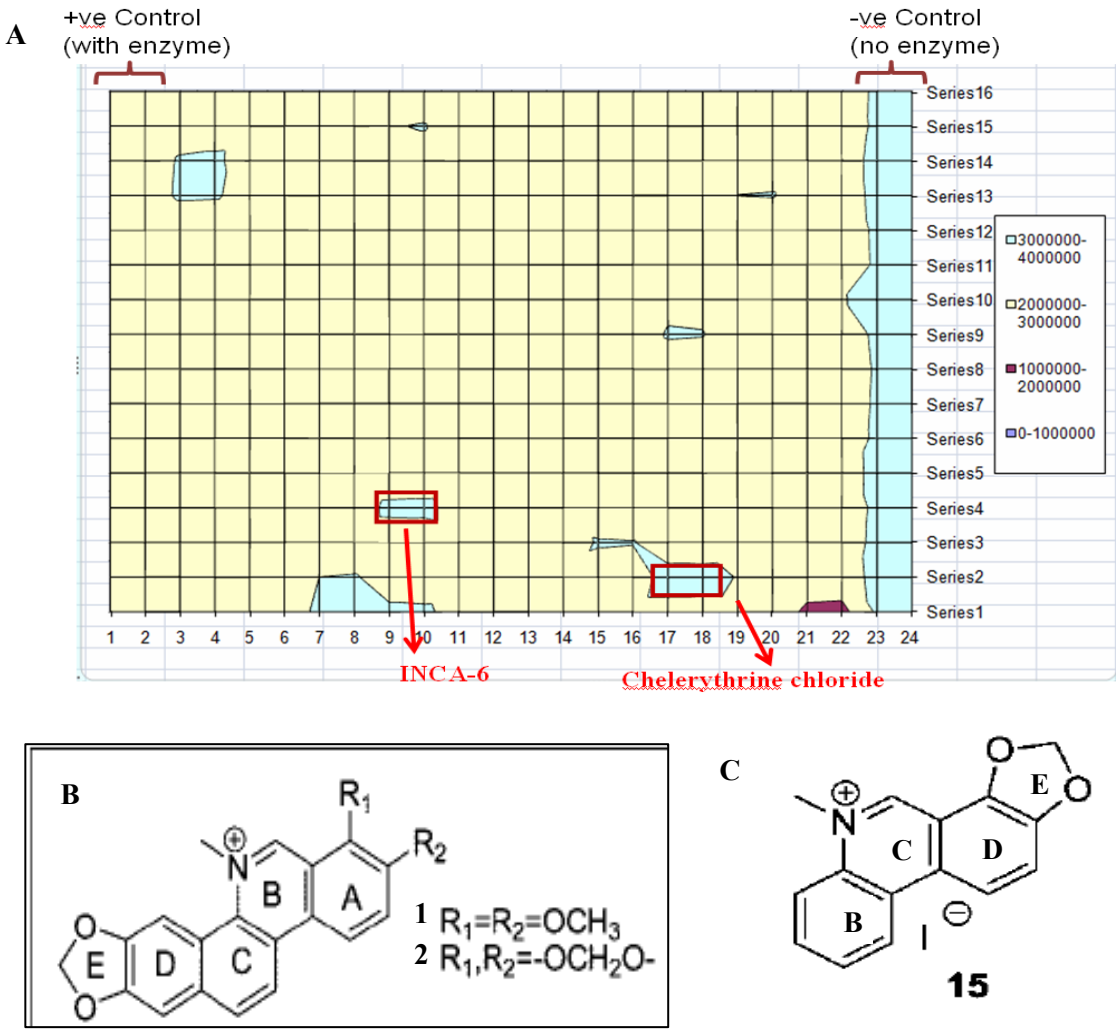


**Fig. 4.2 MRCK inhibitors screening.** (A) Chemical compounds were screened in duplicates in a 384-well format. Two rows at the sites, as indicated, were positive controls (with MRCK but no compound) and negative controls (without MRCK and compound) respectively. The two highest hits were obtained from chelerythrine chloride and INCA-6, which are boxed in red. (B) and (C) The chemical structure of chelerythrine chloride (**1**), sanguinarine (**2**) and compound no. **15**.

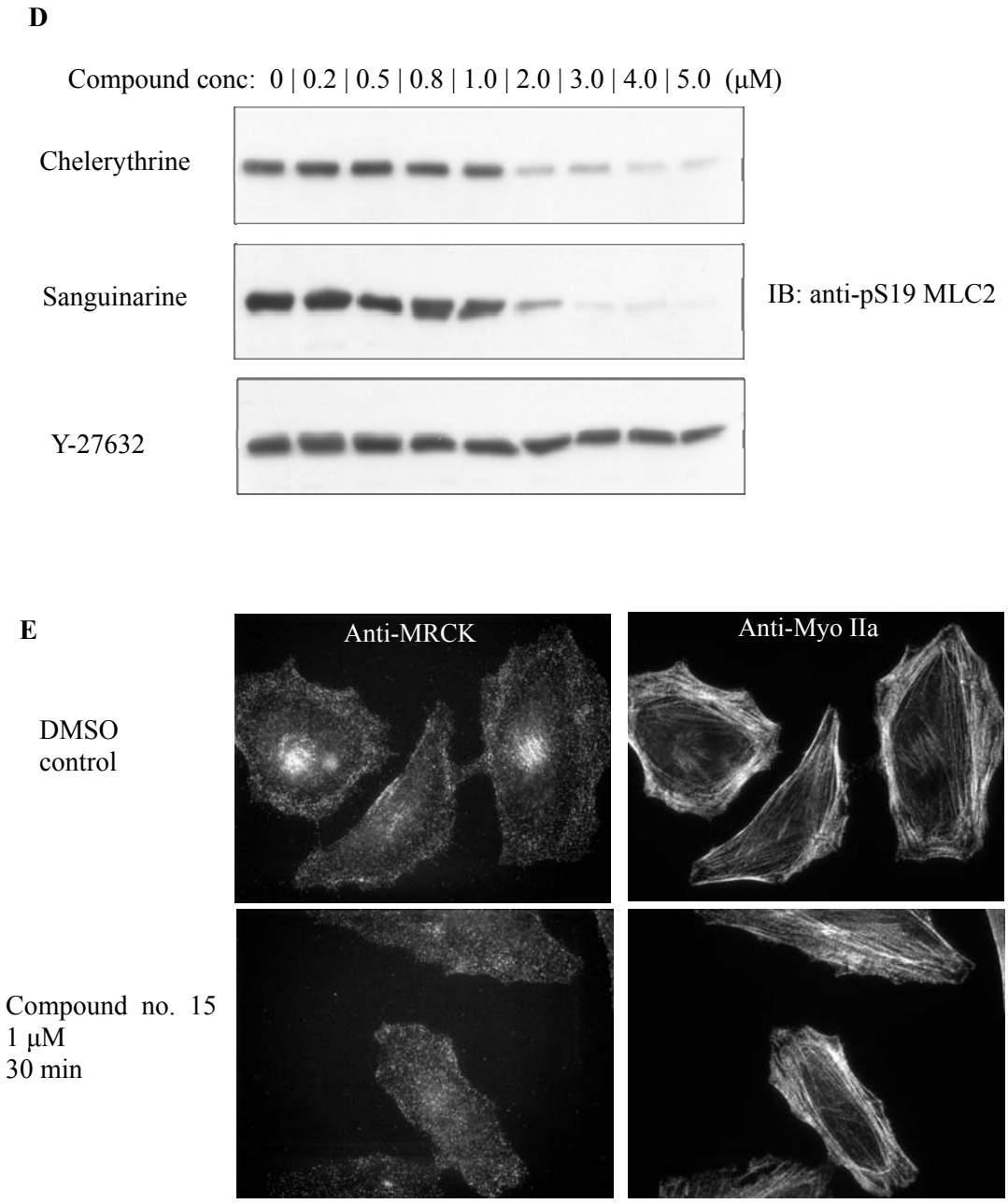


Fig. 4.2 –continued
(D) Serial concentrations of che, sanguinarine, and Y-27632, were tested on MRCK activity using non-radioactive kinase assay. MLC2 was used as substrate in the kinase assay. The phosphorylation of MLC2 was detected by western blot with anti-pS19 MLC2 antibody. Che and sanguinarine, but not Y-27632, can inhibit the activity of MRCK in a dose-dependent manner. (E) Effect of compound no. **15** on MRCK localization in HeLa cells. Cells were co-stained with anti-MRCK and anti-Myosin IIa antibodies. Treatment of compound no. **15** on HeLa cells at 1 μM for 30 min was able to perturb MRCK localization.

### 4.4 Substrate specificity and phosphorylation of MRCK-related kinases

Various recombinant protein kinase including MRCK, ROK, DMPK, CRIK, MLCK, PAK, PKA and PKC were expressed and purified, and their activities in phosphorylating substrates such as PIM and MLC2 were tested and compare. Analyses of MLC2 monophosphorylation on S19 alone or diphosphorylation on T18/S19 were achieved by the use of specific anti-pS19 MLC2 and anti-ppT18/S19 MLC2 antibodies respectively.

As shown in Fig. 4.3B, among all the tested kinases, CRIK was inefficient in phosphorylating PIM. The main function of CRIK is in the regulation of contractile process in cytokinesis (54) that its activity correlates with an increase in diphosphorylated MLC2 level *in vivo* during cytokinesis (103). Its inability to phosphorylate PIM suggests that its regulation on diphosphorylation of MLC2 during cytokinesis does not involve inhibition of myosin phosphatase. In contrast, PIM was effectively phosphorylated by MRCK, ROK, DMPK, PAK and PKA. These *in vitro* results suggest that all these kinases have the potential to inhibit myosin phosphatase and thus cause phosphorylated myosin phosphatase in preserving cellular MLC2 phosphorylation. In fact, ROK's action on MLC2 phosphorylation had been shown to involve myosin phosphatase inhibition (1). In the case of MLC2 phosphorylation, all kinase except DMPK and PKA could phosphorylate MLC2. Earlier reports shown that myosin II with diphosphorylated MLC2 has a higher actin-activated $Mg^{2+}$-ATPase activity than that with monophosphorylated MLC2 (37, 96). In addition, myosin II with diphosphorylated MLC2 resulted in enhanced tension on stress fibers (63). As ROK is implicated in the contraction of actomyosin at the cell rear during cell migration and CRIK in the contractile ring formation in cytokinses, ROK and CRIK induce diphosphorylation of MLC2 to generate a higher mechanical force at the cell rear and cell center respectively for detachment during cell movement and to pull the two cells apart during cytokinesis. In contrast, MLC2 phosphorylation on S19 by MRCK has been shown to localize more to the cell front. This appears to coincide with the dynamic protrusive nature of the cell front during cell migration.

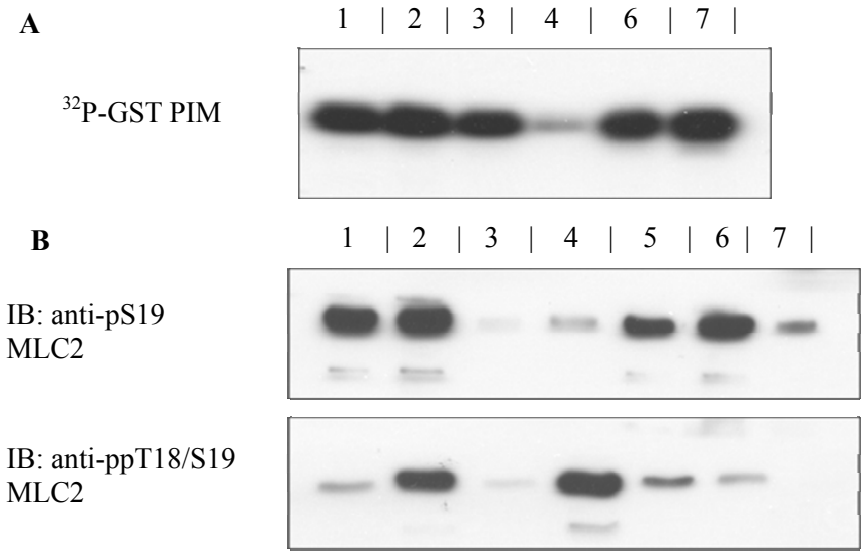


**Fig. 4.3 Substrates, PIM and MLC2, specificities and phosphorylation studies for MRCK and MRCK-related kinases.** (A) Radioactive kinase assay supplement with [γ-$^{32}$P]ATP was used to check the ability of MRCK (lane 1), ROK (lane 2), DMPK (lane 3), CRIK (lane 4), PAK (lane 6) and PKA (lane 7) to phosphorylate PIM. Phosphorylated PIM ($^{32}$P-PIM) containing radioactive signal was detected when exposed onto an X-ray film indicating that PIM is a substrate for that particular kinase. (B) Non-radioactive kinase assay and western blot using anti-pS19 MLC2 and anti-ppT18/S19 MLC2 antibodies were carried out to detect the phosphorylated residue(s) on MLC2 by MRCK (lane 1), ROK (lane 2), DMPK (lane 3), CRIK (lane 4), MLCK (lane 5), PAK (lane 6) and PKA (lane 7). MRCK, ROK, MLCK and PAK can phosphorylate S19 of MLC2 while only ROK and CRIK are able to phosphorylate MLC2 at T18/S19. A lower amount of MLC2 can be phosphorylated by MLCK at T18/S19.

### 4.5 Chelerythrine chloride inhibits MRCK specifically and only inhibits ROK and CRIK at a higher concentration

The selectivity of chelerythrine, using 5 μM and 10 μM as cut off points, was studied on ROK, DMPK, CRIK, MLCK, PAK, PKA and PKCα (Fig 4.4). Expression of kinases was confirmed using western blot analysis with anti-6 histidine and anti-GST antibodies. The kinase activities of some purified enzymes were also tested with their respective inhibitors avalaible: like Y-27632 for ROK, ML-7 for MLCK, H89 for PKA and staurosporine for PKCα. Chelerythrine at 5 μM was found to inhibit MRCK activity almost completely but was unable to inhibit ROK, DMPK, CRIK, MLCK, PAK, PKA and PKCα. However, decreases in ROK and CRIK kinase acitivities were only observed at 10 μM. Chelerythrine only has slight inhibitory effect on PKCα at 10μM, this means that chelerythrine does not effectively inhibit PKCα in agreement with the latest findings (18, 50). Among Y-27632, staurosporine, ML-7 and H89, only 50 nM of staurosporine was found to partially inhibit MRCK among the tested inhibitors. The inhibitory effect of chelerythrine on ROK and CRIK was further investigated in more details in the next section to obtain the $IC_{50}$.

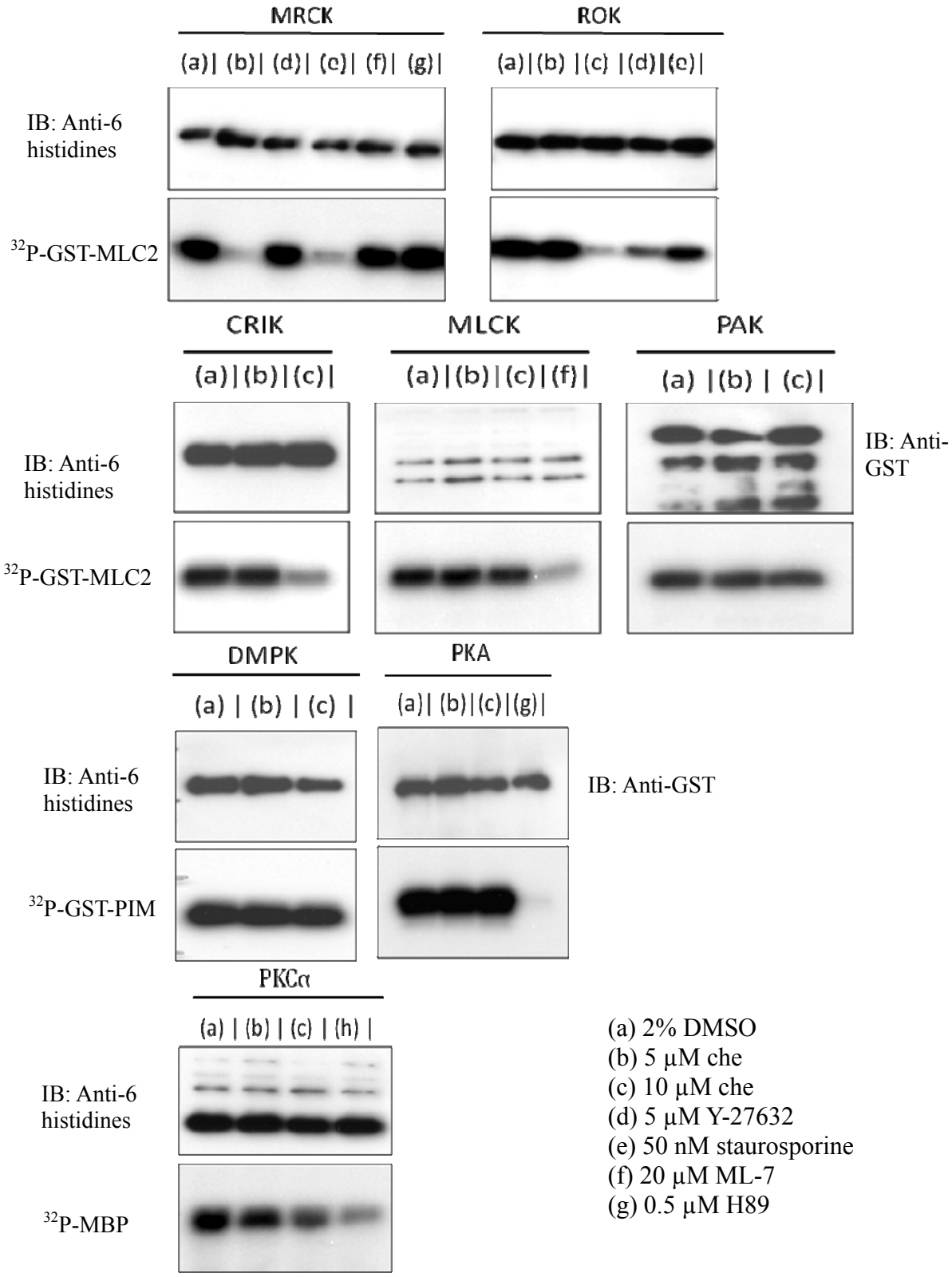


**Fig. 4.4 Selectivity studies of chelerythrine on MRCK, ROK, CRIK, MLCK, PAK, DMPK, PKA and PKCα.** Radioactive kinase assay was used to check the inhibitory effects of chelerythrine and other kinase inhibitors on MRCK-related kinases. The kinases used in each kinase assay were detected by western blot using anti-6 histidines or anti-GST antibodies, depends on the protein tag. The tested chemicals included 2% DMSO as control (lane a), 5 µM che (lane b), 10 µM che (lane c), 5 µM Y-27632 (lane d), 50 nM staurosporine (lane e), 20 µM ML-7 (lane f) and 0.5 µM H89 (lane g).

### 4.6 Kinetics of chelerythrine chloride inhibition of MRCK

In Section 4.3, chelerythrine was shown to inhibit MRCK activity on phosphorylation of MLC2 in a concentration-dependent manner. The inhibition was also comparable to $^{32}$P-ATP-based kinase acitivity wih PIM as substrates (Fig. 4.5A). Previously, it has been shown that Y-27632 inhibited ROK-induced contraction of rabbit aortic strips with a reported $IC_{50}$ of 0.7 μM (94). In comparison, the $IC_{50}$ of chelerythrine on MRCK was found to be approximately 0.86 μM by the *in vitro* kinase assay (Fig. 4.5B) whereas the $IC_{50}$ values of chelerythrine on ROK and CRIK were estimated to be about 8.6 μM and 6.4 μM respectively (Fig. 4.5C). Like MRCK, ROK and CRIK share sequence homology in the kinase domain and substrate specificity, such as PIM and MLC2. Therefore, chelerythrine was expected to exhibit some degree of inhibition both on ROK and CRIK. Our results show that the $IC_{50}$ values on these two kinases are almost 10-fold higher than that for MRCK. Chelerythrine is therefore considered to be more specific towards MRCK as it will only inhibit ROK and CRIK at much higher concentrations.

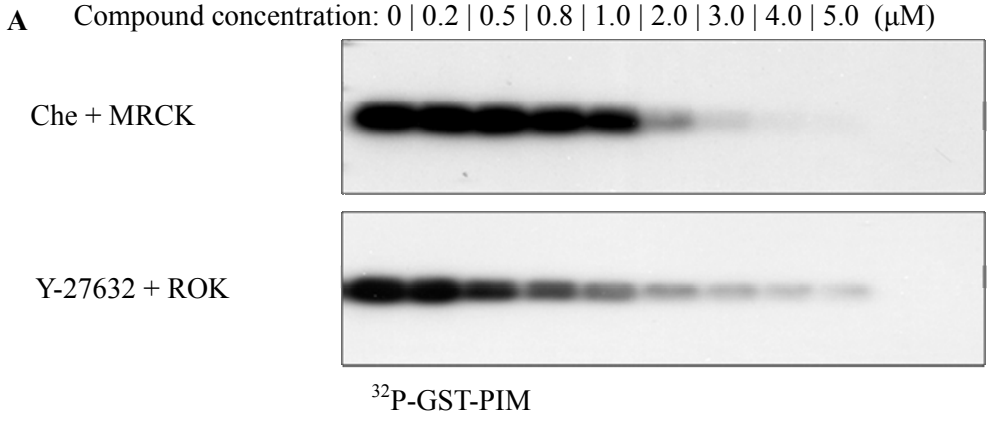


**Fig. 4.5 The calculation of $IC_{50}$ for chelerythrine for MRCK, ROK and CRIK.** (A) Radioactive kinase assay using PIM as substrate and supplement with [γ-$^{32}$P]ATP was carried out to calculate the $IC_{50}$ of chelerythrine on MRCK. ROK activity inhibition with Y-27632 was done for comparison purpose.

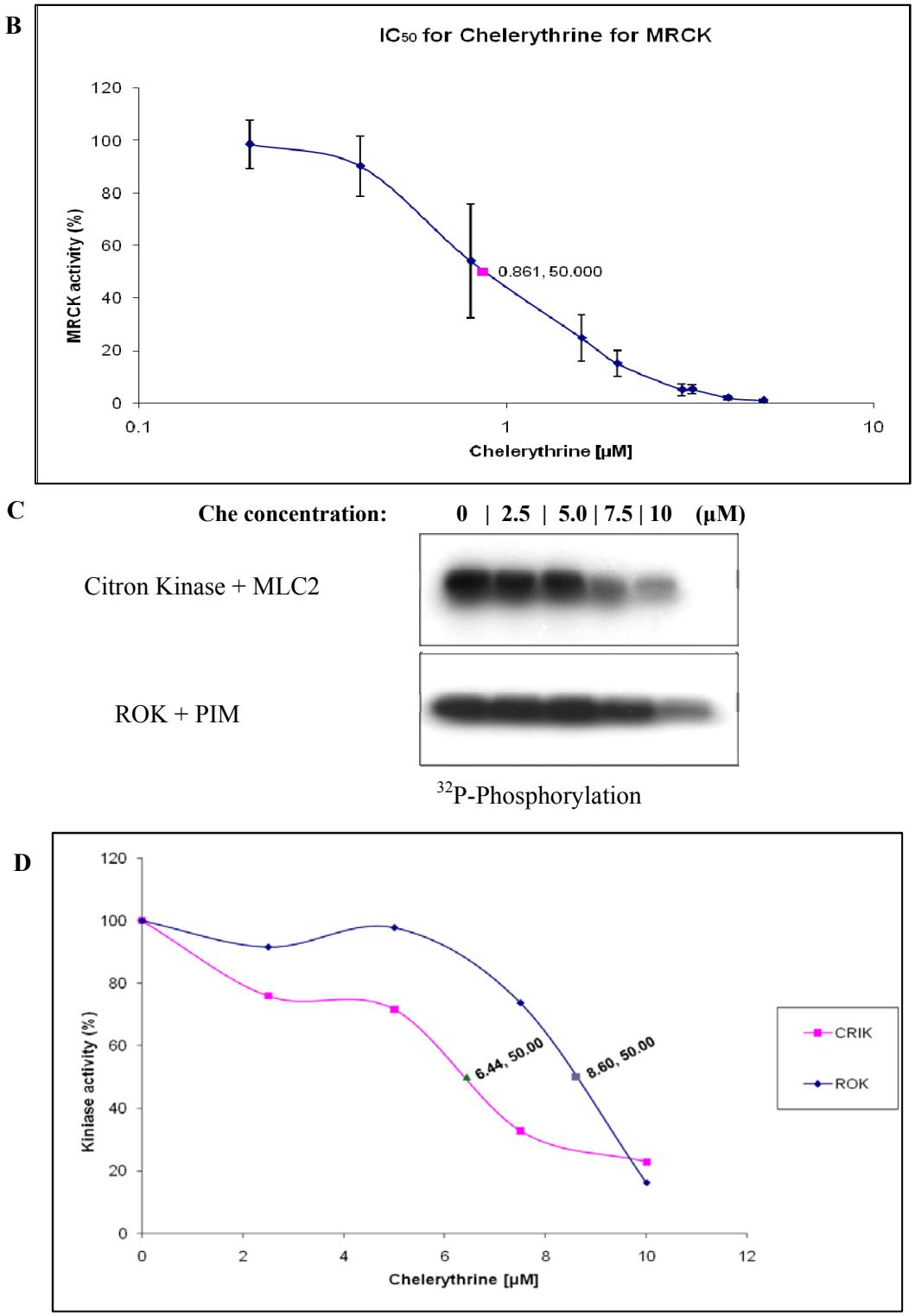


Fig. 4.5-continued

(B) $IC_{50}$ for chelerythrine for MRCK was calculated from the plotted sigmoidal curve. The $IC_{50}$=0.861 µM is at the 50% of kinase activity, which is indicated in the graph. All data are mean ± S.E. of triplicate determinations. (C)Radioactive kinase assay was performed by using PIM as substrate for ROK and MLC2 for CRIK. Che with concentrations at the range of 2.5 µM to 10 µM were tested on ROK and CRIK kinase activity to calculate the $IC_{50}$ values (D) $IC_{50}$ values for chelerythrine for ROK and CRIK were calculated to be about 6.44 µM and 8.6 µM from the plotted curves.

### 4.7 Chelerythrine chloride treatment can perturb endogenous MRCK localization in HeLa cells

The effects of chelerythrine, H89, ML-7 and Y-27632 on MRCK localization in HeLa cells were examined. Endogenous MRCK is mainly localized in the lamella and cell center (88), showing significant co-localization with specific myosin networks as revealed by anti-pS19 MLC2 antibody (Fig. 4.6). Treatment with 5 μM of chelerythrine for 1 hour results in perturbation of MRCK localization and co-localization with the phosphorylated MLC2. This phenomenon was observed to a lesser extent with 2.5 μM of chelerythrine. In contrast, other kinase inhibitors such as H89, ML-7 and Y-27632, did not affect MRCK localization reflecting the specific effect of chelerythrine on MRCK inhibition. Chelerythrine was reported to induce a dose-dependent decrease in the cell viability with $IC_{50}$ of 2.6 μM after 4 hours of treatment (99). Thus, by reducing chelerythrine concentration and duration of the treatment, induction of apoptosis by chelerythrine can be avoided.

As mentioned previously, ROK is able to induce diphosphorylation of MLC2 at both T18 and S19 (Fig. 4.3B). It is expected that a loss of diphosphorylation would indicate a lack of ROK activity. In order to check if chelerythrine would cross-inhibit ROK and CRIK *in vivo*, cells were probed with anti-ppT18/S19 MLC2 antibody. As shown in Fig. 4.7, cells treated with ROK inhibitor, Y-27632, showed normal MRCK localization but the level of diphosphorylated MLC2 was greatly reduced. As ROK is involved in the formation of stress fibers, ROK inhibition also caused the loss of actin bundles at the cell center, which is shown in the decrease of phalloindin staining. In contrast, the level of diphosphorylated MLC2 was not affected in the cells treated with chelerythrine. These results indicate that treatment with 5 μM chelerythrine does not affect cellular ROK activity. The cross-inhibition of chelerythrine on CRIK was not taken in consideration as the main function of CRIK is involved in cytokinesis and our focus is more on cell migration.

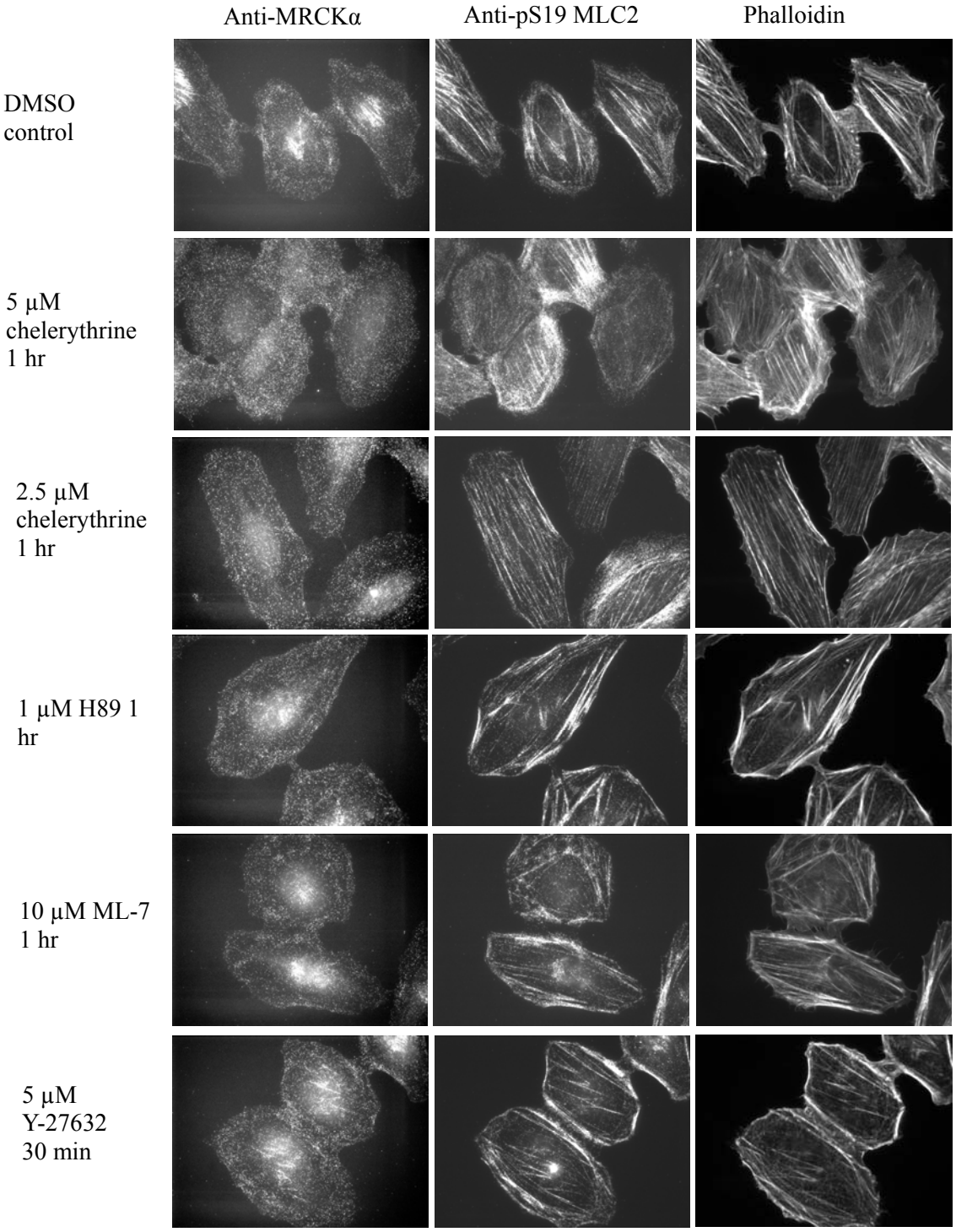


**Fig. 4.6 Localization of endogenous MRCK and phospho-S19 MLC2 in HeLa cells treated with chelerythrine and other kinase inhibitors.** HeLa cells were treated with DMSO as control, 5 μM chelerythrine (1hr), 2.5 μM chelerythrine (1 hr), 1 μM H89 (1 hr), 10 μM ML-7 (1 hr) and 5 μM Y-27632 (30 min).Cells were fixed and stained with anti-MRCKα antibody, anti-pS19 MLC2 antibody and phalloidin.

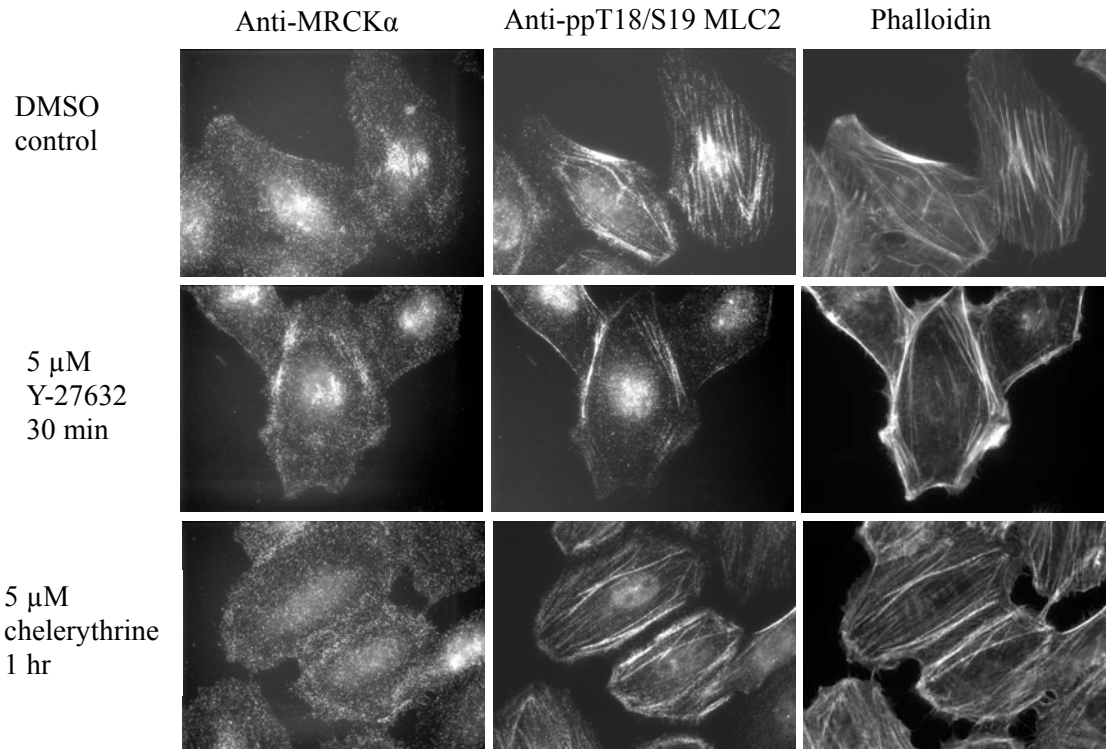


**Fig. 4.7 Effects of chelerythrine and Y-27632 on MRCK.** HeLa cells were either treated with DMSO as positive control, 5 μM Y-27632 as negative control, or 5 μM chelerythrine. The cross-inhibition of chelerythrine on ROK was examined by doing cell staining with anti-MRCKα antibody, anti-ppT18/S19 MLC2 antibody and phalloidin.

### 4.8 Chelerythrine chloride reduces cell migration in U2OS wound healing assay

MRCK has been primarily shown to play an important role in cell migration (88). Therefore, the effect of chelerythrine on cell migration was examined by performing a wound healing assay on U2OS cells. After a wound was made on fully confluent U2OS cells, medium containing either DMSO or 2.5 µM chelerythrine was added. As shown in Fig. 4.8B, the U2OS cells under 2.5 µM chelerythrine treatments migrated slower than the control. Fig. 4.8A depicts the pictures of cell migration in wounded U2OS cells between non-treated and chelerythrine-treated cells. Cells appear to migrate faster and further under normal condition while the migration distance of chelerythrine-treated cells were obviously delayed. Our data suggest that chelerythrine induced MRCK inhibition could indeed reduce cell migration.

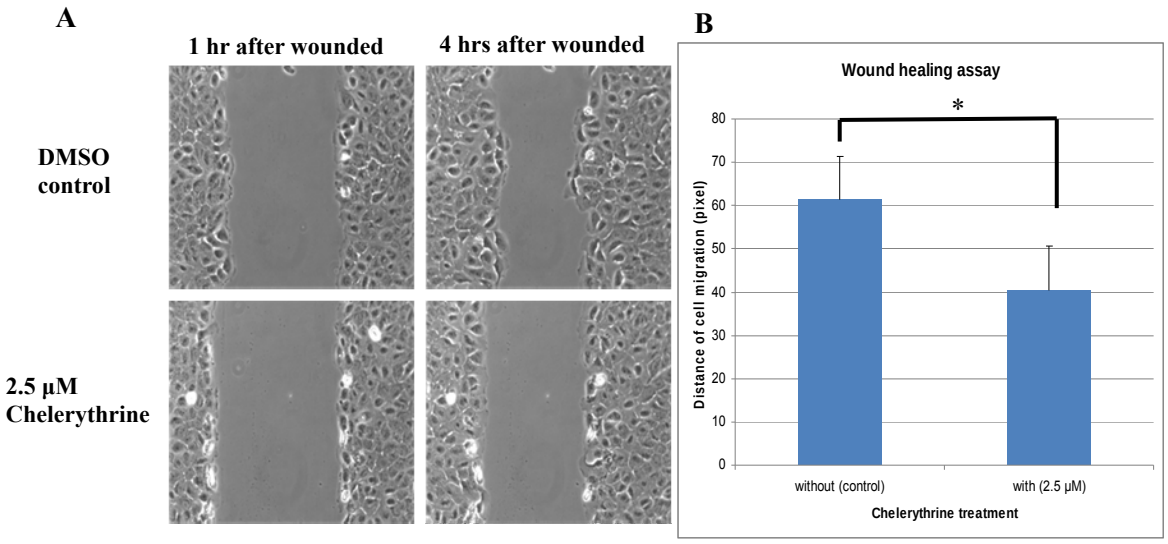


**Fig. 4.8 Effect of chelerythrinee on cell migration.** (A) U2OS cells were grown to 100% confluent onto coverslips and the cells were scratched lightly to generate a wound. Cells were incubated with fresh medium supplement without or with 2.5 µM chelerythrine for 4 hours. The process of cell migration during these 4 hours was recorded. The pictures of the recovery of the wounds at 1 hr and 4 hr after the wounds were shown here. (B) The distances of cell migration under these two treatments were calculated for statistical analysis. About 30 cells were calculated from each treatment and the data was obtained from the mean ± S.E. of the calculated cells from three different sets of experiments. * student t-test p-value<0.05

**4.9 Discussion**

In this section a specific MRCK inhibitor, chelerythrine chloride, was discovered via a chemical compounds screening. Prior to the screening, MRCK enzymatic kinetics were studied. The measurement of MRCK enzymatic kinetics activities apparently revealed some supportive evidences on the previous findings that MRCK catalytic activity is dependent on kinase domain dimerization and trans-autophosphorylation events. MRCK has low kinase activity at low enzyme concentrations (<0.01 μM) presumably due to the lack of dimer formation driven by concentration-dependent process. As the concentration increases, dimerization of MRCK could then occur more readily and this would render the kinase to be active through trans-autophosphorylation as previously reported (87). A similar activation mechanism which requires dimerization and trans-autphosphorylation events have also been disclosed for the two MRCK-related kinases, ROK and DMPK (52).

Substrate specificity profiles of MRCK, ROK, DMPK, CRIK, PAK and PKA were initially studied in this project. These studies are important as the substrate specificity of a kinase may reflect the cellular functions of the kinase. MRCK, ROK and MLCK are the three known MLC2 kinases which are involved in different pathways at different locations and regulate contraction of different networks of actomyosin. In these studies, MRCK, MLCK and PAK were found to be able to monophosphorylate MLC2 at S19 while ROK and CRIK diphosphorylate MLC2 at both T18 and S19. Interestingly it has been reported that monophosphorylated MLC2 was found to localize more towards the protrusive region and diphosphorylated form mainly at the posterior end (46, 78). Our data coincides with the findings that MRCK regulates the myosin II in the lamellar filaments while myosin II regulation by MLCK is in the lamellipodia (88, 91). Phosphorylation of MLC2 by PAK has also been reported but its exact role has yet to be determined (92). As for ROK, its ability in diphosphorylating MLC2 conforms well to its function in causing tail contraction at the retracting cell rear (45, 98). Besides, diphophorylation of MLC2 by CRIK is involved in the contractile process in cytokinesis (54).

Biochemical analysis of MRCK inhibition showed that structurally related compounds chelerythrine and sanguinarine inhibited MRCK in a concentration-dependent manner, similar to the effect of Y-27632 on ROK. The two inhibitors differ only at the R1 and R2 side chains. Based on their similar inhibition profile on MRCK, other compounds which have similar chemical structure to chelerythrine might also be able to inhibit MRCK. Therefore, screening of related compounds with similar structure or modified side chains would facilitate the search of a more potent MRCK inhibitor. The screening of some structural related compounds with fused BCD rings had not yielded any positive results, suggesting that other structural design involving ABC rings may be more desirable (Fig. 4.2B and C).

Although chelerythrine was first discovered to be a potent and selective inhibitor of PKCα (32), it was however disapproved by later studies (8, 18). Furthermore, in agreement with the later studies, our data also shown that chelerythrine has no inhibitory effect on PKC. Chelerythrine has weaker inhibition on ROK and CRIK and only inhibits these two kinases at much higher concentrations for MRCK. The $IC_{50}$ of chelerythrine for MRCK was estimated to be 0.86 μM but was found to be about ten times higher for ROK and CRIK (8.6 μM and 6.4 μM respectively). Chelerythrine is therefore a more specific inhibitor for MRCK than ROK and CRIK. This is in contrast to Y-27632 which is more specific to ROK and can only inhibit MRCK at a higher concentration.

In addition, we also showed that chelerythrine can inhibit MRCK activity *in vivo* and affect its localization in HeLa cells. We also observed that chelerythrine could result in a reduction in cell migration speed as shown in a wound healing assay. This MRCK inhibitory property of chelerythrine can also be exploited as a useful tool for functional studies of MRCK. Besides, it could also be useful in structural analysis on MRCK kinase domain. It will be interesting to find out if this compound might also be beneficial in inhibiting metastasis of cancerous cells in future due to its ability in affecting cell migration. This study should open up potential opportunity for drug design to obtain a better MRCK inhibitor.

**Conclusion**

A new technique named CE was utilized to perform SELEX in the screening of MRCK aptamers. Optimal conditions for carrying out MRCK aptamers selection were determined through method development on CE-SELEX. In the optimization, CE running buffers, phosphate buffer (pH 7) and borate buffer (pH 9), were used to visualize and compare the retention time and migration pattern of MRCK. NaCl concentrations were optimized and the selection buffer with 50 mM Tris, 50 mM NaCl and 5 mM $MgCl_2$ was employed to obtain MRCK-aptamer complex peaks. When borate buffer was used as CE running buffer, the retention time of MRCK was found to be at the region of 8-9 minutes while the retention time of DNA was at 11-12 minutes. An original non-SELEX was used in the initial screen and the best candidate selected, aptamer M6, has an affinity of 125 nM. This aptamer has the ability of detecting the active MRCK but not the inactive MRCK. In the attempt to achieve the purpose of obtaining strong MRCK binders, a modified non-SELEX approach was introduced and carried out in the second screen. The best binder, aptamer F3.11 has a $K_d$ value 109 nM. No significant improvement in MRCK binding affinity could be concluded from the modified approach. Meanwhile, MRCK interactive property of these two aptamers, M6 and F3.11, were further confirmed in an *in vitro* MRCK pull-down assay. When tested on live cells, however, these aptamers were found to be trapped in the cell nucleus and did not appear to have specific localization to MRCK *in vivo*. Further modification on the DNA structure of the aptamers will therefore be helpful to overcome this problem for *in vivo* use in future.

In addition to MRCK aptamers screening, MRCK inhibitors screening from a total of approximately 170 chemical compounds was carried out concurrently. From the result of this chemical screening, Chelerythrine chloride was identified and discovered to have MRCK inhibitory activity with its $IC_{50}$ of 0.86 μM. Sanguinarine, structurally similar to chelerythrine, also displayed MRCK inhibition in a concentration-dependent manner parallel to chelerythrine. In the study of chelerythrine's specificity to MRCK and other kinases, chelerythrine exhibited cross inhibitory effect on the related kinases ROK and CRIK but with higher $IC_{50}$ values of 8.6 μM and 6.4 μM respectively. In the subsequent *in vivo* cell studies,

the co-localization profile of both MRCK and the corresponding monophosphorylated Myosin Light Chain 2 (MLC2) at Serine 19 was readily perturbed by chelerythrine treatment on HeLa cells at a concentration of 5 μM for 1 hour. In contrast, diphosphorylation of MLC2 at Threonine 18/Serine19 was not affected by chelerythrine indicating its specificity toward MRCK. Moreover, a delay in cell migration was observed when U2OS cells were treated with 2.5 μM chelerythrine in a wound healing assay. It is concluded that chelerythrine is a moderately specific inhibitor for MRCK. Further modifications on the chemical structure of chelerythrine should be useful to increase its potency and specificity in the future study.

## References


1. **Amano, M., Y. Fukata, and K. Kaibuchi.** 2000. Regulation and functions of Rho-associated kinase. Exp Cell Res **261:**44-51.
2. **Andre, C., A. Xicluna, and Y. C. Guillaume.** 2005. Aptamer-oligonucleotide binding studied by capillary electrophoresis: cation effect and separation efficiency. Electrophoresis **26:**3247-55.
3. **Asano, T., T. Suzuki, M. Tsuchiya, S. Satoh, I. Ikegaki, M. Shibuya, Y. Suzuki, and H. Hidaka.** 1989. Vasodilator actions of HA1077 in vitro and in vivo putatively mediated by the inhibition of protein kinase. Br J Pharmacol **98:**1091-100.
4. **Bain, J., L. Plater, M. Elliott, N. Shpiro, C. J. Hastie, H. McLauchlan, I. Klevernic, J. S. Arthur, D. R. Alessi, and P. Cohen.** 2007. The selectivity of protein kinase inhibitors: a further update. Biochem J **408:**297-315.
5. **Berezovski, M., A. Drabovich, S. M. Krylova, M. Musheev, V. Okhonin, A. Petrov, and S. N. Krylov.** 2005. Nonequilibrium capillary electrophoresis of equilibrium mixtures: a universal tool for development of aptamers. J Am Chem Soc **127:**3165-71.
6. **Berezovski, M., M. Musheev, A. Drabovich, and S. N. Krylov.** 2006. Non-SELEX selection of aptamers. J Am Chem Soc **128:**1410-1.
7. **Berezovski, M. V., M. U. Musheev, A. P. Drabovich, J. V. Jitkova, and S. N. Krylov.** 2006. Non-SELEX: selection of aptamers without intermediate amplification of candidate oligonucleotides. Nat Protoc **1:**1359-69.
8. **Bernardo, P., K. Wan, T. Sivaraman, J. Xu, F. Moore, A. Hung, H. Mok, V. Yu, and C. Chai.** 2008. Structure-activity relationship studies of phenanthridine-based Bcl-XL inhibitors. J Med Chem **51:**6699-710.
9. **Blank, M., and M. Blind.** 2005. Aptamers as tools for target validation. Curr Opin Chem Biol **9:**336-42.
10. **Bock, L. C., L. C. Griffin, J. A. Latham, E. H. Vermaas, and J. J. Toole.** 1992. Selection of single-stranded DNA molecules that bind and inhibit human thrombin. Nature **355:**564-6.
11. **Brook, J. D., M. E. McCurrach, H. G. Harley, A. J. Buckler, D. Church, H. Aburatani, K. Hunter, V. P. Stanton, J. P. Thirion, and T. Hudson.** 1992. Molecular basis of myotonic dystrophy: expansion of a trinucleotide (CTG) repeat at the 3' end of a transcript encoding a protein kinase family member. Cell **69:**385.
12. **Buchanan, D. D., E. E. Jameson, J. Perlette, A. Malik, and R. T. Kennedy.** 2003. Effect of buffer, electric field, and separation time on detection of aptamer-ligand complexes for affinity probe capillary electrophoresis. Electrophoresis **24:**1375-82.
13. **Bunka, D. H., B. J. Mantle, I. J. Morten, G. A. Tennent, S. E. Radford, and P. G. Stockley.** 2007. Production and characterization of RNA aptamers specific for amyloid fibril epitopes. J Biol Chem **282:**34500-9.
14. **Bunka, D. H., and P. G. Stockley.** 2006. Aptamers come of age - at last. Nat Rev Microbiol **4:**588-96.
15. **Burmeister, P. E., C. Wang, J. R. Killough, S. D. Lewis, L. R. Horwitz, A. Ferguson, K. M. Thompson, P. S. Pendergrast, T. G. McCauley, M. Kurz, J. Diener, S. T. Cload, C. Wilson, and A. D. Keefe.** 2006. 2'-Deoxy purine, 2'-O-methyl pyrimidine (dRmY) aptamers as candidate therapeutics. Oligonucleotides **16:**337-51.
16. **Chen, X. Q., I. Tan, T. Leung, and L. Lim.** 1999. The myotonic dystrophy kinase-related Cdc42-binding kinase is involved in the regulation of neurite outgrowth in PC12 cells. J Biol Chem **274:**19901-5.
17. **Davidson, E. A., and A. D. Ellington.** 2005. Engineering regulatory RNAs. Trends Biotechnol **23:**109-12.
18. **Davies, S. P., H. Reddy, M. Caivano, and P. Cohen.** 2000. Specificity and mechanism of action of some commonly used protein kinase inhibitors. Biochem J **351:**95-105.
19. **Deissler, H. L., and G. E. Lang.** 2008. [Effect of VEGF165 and the VEGF aptamer pegaptanib (Macugen) on the protein composition of tight junctions in microvascular endothelial cells of the retina]. Klin Monatsbl Augenheilkd **225:**863-7.
20. **Dormann, D., and C. J. Weijer.** 2006. Imaging of cell migration. EMBO J **25:**3480-93.
21. **Drabovich, A., M. Berezovski, and S. N. Krylov.** 2005. Selection of smart aptamers by equilibrium capillary electrophoresis of equilibrium mixtures (ECEEM). J Am Chem Soc **127:**11224-5.
22. **Drabovich, A. P., M. Berezovski, V. Okhonin, and S. N. Krylov.** 2006. Selection of smart

aptamers by methods of kinetic capillary electrophoresis. Anal Chem **78:**3171-8.
23. **Ellington, A. D., and J. W. Szostak.** 1990. In vitro selection of RNA molecules that bind specific ligands. Nature **346:**818-22.
24. **Etienne-Manneville, S., and A. Hall.** 2002. Rho GTPases in cell biology. Nature **420:**629-35.
25. **Famulok, M., and G. Mayer.** 2005. Intramers and aptamers: applications in protein-function analyses and potential for drug screening. Chembiochem **6:**19-26.
26. **Famulok, M., G. Mayer, and M. Blind.** 2000. Nucleic acid aptamers-from selection in vitro to applications in vivo. Acc Chem Res **33:**591-9.
27. **Feng, Y., Y. Yin, A. Weiser, E. Griffin, M. D. Cameron, L. Lin, C. Ruiz, S. C. Schürer, T. Inoue, P. V. Rao, T. Schröter, and P. Lograsso.** 2008. Discovery of substituted 4-(pyrazol-4-yl)-phenylbenzodioxane-2-carboxamides as potent and highly selective Rho kinase (ROCK-II) inhibitors. J Med Chem **51:**6642-5.
28. **Friedmann, Y., A. Shriki, E. R. Bennett, S. Golos, R. Diskin, I. Marbach, E. Bengal, and D. Engelberg.** 2006. JX401, A p38alpha inhibitor containing a 4-benzylpiperidine motif, identified via a novel screening system in yeast. Mol Pharmacol **70:**1395-405.
29. **Fu, Y. H., A. Pizzuti, R. G. Fenwick, Jr., J. King, S. Rajnarayan, P. W. Dunne, J. Dubel, G. A. Nasser, T. Ashizawa, and P. de Jong.** 1992. An unstable triplet repeat in a gene related to myotonic muscular dystrophy. Science **255:**1256-8.
30. **Gatto, B., M. Palumbo, and C. Sissi.** 2009. Nucleic Acid aptamers based on the g-quadruplex structure: therapeutic and diagnostic potential. Curr Med Chem **16:**1248-65.
31. **Gomes, E. R., S. Jani, and G. G. Gundersen.** 2005. Nuclear movement regulated by Cdc42, MRCK, myosin, and actin flow establishes MTOC polarization in migrating cells. Cell **121:**451-63.
32. **Herbert, J. M., J. M. Augereau, J. Gleye, and J. P. Maffrand.** 1990. Chelerythrine is a potent and specific inhibitor of protein kinase C. Biochem Biophys Res Commun **172:**993-9.
33. **Hermann, T., and D. J. Patel.** 2000. Adaptive recognition by nucleic acid aptamers. Science **287:**820-5.
34. **Hesselberth, J., M. P. Robertson, S. Jhaveri, and A. D. Ellington.** 2000. In vitro selection of nucleic acids for diagnostic applications. J Biotechnol **74:**15-25.
35. **Hillmen, P., N. S. Young, J. Schubert, R. A. Brodsky, G. Socié, P. Muus, A. Röth, J. Szer, M. O. Elebute, R. Nakamura, P. Browne, A. M. Risitano, A. Hill, H. Schrezenmeier, C. L. Fu, J. Maciejewski, S. A. Rollins, C. F. Mojcik, R. P. Rother, and L. Luzzatto.** 2006. The complement inhibitor eculizumab in paroxysmal nocturnal hemoglobinuria. N Engl J Med **355:**1233-43.
36. **Ikebe, M., and D. J. Hartshorne.** 1985. Phosphorylation of smooth muscle myosin at two distinct sites by myosin light chain kinase. J Biol Chem **260:**10027-31.
37. **Ikebe, M., J. Koretz, and D. J. Hartshorne.** 1988. Effects of phosphorylation of light chain residues threonine 18 and serine 19 on the properties and conformation of smooth muscle myosin. J Biol Chem **263:**6432-7.
38. **Ikenoya, M., H. Hidaka, T. Hosoya, M. Suzuki, N. Yamamoto, and Y. Sasaki.** 2002. Inhibition of rho-kinase-induced myristoylated alanine-rich C kinase substrate (MARCKS) phosphorylation in human neuronal cells by H-1152, a novel and specific Rho-kinase inhibitor. J Neurochem **81:**9-16.
39. **Ishizaki, T., M. Maekawa, K. Fujisawa, K. Okawa, A. Iwamatsu, A. Fujita, N. Watanabe, Y. Saito, A. Kakizuka, N. Morii, and S. Narumiya.** 1996. The small GTP-binding protein Rho binds to and activates a 160 kDa Ser/Thr protein kinase homologous to myotonic dystrophy kinase. EMBO J **15:**1885-93.
40. **Itoh, K., K. Yoshioka, H. Akedo, M. Uehata, T. Ishizaki, and S. Narumiya.** 1999. An essential part for Rho-associated kinase in the transcellular invasion of tumor cells. Nat Med **5:**221-5.
41. **Joberty, G., R. R. Perlungher, and I. G. Macara.** 1999. The Borgs, a new family of Cdc42 and TC10 GTPase-interacting proteins. Mol Cell Biol **19:**6585-97.
42. **Kaliman, P., and E. Llagostera.** 2008. Myotonic dystrophy protein kinase (DMPK) and its role in the pathogenesis of myotonic dystrophy 1. Cell Signal **20:**1935-41.
43. **Kimura, K., M. Ito, M. Amano, K. Chihara, Y. Fukata, M. Nakafuku, B. Yamamori, J. Feng, T. Nakano, K. Okawa, A. Iwamatsu, and K. Kaibuchi.** 1996. Regulation of myosin phosphatase by Rho and Rho-associated kinase (Rho-kinase). Science **273:**245-8.
44. **Klug, S. J., and M. Famulok.** 1994. All you wanted to know about SELEX. Mol Biol Rep **20:**97-107.
45. **Kolega, J.** 2003. Asymmetric distribution of myosin IIB in migrating endothelial cells is

regulated by a rho-dependent kinase and contributes to tail retraction. Mol Biol Cell **14:**4745-57.

46. **Komatsu, S., and M. Ikebe.** 2004. ZIP kinase is responsible for the phosphorylation of myosin II and necessary for cell motility in mammalian fibroblasts. J Cell Biol **165:**243-54.
47. **Kozma, R., S. Ahmed, A. Best, and L. Lim.** 1995. The Ras-related protein Cdc42Hs and bradykinin promote formation of peripheral actin microspikes and filopodia in Swiss 3T3 fibroblasts. Mol Cell Biol **15:**1942-52.
48. **Kureishi, Y., S. Kobayashi, M. Amano, K. Kimura, H. Kanaide, T. Nakano, K. Kaibuchi, and M. Ito.** 1997. Rho-associated kinase directly induces smooth muscle contraction through myosin light chain phosphorylation. J Biol Chem **272:**12257-60.
49. **Lauffenburger, D. A., and A. F. Horwitz.** 1996. Cell migration: a physically integrated molecular process. Cell **84:**359-69.
50. **Lee, S. K., W. G. Qing, W. Mar, L. Luyengi, R. G. Mehta, K. Kawanishi, H. H. Fong, C. W. Beecher, A. D. Kinghorn, and J. M. Pezzuto.** 1998. Angoline and chelerythrine, benzophenanthridine alkaloids that do not inhibit protein kinase C. J Biol Chem **273:**19829-33.
51. **Leung, T., X. Chen, I. Tan, E. Manser, and L. Lim.** 1998. Myotonic dystrophy kinase-related Cdc42-binding kinase acts as a Cdc42 effector in promoting cytoskeletal reorganization. Mol Cell Biol **18:**130-40.
52. **Leung, T., X. Q. Chen, E. Manser, and L. Lim.** 1996. The p160 RhoA-binding kinase ROK alpha is a member of a kinase family and is involved in the reorganization of the cytoskeleton. Mol Cell Biol **16:**5313-27.
53. **Li, J., X. Fang, S. Schuster, and W. Tan.** 2000. Molecular Beacons: A Novel Approach to Detect Protein - DNA Interactions This work was partially supported by a U.S. NSF Career Award (CHE-9733650) and by a U.S. Office of Naval Research Young Investigator Award (N00014-98-1-0621). Angew Chem Int Ed Engl **39:**1049-1052.
54. **Madaule, P., M. Eda, N. Watanabe, K. Fujisawa, T. Matsuoka, H. Bito, T. Ishizaki, and S. Narumiya.** 1998. Role of citron kinase as a target of the small GTPase Rho in cytokinesis. Nature **394:**491-4.
55. **Mallikaratchy, P., R. V. Stahelin, Z. Cao, W. Cho, and W. Tan.** 2006. Selection of DNA ligands for protein kinase C-delta. Chem Commun (Camb)**:**3229-31.
56. **Matsui, T., M. Amano, T. Yamamoto, K. Chihara, M. Nakafuku, M. Ito, T. Nakano, K. Okawa, A. Iwamatsu, and K. Kaibuchi.** 1996. Rho-associated kinase, a novel serine/threonine kinase, as a putative target for small GTP binding protein Rho. EMBO J **15:**2208-16.
57. **Mayer, G., and A. Jenne.** 2004. Aptamers in research and drug development. BioDrugs **18:**351-9.
58. **Mendonsa, S. D., and M. T. Bowser.** 2004. In vitro evolution of functional DNA using capillary electrophoresis. J Am Chem Soc **126:**20-1.
59. **Mendonsa, S. D., and M. T. Bowser.** 2005. In vitro selection of aptamers with affinity for neuropeptide Y using capillary electrophoresis. J Am Chem Soc **127:**9382-3.
60. **Mendonsa, S. D., and M. T. Bowser.** 2004. In vitro selection of high-affinity DNA ligands for human IgE using capillary electrophoresis. Anal Chem **76:**5387-92.
61. **Mhlanga, M. M., D. Y. Vargas, C. W. Fung, F. R. Kramer, and S. Tyagi.** 2005. tRNA-linked molecular beacons for imaging mRNAs in the cytoplasm of living cells. Nucleic Acids Res **33:**1902-12.
62. **Midtvedt, K., P. Fauchald, B. Lien, A. Hartmann, D. Albrechtsen, B. L. Bjerkely, T. Leivestad, and I. B. Brekke.** 2003. Individualized T cell monitored administration of ATG versus OKT3 in steroid-resistant kidney graft rejection. Clin Transplant **17:**69-74.
63. **Mizutani, T., H. Haga, Y. Koyama, M. Takahashi, and K. Kawabata.** 2006. Diphosphorylation of the myosin regulatory light chain enhances the tension acting on stress fibers in fibroblasts. J Cell Physiol **209:**726-31.
64. **Mosing, R. K., S. D. Mendonsa, and M. T. Bowser.** 2005. Capillary electrophoresis-SELEX selection of aptamers with affinity for HIV-1 reverse transcriptase. Anal Chem **77:**6107-12.
65. **Murányi, A., R. Zhang, F. Liu, K. Hirano, M. Ito, H. Epstein, and D. Hartshorne.** 2001. Myotonic dystrophy protein kinase phosphorylates the myosin phosphatase targeting subunit and inhibits myosin phosphatase activity. FEBS Lett **493:**80-4.
66. **Niggli, V.** 1999. Rho-kinase in human neutrophils: a role in signalling for myosin light chain phosphorylation and cell migration. FEBS Lett **445:**69-72.
67. **Nobes, C. D., and A. Hall.** 1995. Rho, rac and cdc42 GTPases: regulators of actin structures, cell adhesion and motility. Biochem Soc Trans **23:**456-9.

68. **Pestourie, C., B. Tavitian, and F. Duconge.** Aptamers against extracellular targets for in vivo applications. Biochimie **87:**921-30.
69. **Pieramici, D. J., and M. D. Rabena.** 2008. Anti-VEGF therapy: comparison of current and future agents. Eye **22:**1330-6.
70. **Pirone, D. M., D. E. Carter, and P. D. Burbelo.** 2001. Evolutionary expansion of CRIB-containing Cdc42 effector proteins. Trends Genet **17:**370-3.
71. **Raftopoulou, M., and A. Hall.** 2004. Cell migration: Rho GTPases lead the way. Dev Biol **265:**23-32.
72. **Ravelet, C., C. Grosset, and E. Peyrin.** 2006. Liquid chromatography, electrochromatography and capillary electrophoresis applications of DNA and RNA aptamers. J Chromatogr A **1117:**1-10.
73. **Ridley, A., H. Paterson, C. Johnston, D. Diekmann, and A. Hall.** 1992. The small GTP-binding protein rac regulates growth factor-induced membrane ruffling. Cell **70:**401-10.
74. **Ridley, A. J., M. A. Schwartz, K. Burridge, R. A. Firtel, M. H. Ginsberg, G. Borisy, J. T. Parsons, and A. R. Horwitz.** 2003. Cell migration: integrating signals from front to back. Science **302:**1704-9.
75. **Roehrl, M. H., S. Kang, J. Aramburu, G. Wagner, A. Rao, and P. G. Hogan.** 2004. Selective inhibition of calcineurin-NFAT signaling by blocking protein-protein interaction with small organic molecules. Proc Natl Acad Sci U S A **101:**7554-9.
76. **Ruckman, J., L. S. Green, J. Beeson, S. Waugh, W. L. Gillette, D. D. Henninger, L. Claesson-Welsh, and N. Janjić.** 1998. 2'-Fluoropyrimidine RNA-based aptamers to the 165-amino acid form of vascular endothelial growth factor (VEGF165). Inhibition of receptor binding and VEGF-induced vascular permeability through interactions requiring the exon 7-encoded domain. J Biol Chem **273:**20556-67.
77. **Sahai, E., T. Ishizaki, S. Narumiya, and R. Treisman.** 1999. Transformation mediated by RhoA requires activity of ROCK kinases. Curr Biol **9:**136-45.
78. **Saitoh, T., S. Takemura, K. Ueda, H. Hosoya, M. Nagayama, H. Haga, K. Kawabata, A. Yamagishi, and M. Takahashi.** 2001. Differential localization of non-muscle myosin II isoforms and phosphorylated regulatory light chains in human MRC-5 fibroblasts. FEBS Lett **509:**365-9.
79. **Sayer, N. M., M. Cubin, A. Rhie, M. Bullock, A. Tahiri-Alaoui, and W. James.** 2004. Structural determinants of conformationally selective, prion-binding aptamers. J Biol Chem **279:**13102-9.
80. **Sin, W. C., X. Q. Chen, T. Leung, and L. Lim.** 1998. RhoA-binding kinase alpha translocation is facilitated by the collapse of the vimentin intermediate filament network. Mol Cell Biol **18:**6325-39.
81. **Sokol, D. L., X. Zhang, P. Lu, and A. M. Gewirtz.** 1998. Real time detection of DNA.RNA hybridization in living cells. Proc Natl Acad Sci U S A **95:**11538-43.
82. **Stanlis, K. K., and J. R. McIntosh.** 2003. Single-strand DNA aptamers as probes for protein localization in cells. J Histochem Cytochem **51:**797-808.
83. **Sweeney, S. J., P. Campbell, and G. Bosco.** 2008. Drosophila sticky/citron kinase is a regulator of cell-cycle progression, genetically interacts with Argonaute 1 and modulates epigenetic gene silencing. Genetics **178:**1311-25.
84. **Tachibana, E., T. Harada, M. Shibuya, K. Saito, M. Takayasu, Y. Suzuki, and J. Yoshida.** 1999. Intra-arterial infusion of fasudil hydrochloride for treating vasospasm following subarachnoid haemorrhage. Acta Neurochir (Wien) **141:**13-9.
85. **Takami, A., M. Iwakubo, Y. Okada, T. Kawata, H. Odai, N. Takahashi, K. Shindo, K. Kimura, Y. Tagami, M. Miyake, K. Fukushima, M. Inagaki, M. Amano, K. Kaibuchi, and H. Iijima.** 2004. Design and synthesis of Rho kinase inhibitors (I). Bioorg Med Chem **12:**2115-37.
86. **Tan, I., C. Ng, L. Lim, and T. Leung.** 2001. Phosphorylation of a novel myosin binding subunit of protein phosphatase 1 reveals a conserved mechanism in the regulation of actin cytoskeleton. J Biol Chem **276:**21209-16.
87. **Tan, I., K. Seow, L. Lim, and T. Leung.** 2001. Intermolecular and intramolecular interactions regulate catalytic activity of myotonic dystrophy kinase-related Cdc42-binding kinase alpha. Mol Cell Biol **21:**2767-78.
88. **Tan, I., J. Yong, J. Dong, L. Lim, and T. Leung.** 2008. A tripartite complex containing MRCK modulates lamellar actomyosin retrograde flow. Cell **135:**123-36.
89. **Tang, J., J. Xie, N. Shao, and Y. Yan.** 2006. The DNA aptamers that specifically recognize ricin toxin are selected by two in vitro selection methods. Electrophoresis **27:**1303-11.

90. **Tombelli, S., M. Minunni, and M. Mascini.** 2005. Analytical applications of aptamers. Biosens Bioelectron **20:**2424-34.
91. **Totsukawa, G., Y. Wu, Y. Sasaki, D. J. Hartshorne, Y. Yamakita, S. Yamashiro, and F. Matsumura.** 2004. Distinct roles of MLCK and ROCK in the regulation of membrane protrusions and focal adhesion dynamics during cell migration of fibroblasts. J Cell Biol **164:**427-39.
92. **Tuazon, P. T., and J. A. Traugh.** 1984. Activation of actin-activated ATPase in smooth muscle by phosphorylation of myosin light chain with protease-activated kinase I. J Biol Chem **259:**541-6.
93. **Tuerk, C., and L. Gold.** 1990. Systematic evolution of ligands by exponential enrichment: RNA ligands to bacteriophage T4 DNA polymerase. Science **249:**505-10.
94. **Uehata, M., T. Ishizaki, H. Satoh, T. Ono, T. Kawahara, T. Morishita, H. Tamakawa, K. Yamagami, J. Inui, M. Maekawa, and S. Narumiya.** 1997. Calcium sensitization of smooth muscle mediated by a Rho-associated protein kinase in hypertension. Nature **389:**990-4.
95. **Ulrich, H., A. H. Martins, and J. B. Pesquero.** 2004. RNA and DNA aptamers in cytomics analysis. Cytometry A **59:**220-31.
96. **Umemoto, S., A. R. Bengur, and J. R. Sellers.** 1989. Effect of multiple phosphorylations of smooth muscle and cytoplasmic myosins on movement in an in vitro motility assay. J Biol Chem **264:**1431-6.
97. **Vavvas, D., and D. J. D'Amico.** 2006. Pegaptanib (Macugen): treating neovascular age-related macular degeneration and current role in clinical practice. Ophthalmol Clin North Am **19:**353-60.
98. **Vicente-Manzanares, M., M. A. Koach, L. Whitmore, M. L. Lamers, and A. F. Horwitz.** 2008. Segregation and activation of myosin IIB creates a rear in migrating cells. J Cell Biol **183:**543-54.
99. **Vrba, J., P. Dolezel, J. Vicar, M. Modrianský, and J. Ulrichová.** 2008. Chelerythrine and dihydrochelerythrine induce G1 phase arrest and bimodal cell death in human leukemia HL-60 cells. Toxicol In Vitro **22:**1008-17.
100. **Wan, K. F., S. L. Chan, S. K. Sukumaran, M. C. Lee, and V. C. Yu.** 2008. Chelerythrine induces apoptosis through a Bax/Bak-independent mitochondrial mechanism. J Biol Chem **283:**8423-33.
101. **Wilkinson, S., H. F. Paterson, and C. J. Marshall.** 2005. Cdc42-MRCK and Rho-ROCK signalling cooperate in myosin phosphorylation and cell invasion. Nat Cell Biol **7:**255-61.
102. **Wilson, D. S., and J. W. Szostak.** 1999. In vitro selection of functional nucleic acids. Annu Rev Biochem **68:**611-47.
103. **Yamashiro, S., G. Totsukawa, Y. Yamakita, Y. Sasaki, P. Madaule, T. Ishizaki, S. Narumiya, and F. Matsumura.** 2003. Citron kinase, a Rho-dependent kinase, induces di-phosphorylation of regulatory light chain of myosin II. Mol Biol Cell **14:**1745-56.
104. **Yang, Y., D. Yang, H. J. Schluesener, and Z. Zhang.** 2007. Advances in SELEX and application of aptamers in the central nervous system. Biomol Eng **24:**583-92.
105. **Yarrow, J. C., G. Totsukawa, G. T. Charras, and T. J. Mitchison.** 2005. Screening for cell migration inhibitors via automated microscopy reveals a Rho-kinase inhibitor. Chem Biol **12:**385-95.
106. **Ylera, F., R. Lurz, V. A. Erdmann, and J. P. Fürste.** 2002. Selection of RNA aptamers to the Alzheimer's disease amyloid peptide. Biochem Biophys Res Commun **290:**1583-8.

## Appendix

| | ***Conventional SELEX*** | ***Modern SELEX*** | |
|---|---|---|---|
| | | ***CE-SELEX*** | ***Non-SELEX*** |
| | ***Similarities*** | | |
| | (1) *In vitro* method used to select DNA/RNA which have binding affinity to a particular target protein | | |
| | (2) Selection starts from a random sequences of DNA/RNA library | | |
| | (3) Selected DNA/RNA are identified via molecular cloning and sequencing | | |
| | | | |
| ***Differences*** | | | |
| | ***Conventional SELEX*** | ***CE-SELEX*** | ***Non-SELEX*** |
| (1) Amplification of selected DNA/RNA | Required between each round of selection | Required between each round of selection | Not required |
| (2) Rounds of selection required | Average 8-12 rounds | 3-4 rounds | 3-4 rounds |
| (3) Duration of whole selection process | Month(s) | Weeks | Days |
| (4) Amount of target protein | High (in terms of μg) | Low (in terms of ng) | Low (in terms of ng) |
| (5) Volume of sample during selection | Microliter | Nanoliter | Nanoliter |
| (6) Fashion of technique(s) performance | Manual | Manual and automated | Can be fully automated |
| (7) Blocking step before selection | Required | Not required | Not required |

**Table 8. The similarities and differences of conventional SELEX, CE-SELEX and Non-SELEX.**